Title

The Evolution of Form and Function in Teleost Fishes

Author

Corn, Katherine Anne Preisig

Publication Date

2022

Peer reviewed|Thesis/dissertation

The Evolution of Form and Function in Teleost Fishes

By

KATHERINE ANNE PREISIG CORN

DISSERTATION

Submitted in partial satisfaction of the requirements for the degree of

DOCTOR OF PHILOSOPHY

in

Population Biology

in the

OFFICE OF GRADUATE STUDIES

of the

UNIVERSITY OF CALIFORNIA

DAVIS

Approved:

Peter C. Wainwright, Chair

Michael Turelli

Stacey A. Combes

Committee in Charge

2022

ABSTRACT

Though environments change across space and time, living organisms must always find ways to succeed under the mechanical constraints posed by the world around them. The nearly 25,000 species of teleost fishes inhabit nearly every imaginable aquatic habitat and have amazing diversity of shapes, sizes, and color patterns. Yet all fishes must eat, and almost every living teleost fish is capable of using 'suction feeding' for prey capture. Suction is a dynamic feeding mechanism that leverages the density and viscosity of water to pull in water and a prey item via rapid expansion of the head. But there are many common prey, like algae, sponges, or coral, that are not easily suctioned in by a hungry critter: and thus, some fishes use 'biting' to graze, scrape, or yank prey from an attachment to the substrate. My dissertation explores how the interactions between animals and their physical world shape evolutionary processes over millions of years, seeking to understand the drivers of diversity in form and function.

In my first chapter, I explored the potential for a fundamental mechanical trade-off to constrain the evolution of biters. Fishes that use biting for prey capture can also use suction, but this may create a trade-off between cranial expansion for suction and force transmission for biting. I studied how this mechanical trade-off affects diversification of both head shape and feeding kinematics. I filmed high-speed videos of feeding strikes of fishes of both groups, then used geometric morphometrics to calculate the amount of motion of the anatomy of the head during feeding, which I refer to as "cranial mobility." I then compared rates of evolution of cranial mobility and of head shape between biters and suction feeders. I demonstrated that the trade-off results in less diversity of kinematics, which evolve more slowly in biters, but accelerates evolution of morphology,

as biters evolve head shape more rapidly than suction feeders. These results show the potential for trade-offs to provide differing evolutionary constraints on the evolution of morphology and kinematics, and to create a mismatch between the adaptive landscapes of form and function.

In my second chapter, I reconstructed the history of feeding mode among 1,530 species of reef fishes and found that prior to the end-Cretaceous mass extinction, over 96% of reef-associated lineages were suction feeders. But I found that there has been a trophic revolution among fishes since then, and benthic grazers make up fully 40% of modern reef fish species diversity. Alongside ecological shifts in the structure of reefs, innovations for improved biting by fishes at the dawn of the Cenozoic may have provided opportunities for biters to thrive and resulted in a trophic revolution among reef fishes. Using body shape data for all 1,530 species, I showed that benthic grazers are evolving body shapes 1.7x faster than suction feeders. These results suggest that benthic grazing may inherently elevate evolutionary potential by providing access to attached prey with diverse functional properties. This study demonstrates that there has been a transformation the trophic makeup of reef fishes in the last 65 million years, and that biting has been a major contributor to the ecological and phenotypic diversity of reefs.

In my third chapter, I leveraged body shape data from 5,940 species of teleost fishes across 392 families from a dataset that I helped collect at the National Museum of Natural History to understand evolution of extreme body shapes in fishes. Fishes range from pancake-like, dorsoventrally flattened goosefishes to species that have been laterally compressed into a disc-like shape, such as surgeonfishes, and even to slender, elongate eels. Yet fishes of all these shapes are subject to the same physical constraints

of life underwater. How, then, is it possible for some lineages to “break the rules” and evolve extreme body shapes? One intuitive possibility is that fishes are concentrated in shape space because it is hard to evolve or function with these odd shapes, and so evolution towards extreme shapes is a long, slow battle against the physics of aquatic life. Yet this work found that species further in shape space from the average body shape are evolving more rapidly, suggesting that the evolution of an extreme body shape requires the release of the constraints on the formation of a typical body shape, such as a major developmental or ecological shift, likely paired with a major shift in adaptive zone. Such a shift in adaptive zone may result in dramatic evolution of body shapes and allow the evolution of extreme or unique body shapes.

ACKNOWLEDGEMENTS

It is amazing how the six years of this PhD feels like it has passed in the blink of an eye, and simultaneously feels like I've been doing this as long as I can remember. I would not have been able to even start this degree without incredible mentorship as an undergraduate. At Bard College at Simon's Rock, Patty Dooley made me feel like I could do anything I set my mind to. At Cornell University, Stacy Farina was both a mentor and a friend: our "professional development" talks helped me become both a better scientist and person. At Friday Harbor Marine Labs, Adam Summers took a chance on an undergrad and showed me that it was not just acceptable but essential to love my study organisms.

Peter Wainwright has been the best PhD advisor I could imagine. I came into this PhD at 21, bright eyed and terribly enthusiastic about fishes, and Peter taught me how to channel that passion into a fruitful career. Peter is not just an incredible scientist, but a person who lives every day thoughtfully and with integrity, and he has shown me how to be a better person in his example. Peter expects the best, because he knows you can do it; in reaching those expectations I have achieved things I never could have dreamed for myself.

The Center for Population Biology has been an unparalleled place to work on a PhD. The community here is both brilliant and welcoming in a rare fashion. The instruction in the Pop Bio Core made me into a better, broader, and more integrative scientist. I could not think of a more delightful group of folks to go through a PhD alongside than my cohort (Asher, Elise, Fernanda, and Sivan). My Qualifying Exam committee (Stacey Combes, Ryosuke Motani, Sharon Strauss, Michael Turelli, and Phil Ward) helped me learn how

to make my work appeal to all kinds of biologists. Michael and Stacey continued as my dissertation committee and have been invaluable; they both truly lead by example and encouraged me to aim higher and be better. Michael instilled in me a deep and undying love for Brownian Motion that forms the foundation of my phylogenetic comparative methods today.

I have been lucky enough to call Wainwright Lab my home for six years. I would be utterly lost without my labmates: Anthony Barley, Ed Burress, Jen Hodge, Sarah Longo, Chris Martinez, Nick Peoples, Sam Price, Max Rupp, Khalil Russell, Darien Satterfield, and Dylan Wainwright; and most of all, my work wives: Sarah Friedman and Alexus Roberts Hugghis. My beloved Fish Friends have been there for everything from jokes to ethical discussions. Few people get to say that their labmates are also close friends: it is a gift.

I have been supported from near and afar by the very best friends anyone could ask for. Jared Weiss and Spencer Zeitel have been my brothers, providing in equal measure both deep thoughts and reminders not to take myself too seriously. Lucia You and Erica Oliver have cheered me on in every part of my life, from eloping privately to graduating publicly. Elska Kaczmarek has encouraged me to think critically about how I approach the world, and to embrace the spontaneity and beauty of life. Alexus Roberts Hugghis has been both work wife and a friend whom I could talk with forever, about anything. Since 1997, Rachel Crawford has given me pep talks and let me be myself. I have looked forward to thoughtful discussions with Noah Randolph-Flagg, Alex Long, and Rob Kaye over many pots of extremely strong coffee. Very high quality coffee, hand-

ground by Iris Holzer and Heath Goertzen, has fueled much of this last year. Paula Mara has provided endless wisdom and suggestions in the park every week.

Time with my family has grounded me. All four of my grandparents were teachers, and we have always valued education deeply. The Corn family has cheered me on and reminded me where I came from. The Preisig family has shown me how to reach higher and think bigger. My late grandfather, Chuck, encouraged a young scientist to follow her passion. The Bowman-Rath family has welcomed me with open arms and shown me new ways to understand my place in the world.

My parents raised a young woman to stand on her own two feet and reach for the stars. My stepmom, Rebecca, taught me to assert myself. My dad, Kim, taught me to value myself. My mom, Carol, has believed I can do great things, probably since I was in diapers! Making you three proud is one of my greatest honors, and I am grateful for your support every day.

My husband, Daniel Rath, is the sun in the sky of my life. Thank you for being my best friend. My life would be less in every way without you in it.

Finally, thank you to the fish. The world would be not nearly as much fun without fish doing all the wacky things they do.

CONTENTS

Dissertation Abstract ii

Acknowledgements v

Contents viii

Chapter 1: A multifunction trade-off has contrasting effects on the evolution of form and function 1

Introduction 2

Materials & Methods 4

Results 10

Discussion 14

Figures & Tables 20

Chapter 2: The rise of biting in the Cenozoic fueled reef fish body shape diversification 29

Introduction 30

Materials & Methods 33

Results 38

Discussion 42

Figures & Tables 49

Chapter 3: Faster body shape evolution at the edges of fish morphospace 55

Introduction 56

Materials & Methods 58

Results 63

Discussion 66

Figures & Tables 73

Literature Cited 80

Appendix 1: Supplementary Materials for Chapter 1 96

Appendix 2: Supplementary Materials for Chapter 2 110

Appendix 3: Supplementary Materials for Chapter 3 125

CHAPTER 1

A MULTIFUNCTION TRADE-OFF HAS CONTRASTING EFFECTS ON THE EVOLUTION OF FORM AND FUNCTION

INTRODUCTION

Morphological systems with more than one function may experience trade-offs tied to an inability to simultaneously optimize alternative functions (Futuyma and Moreno 1988; Wilson and Yoshimura 1994; Koehl 1997; Wainwright 2007). The compromises inherent in trade-offs suggest that multifunctionality discourages the incorporation of novel functions into existing repertoires, thereby limiting diversification of these systems (Schaefer and Lauder 1996; Gatesy and Middleton 1997; Bennett and Lenski 2007; Walker 2007; Farina et al. 2019). But, the efficacy of this suppressive effect has been called into question by recent research that finds that traits most closely tied to trade-offs show elevated rates of evolutionary diversification, demonstrating that trade-offs can sometimes promote rather than limit diversification (Holzman et al. 2012; Muñoz et al. 2017, 2018). These contrasting observations indicate a need for specific tests of multifunctional constraint, particularly as they suggest that the impact of a trade-off may be context-dependent. Furthermore, most studies of multifunctionality focus on underlying anatomical traits, but because the mapping of form to function can be complex, it is important to explore diversification at both levels (Koehl 1997). In this study, we asked how multifunctionality affects evolution of the feeding mechanisms in fishes. We compared prey capture kinematics in fishes that feed with one mechanism, suction, with those of fishes potentially exposed to a trade-off invoked by having two prey capture mechanisms: suction and biting.

Suction feeding is used by nearly all aquatic vertebrates for prey capture. Highly versatile, suction is used to capture virtually any free-moving prey, including fishes, crustaceans, polychaetes, zooplankton, and insects (Lauder 1985). A suction strike involves rapid

expansion of the skull that draws in water and prey, made possible by mobile cranial elements and by the high density and viscosity of water (Lauder 1980a; Sanford and Wainwright 2002; Westneat 2006). Across ray-finned fishes (Actinopterygii), for whom suction feeding is the ancestral mode of prey capture, skull expansion is achieved by way of flexible joints and many independently moving components (Schaeffer and Rosen 1961; Anker 1974; Elshoud-Oldenhave 1979; Lauder 1980a; Westneat 2006). Some fishes, especially in reef habitats, have expanded their feeding repertoire, using direct biting actions to remove attached prey not easily captured with suction (hereafter termed "biters") (Liem 1978, 1980; McKaye and Marsh 1983; Bellwood and Choat 1990; Konow and Bellwood 2005; Konow et al. 2008; Gibb et al. 2015). Biters continue to use suction, but habitual biting or grazing places novel functional requirements on their cranial anatomy (Bemis and Lauder 1986; Gillis and Lauder 1995; Van Wassenbergh et al. 2007; Ferry et al. 2012; Mackey et al. 2014). A biting strike typically transmits greater forces through the jaws to the prey or substrate than a suction strike (Liem 1979; McGee et al. 2016). Elevated forces in biters are expected to lead to greater cranial strength and stability, but a reduction in mobility as a result of a fundamental trade-off between transmitting motion versus force through the musculoskeletal levers that form the kinetic fish skull (Kotrschal 1988; Westneat 1994; Ferry-Graham and Konow 2010; McGee et al. 2016; Martinez et al. 2018).

We explored the impact of multifunctionality associated with biting on diversification of the feeding mechanism by comparing the rates of evolution of cranial mobility measured during prey capture in 44 species of suction feeders and biters spanning 28 families of fishes of percomorph fishes (Percomorpha includes about 160

families). Using landmark morphometrics applied to high-speed videos of fishes feeding, we generated a dataset consisting of seven traits capturing cranial motions during suction feeding. We then estimated rates of evolution, trait optima, and convergence of suction kinematics, as well as the evolutionary rate of cranial morphology. We used two contrasting approaches to assess evolutionary rates of cranial mobility (e.g., kinesis) and major components of kinesis (e.g., jaw protrusion, rotation, gape, etc.), one based on a univariate Brownian-Motion and Ornstein-Uhlenbeck model-fitting framework, and a second with a Bayesian, relaxed clock, state-dependent, multivariate model of Brownian Motion. If a trade-off between mobility and force transmission constrains the evolution of prey capture kinematics, we should see slower rates of evolution in species that use both biting and suction, versus those using suction alone.

MATERIALS & METHODS

Dataset Construction

Feeding mode distribution. We categorized species in our study as either “biting”, referencing those species that use both biting and suction, or “suction feeding” based on published information about their feeding ecology and our own observations in the lab and the field (Purcell and Bellwood 1993; Westneat 1995; Randall et al. 1997; Ferry-Graham et al. 2001; Wainwright and Bellwood 2002; Konow et al. 2008; Oufiero et al. 2012; Copus and Gibb 2013). We classified a “biting” feeding mode as one where the fish uses suction as well as direct biting actions. A direct biting action was designated as one where the fish’s closing jaws make contact with the prey item to either grip it or scrape it

from a holdfast. We identified 31 suction feeders and 13 biters in our dataset of 44 species (Table S1).

Feeding videos & landmark morphometrics. We collected 175 lateral view high-speed videos of suction-based feeding strikes in 44 species of fishes from 28 families within Percomorpha for which we had identified feeding mode. To calculate overall cranial kinesis, we used the method described by Martinez et al. (2018), summarized here. Landmark morphometrics were used to digitally capture head shape at ten equidistant time points during each feeding strike, starting with onset of mouth opening and ending when maximum gape was achieved. We used tpsDig2 (Rohlf 2015) to place 18 landmarks on the fish's head: 10 fixed landmarks denoted functionally informed, homologous points of the cranial anatomy and 8 sliding semi-landmarks along the ventral margin of the head captured the motion of the lower jaw and depression of the hyoid apparatus of the throat, which we refer to as "buccal depression" (Fig. S1; doi: 10.25338/B8703S). Landmark data were analyzed in the statistical software R v. 3.6.3 (R Core Team 2019) using the package geomorph v. 3.1.2 (Adams and Otárola-Castillo 2013). A generalized Procrustes analysis (GPA) was performed to align the data, an iterative process of scaling, rotating, and translating all shapes to reduce the Procrustes distance between them (Rohlf and Slice 1990). Alignment of sliding semi-landmarks during GPA was done in a manner that reduced Procrustes distance (Gunz and Mitteroecker 2013). We extracted head shape data from the starting image of each strike, when the mouth was closed, computed a separate alignment for those shapes, and then averaged them by specimen and then by species. This procedure for extracting head shape data from video sequences resulted in

a morphological dataset in which all downstream analyses of head shape were independent of scale.

Calculating total cranial kinesis and kinematic components. We visualized each feeding strike as a trajectory of head shape change. The length of this trajectory was quantified using Procrustes distance, which represents the distance between two points (i.e., shapes) in shape space (Kendall 1984; Adams and Otárola-Castillo 2013) (distances ij in Fig. 1b). This resulted in nine distances between the ten head shapes representing a strike sequence, which we summed to get the total trajectory length, representing overall cranial kinesis (sum of i1:i9 in Fig. 1b). A longer shape change trajectory represented higher kinesis, with a greater range of motion of cranial bones (Martinez et al. 2018; Martinez and Wainwright 2019). We separately measured six components of cranial kinesis from the landmark data, which we refer to as "kinematic components" (Fig. S2). These measurements included the peak values of major elements of the expansive phase of a suction strike: upper jaw protrusion, mouth gape, cranial elevation, upper jaw rotation, lower jaw rotation, and buccal depression (Fig. S2). These kinematic components are functionally integrated in a suction feeding strike and their sequential, coordinated activation is a defining feature of suction feeding (Gibb and Ferry-Graham 2005; Bishop et al. 2008; Olsen et al. 2019). All measurements, including overall cranial kinesis and all six kinematic components, were computed for each feeding strike and averaged at the specimen-, then species-levels prior to conducting statistical analyses.

Data Analysis

Phylogenetic comparative methods. To account for the effects of shared evolutionary history on kinematic and morphological traits, we employed a dual model-fitting approach

to estimate the impact of native feeding mode (suction or biting) on the rate of evolutionary diversification of kinematics during suction-based feeding events. We pruned a large phylogeny of ray-finned fishes (Rabosky et al. 2018) to the species in our dataset and used the R packages stats, ape v 5.3 (Paradis et al. 2004), and phytools 0.6-99 (Revell 2012) to explore evolutionary patterns. Where species in our dataset were not present in the phylogeny, we substituted them with a species chosen at random from those in the same genus or the most closely related genus that were sampled in the tree; four species required this substitution (genera: within-Choerodon; Oxycirrhites to Paracirrhites; Cyprinocirrhites to Notocirrhitus; Terelabrus to Bodianus).

We estimated disparity separately for each kinematic trait using morphol.disparity in geomorph, and also took the average of all 7 values. Separate phylogenetic ANOVAs using procD.pgls in geomorph were used to compare overall cranial kinesis and individual kinematic components by feeding mode (at $\alpha = 0.05$). We used principal component analysis (PCA) on the correlation matrix to visualize the multivariate kinematic data. Lastly, to compare head morphology, we visualized the morphospace of interspecific head shape variation from landmark data using the plotTangentSpace function in geomorph and measured overall morphological disparity with the morphol.disparity function in that R package.

Convergent evolution. We used two distance-based metrics of evolutionary convergence, as implemented in the package convevol v 1.3 (Stayton 2015). We estimated convergent evolution among biting lineages in our kinematic data, including overall cranial kinesis and the six kinematic components. C1 estimates the proportion of phenotypic distance closed by evolution of the putatively convergent tips, given the

maximum distance in phenotypic space between lineages, including estimated ancestral states at nodes (Stayton 2015). We also compared C3, which estimates the proportion of the total evolution of the putatively convergent taxa distance that brings taxa closer together, or that which is "attributable to convergence." We ran significance tests using 500 simulations of convratsig when estimating the degree of convergence in kinematic data, which iterates the distance-based convergence tests.

Evolutionary rate and trait optima estimates. There are no reliable methods yet to model the effect of a discrete trait in a multivariate Ornstein-Uhlenbeck framework for very high-dimensional data, like the morphometric landmarks that we used to capture head shape (Adams and Collyer 2018, 2019). Therefore, we used multivariate Brownian Motion models implemented in geomorph to estimate evolutionary rates and compared the fit of single- and multi-rate Brownian motion models (Adams and Otárola-Castillo 2013; Adams 2014). We used feeding mode as a binary discrete trait.

We used a two-fold methodology to estimate rates of character evolution for kinematic components and kinesis for biters and suction feeders. In the first approach, we fit a series of Brownian Motion (BM) and Ornstein-Uhlenbeck (OU) models of trait evolution to estimate univariate evolutionary rates. Both BM and OU models can be used to estimate evolutionary rate of a continuous character and to test for the effect of discrete trait history on continuous character evolution. We used feeding mode as a binary discrete character and generated a distribution of 1,000 stochastic character maps using phytools (Revell 2012). For kinesis and each kinematic component, we then fit five BM or OU models on each stochastic character map using OUwie (Beaulieu et al. 2012). We fit single-rate Brownian Motion, "BM1"; multi-rate Brownian Motion, "BMS"; single rate,

single optimum Ornstein-Uhlenbeck, “OU1”; multi-optimum, single rate Ornstein-Uhlenbeck, “OUM”, and multi-rate, multi-peak Ornstein-Uhlenbeck, “OUMV”. We elected not to fit multi-rate, multi-peak, multi-selection Ornstein-Uhlenbeck models with a separately estimated sigma-squared and alpha (OUMVA) because of difficulties with interpreting values of sigma-squared under different estimates of the alpha parameter (Ho and Ané 2014; Cooper et al. 2016). We compared the fit of models across all 1,000 stochastic character maps using AICc, with a distinguishability cutoff of 2.0.

Secondly, we fit estimated rates of kinematic evolution in suction feeders and biters with a Bayesian approach, using a relaxed clock, state-dependent, multivariate BM model of evolution, implemented with the MuSSCRat model and executed in RevBayes (Höhna et al. 2016; May and Moore 2019). We used the MuSSCRat model for estimates of evolutionary rate because it allows multivariate estimates of the Brownian rate parameter, jointly estimates evolution of the discrete trait and the continuous traits avoiding a source of bias in rate estimates (Revell 2013), and uses a relaxed-clock model incorporating background rate variation that provides improved type-I error rates (May and Moore 2019). Most common implementations of BM or OU are univariate, allowing only one continuous character at a time (Adams 2014; Denton and Adams 2015; Adams and Collyer 2018, 2019). However, the multiple kinematic components measured in our fishes are mechanically linked and are concurrently activated during a feeding strike. For this reason, a multivariate approach that allows us to capture that covariation is valuable. Furthermore, a state-dependent, relaxed-clock model allowed us to directly test our hypothesis that the rate of evolution depends on feeding mode, at the exclusion of other sources of rate variation.

We ran three separate MCMCs of the MuSSCRat model due to unit incommensurability between the three forms of measurement data (Huttegger and Mitteroecker 2011; Adams and Collyer 2019). We fit independent models with the three angular kinematic components, the three linear distance components, and overall cranial kinesis as continuous characters and used feeding mode (biting and suction feeding) as a binary discrete trait. The MCMCs ran for 500,000 generations (distances), 1 million generations (angles), or 2 million generations (kinesis) with a 10% burn-in, and we set a prior expectation on the number of transitions between discrete states at 5 for all models. We drew transition rates from a log-normal prior and set a log-uniform prior on the probability that the rate of the continuous characters was state-dependent. A log-normal prior informed the rate shift distribution. We describe how we evaluated the influence of priors on the number of rate shifts on posterior parameter estimates in Appendix 1 (Fig. S5).

RESULTS

Diversity in kinematics and morphology

Overall cranial kinesis and kinematic components. Suction feeding fishes had greater overall cranial kinesis, undergoing greater total shape change during feeding strikes, than did biters (Fig. 1). Across six components of cranial mobility, suction feeders had more diverse feeding kinematics, possessing an average of 13.53-fold greater variance among species than in biters (Table S2). Additionally, fishes that use biting had smaller mean values than those that use only suction for all kinematic components except for lower jaw

rotation, and also displayed lower overall cranial kinesis (Fig. 2; Table S3). A PCA of the six kinematic components resulted in all variables loading positively on PC1, which accounted for 65.9% of total variation and represented an axis of low to high mobility, with biters clustered low on PC1. PC2 (17.8% of total variation) primarily captured variation among suction feeders, with upper jaw protrusion and maxillary rotation loading positively and highly, but maximum gape loading strongly, but negatively on this axis (Fig. 3a; Fig. S3; Table S4).

Head shape diversity. Feeding mode had a strong effect on head shape. When visualized in the first two axes of a PCA, feeding mode separated species into two minimally overlapping groups (Fig. 3b). Head depth and mouth size were major contributors to this separation, correlating most strongly with PC1 (40% of total variation) and PC2, respectively (29.1% of total variation). Biters occupied parts of the morphospace associated with deeper heads and smaller mouths as compared to suction feeders. Disparity (i.e., variance) of head shape in suction feeders was 1.54x that of biters but was not statistically different ($p = 0.15$).

Convergence among biters. We found strong evidence for convergent evolution in kinematics of species that use both biting and suction ($C1=0.404$; $p < 0.0001$), indicating that biters have closed 40% of the maximum distance in kinematic phenotype space between their lineages. An estimated 20.2% of the total evolution of kinematic components and total cranial kinesis in biters brought these putatively convergent taxa closer together (C3) (Fig. 4). Consistent with the results for trait means and variances, biters converged on lower cranial kinesis and lower variation among species in kinesis than suction feeding species.

Models of Evolution

Stochastic character maps. A distribution of 1,000 stochastic character maps, simulating the discrete character history of feeding mode, recovered an average of 9.00 transitions between states, including some from suction to biting, and others back again from biting to suction (Fig. 5a). Reconstructions predict the ancestral character state of the sampled taxa to be suction feeding.

Morphological evolution. Head shape evolved faster in biters than in suction feeders, with the former having about a 1.62-fold faster rate of evolution. Model fitting significantly favored different rates for feeding mode groups over a single-rate model (BMS preferred over BM1, $p = 0.01$). Though biters have an elevated rate of head shape evolution compared to suction feeders, their slightly lower disparity is likely due to the smaller proportion of time on the phylogeny spent in a biting state.

Kinematic evolution. In a Brownian Motion and Ornstein-Uhlenbeck model fitting framework, suction feeders had elevated rates of evolution when compared to biters in all six kinematic components as well as total cranial kinesis (Fig. 5b, Table 1). All traits were best fit by a multi-rate, multi-optima model of evolution (OUMV), but some traits were equally well fit by either multi-rate Brownian Motion with no adaptive optima (BMS; buccal depression, head rotation) or a single-rate, multi-optima model (OUM; lower jaw rotation, maximum gape). As all traits were equally well or best fit by the OUMV model, we reference its parameters for the rest of this manuscript, particularly when comparing this model-fitting framework to an alternative approach used, below. Suction feeders always had an optimum associated with larger trait values than biters (Fig. 2). Furthermore, in suction feeders, model-predicted trait optima were largely aligned with

the central peaks of empirically measured trait values, but observed trait distributions in biters were often centered on a peak associated with slightly higher trait values than those predicted by the model. Rates of evolution for kinematic traits were, on average, 16.53 times faster in suction feeders than biters, with the difference ranging from a 2.99-fold faster rate in maximum gape to an exceptional 47.40-fold faster rate of upper jaw protrusion in suction feeders.

An alternate method for rate estimation, using Bayesian relaxed-clock, multivariate, state-dependent models of evolution, reported an average of 13.50-fold faster evolution of kinematics in suction feeders than in biters while accounting for background rate variation, across three models (Fig. 6). Suction feeders evolved kinesis 15.13 times faster than biters, with a posterior probability of separate rates for each discrete state of 0.997 and an estimated 5.29 rate shifts. For linear distance-based components, suction feeders evolved 22.46-fold faster than biters, with a posterior probability of 1.00 for state dependence of the rate and an estimated 8.34 rate shifts. For angle-based components, suction feeders evolved 2.91 times faster than biters, with a posterior probability of state dependence of 0.91 and an estimated 7.13 rate shifts. The magnitude of the effect of feeding mode on trait evolution was variable; in kinesis, there was a strikingly strong correspondence between variation in rates that was attributed to the discrete trait and the overall rates for each branch (Fig. 6, Fig. S4). In contrast, the distance component traits and angle component traits showed a more moderate role for background rate variation contributing to overall branch rates.

DISCUSSION

We found patterns of diversity in fish feeding motions that are consistent with a trade-off constraining evolution in species with multifunctional jaws used for both biting and suction, compared to species that feed only by suction. Our results show a dominant role of multifunctionality in governing the evolution of suction strikes and of cranial mobility, with exceptional rate differences between groups: 16.5-fold per-trait average or a still high 13.5-fold (multivariate BM rate) faster evolution of species that use just suction feeding, even when accounting for background rate evolution. This very strong effect of feeding mode is underscored by the remarkable similarity in the evolution of total cranial kinesis between overall branch rates of evolution (Fig. 6a, center) and rate attributed to feeding mode, indicating that feeding mode accounts for nearly the full range of rates of evolution of suction feeding kinematics (Fig. 6a, right). We found that the constraints of the trade-off have limited both the degree of kinesis as well as the diversity of kinematic combinations in species that use both biting and suction when they feed using suction. In contrast, suction feeders have elevated kinematic diversity in part because of the higher degree of cranial kinesis, but also because they couple their highly mobile strikes with varied contributions from different kinematic components to the overall feeding motion (Fig. 3a). For example, two of the highest kinesis suction feeders, Antennarius hispidus and Epibulus insidiator, have either high buccal expansion and comparatively modest jaw protrusion, or exceptional jaw protrusion with little buccal expansion, respectively.

Reduced kinesis appears to be adaptive for biting fishes with a multifunctional feeding apparatus, with lower rates of kinematic evolution across multiple model-fitting methods. Because of the inherent mechanical trade-off in levers between transmission of

force and motion (Westneat 1994, 2003), adaptation in a feeding system that uses biting toward the transmission and application of force during biting results in less mobility during suction strikes. In a biting strike, the force applied to the prey item is transmitted directly through the jaw lever systems, which may lead to the evolution of efficient muscular force transmission and constraint of skeletal movement to minimize misalignment of force and motion (Tedman 1980; Kotrschal 1988; Bellwood and Choat 1990; Vial and Ojeda 1990; Friel and Wainwright 1997; Wainwright and Bellwood 2002; Ferry-Graham and Konow 2010; McGee et al. 2016). These expectations for the design of a biting feeding system contrast with characteristics of suction strikes, which often include a large expansion of the buccal cavity to drive the flow of water into the mouth (Elshoud-Oldenhave 1979; Lauder 1980b; Camp et al. 2015; Jacobs and Holzman 2018), including jaw protrusion that increases the hydrodynamic forces that suction feeders exert on prey (Holzman et al. 2008; Staab et al. 2012).

Many biting taxa in our study have lost independent mobility between the two major bones of the upper jaw (Gosline 1987; Kotrschal 1988; Purcell and Bellwood 1993). Loss of independent upper jaw mobility results in less complex motion of the bones and, in most cases, the loss of upper jaw protrusion altogether, likely contributing to the extreme difference between groups in evolutionary rates for this trait (47.4-fold faster in suction feeders). The relationship between loss of mobility and reduced diversity of kinematics is reminiscent of the pattern in terrestrial vertebrate locomotion where an increased number of mobile elements is associated with diversity in locomotor patterns (Mosauer 1932; Dagg 1973; Hildebrand 1989). For example, mammals that almost exclusively move their hind legs synchronously, like adult rabbits, have fewer gaits than animals that routinely

move each of their four limbs in different patterns (e.g., horses). Such a relationship between diversification and number of independent elements is consistent with literature on modularity, which suggests that an elevated number of modules may increase the evolvability of the system, or its ability to vary (Hallgrímsson et al. 2009). Interestingly, the observed distribution of biters for each kinematic trait is centered around a slightly larger value than the optima estimated by Ornstein-Uhlenbeck models (Fig. 2), possibly reflecting compromises required to maintain adequate mobility to produce effective suction or that these species have yet to reach the optimal trait values. We conclude that convergent evolution of reduced cranial mobility during suction feeding may be a consequence of trade-offs that are characteristic of a multifunctional feeding apparatus, providing an example of how specialization for one function may have major consequences for another, within the context of a multifunctional apparatus.

Much of the observed diversity among suction feeders appears to be associated with the different prey that these species normally feed on. Our sample includes piscivores with a large mouth opening and substantial buccal expansion (e.g., Antennarius hispidus, Epinephelus ongus), predators of small fish and elusive invertebrates with a high degree of upper jaw rotation (e.g., Epibulus insidiator, Oxycirrhites typus), and species that crush shelled prey in the pharyngeal jaws but capture them with suction (e.g., Cheilinus trilobatus) (Hiatt and Strasburg 1960; Grobecker and Pietsch 1979; Ormond 1980; Cornic 1987; Myers 1991; Wainwright and Richard 1995; Randall et al. 1997; Craig 2007). The higher rate of kinematic evolution in native suction feeders suggests that changes to kinematic pattern, achieved by varying the amount and relative contribution of different skull motions, are a key part of the

adaptive diversification of this feeding behavior, an insight that is supported by literature pointing to trends between feeding kinematics and trophic ecology (Liem 1978, 1979, 1980; Norton and Brainerd 1993; Norton 1995; Rupp and Hulsey 2014; Longo et al. 2016; Martinez et al. 2018).

Surprisingly, the observed difference in the rate of evolution of feeding kinematics is not associated with a parallel pattern in cranial morphology, as we found that relative to biters, suction feeders have an average of at least 13.50-fold faster kinematic evolution, but biters have 1.62-fold faster rates of evolution of head shape (Fig. 5b). It is possible that the substantial kinematic constraints imposed by a biting feeding mode have spurred evolution of the cranial morphology to meet those requirements. While a more detailed exploration of morphology may reveal greater anatomical diversity in specific structures in suction feeders, this result indicates that kinematic evolution reflects something more than a simple mapping of function onto morphology (Koehl 1997; Wainwright 2007). By extension, the impressive morphological diversity of suction feeding ray-finned fishes may substantially underestimate their kinematic diversity, whereas fishes that rely on biting have less kinematic diversity than would be expected from their morphological variation. This result also suggests that caution is warranted when inferring functional traits from morphology, a key step in many ecomorphological studies (Feilich and López-Fernández 2019).

Our study demonstrates that the effects of multifunctional trade-offs are not restricted to phenotype or functional space occupation, but also affect evolutionary rates in the involved traits and functions. The role of trade-offs in determining the occupation of morphospace have been documented in some taxa. In turtles, interactions of

hydrodynamics, self-righting ability, and mechanical stiffness constrain shell shape, and the trade-offs between these functions can pull species between optima (Polly et al. 2016; Stayton 2019; Polly 2020); in birds, release of trade-offs on the hindlimbs as the forelimbs evolve to be used for flight results in elevated diversity of the hindlimb (Gatesy and Middleton 1997); and in land plants, an adaptive landscape with multiple functional obligations contributing to fitness results in greater morphospace occupation than a landscape with just one function (Niklas 1994). Our results conceptually extend these principles to show that the effects of trade-offs may not be to just move lineages between adaptive peaks but also to increase or decrease the rate at which they traverse functional and phenotypic space.

Multifunctionality is widespread in organismal systems and our study indicates that it can elevate the exposure of these systems to trade-offs, with substantial consequences for the evolutionary dynamics of functional attributes. Nearly all organismal systems are multifunctional in some form, but the fundamental physical principles underlying organismal design provide opportunities to understand the effects of the consequential trade-offs on evolution of those very same systems. A key goal in future work will be to test the generality of how multifunctionality impacts diversification, especially the degree to which variation among taxa in the level of multifunctionality is a major regulator of the pace of functional evolution.

Coauthors. Edward D. Burress, Christopher M. Martinez, Peter C. Wainwright

Chapter Acknowledgements. We thank Maxwell Rupp and Angelly Tovar for assistance with films, and Michael May for his assistance with the MuSSCRat model. Michael Turelli provided valuable feedback on the manuscript. We are grateful to the many past members of the Wainwright Lab who contributed to the videos used in this study. K.A.C. thanks Alexus Roberts and Daniel Rath for their support during this project, and Sarah Friedman for her help with tidy code.

Funding. K.A.C. was supported by the Achievement Rewards for College Scientists Foundation. This research was supported by NSF grants IOS-0444554, IOS-0924489, and DEB-1061981 to P.C.W. and research awards from the Center for Population Biology to K.A.C.

FIGURES & TABLES

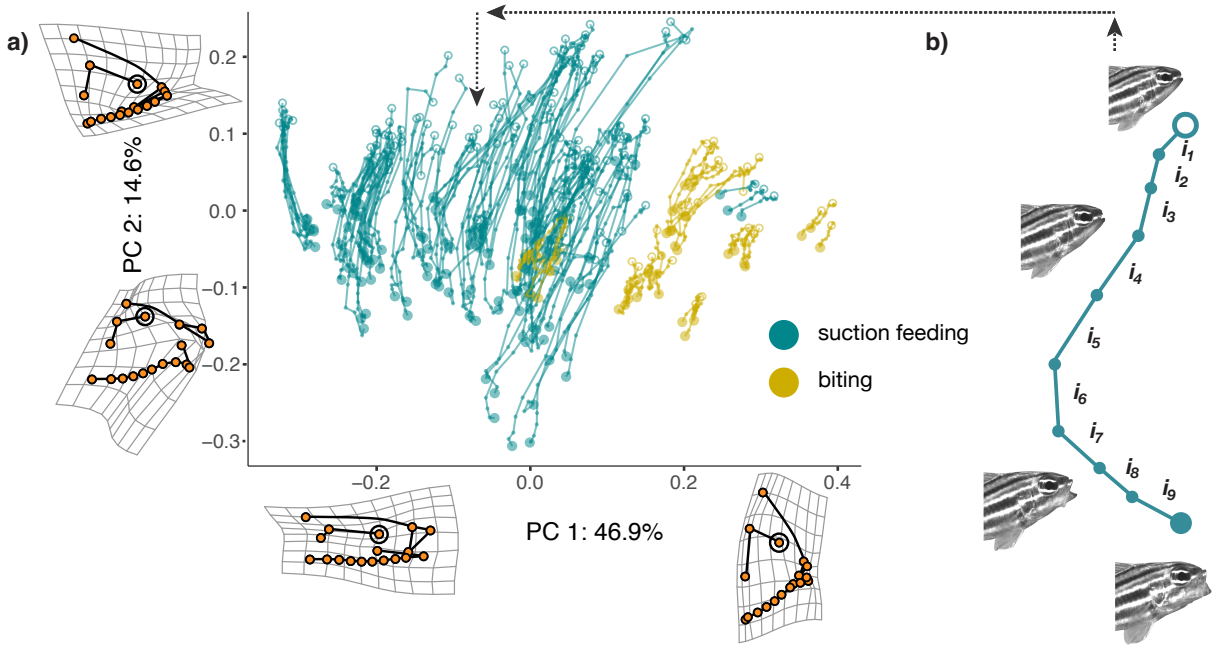

Fig. 1. Comparison of motion trajectories of suction-feeding strikes by fishes that naturally feed with either a biting or suction-based feeding mode. a) 175 feeding sequence motion trajectories displayed on PCs 1 and 2, colored by feeding mode. Individual lines connect frames that are part of a single feeding sequence, and each point along the lines reflects head shape during one of the 10 sampled frames of the video sequence. Larger points at the ends of lines indicate starting postures (i.e., closed mouth, shown as an open point) and maximum gape (closed point), and smaller points represent intermediate motion points. All strikes proceed in a generally downward direction on the plot. Deformation grids indicate landmark positions at minima and maxima for each PC; the position of the eye is circled. The major axis of variation corresponded with head shape diversity (PC1), followed by an axis of shape change largely associated with feeding motions (PC2). b) Mock illustration in the style of sequences shown in a, displaying shape change of a fish head during a single suction feeding event and the resulting shape trajectory.

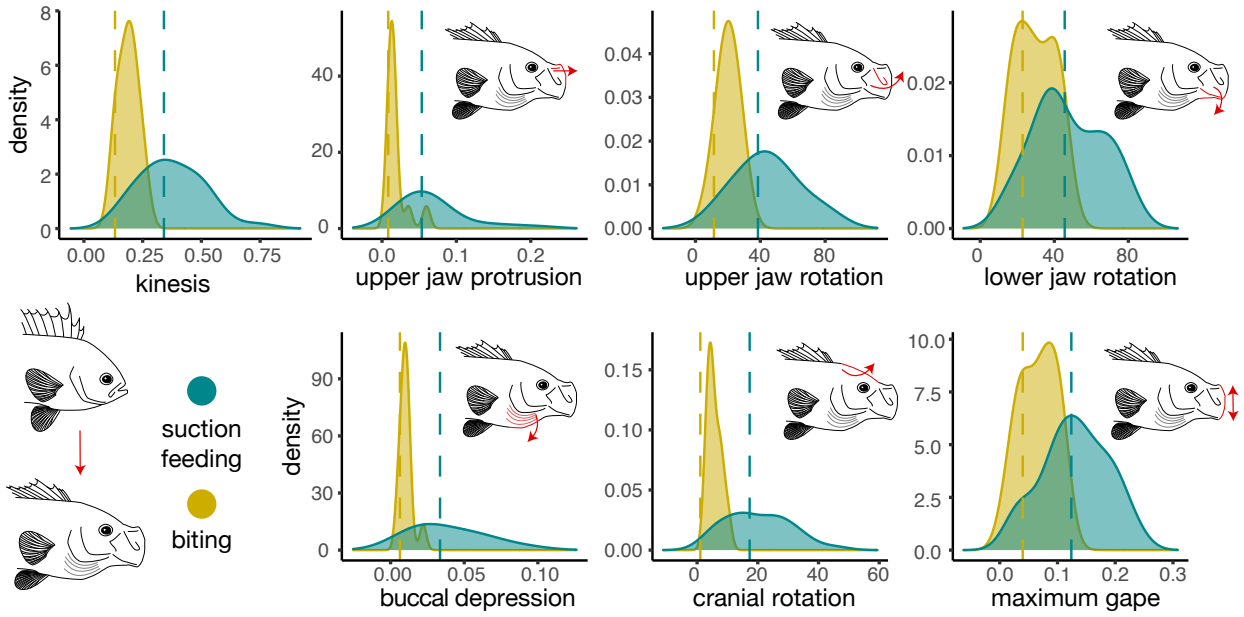

Fig. 2. Major kinematic components in fishes that use suction and biting feeding modes and their evolutionary optima. Density plots depict the maximum value of each measured variable attained during a feeding sequence, averaged by species. Dashed lines indicate the evolutionary optima (theta) estimated by the multi-rate, multi-optima Ornstein-Uhlenbeck model (OUMV), colored by feeding group. Phylogenetic ANOVAs for all kinematic traits were significant at $\alpha = 0.05$, except for lower jaw rotation. In every measured kinematic component and in overall kinesis, biters have both lower values and lower variance among-species, relative to suction feeders. Illustrated on the left are starting and maximum gape postures of *Paranthias furcifer*; illustrated at each panel is the motion measured by that kinematic component. Red lines on the illustrated fish indicate mobile anatomy that has been measured and arrows show the direction of motion.

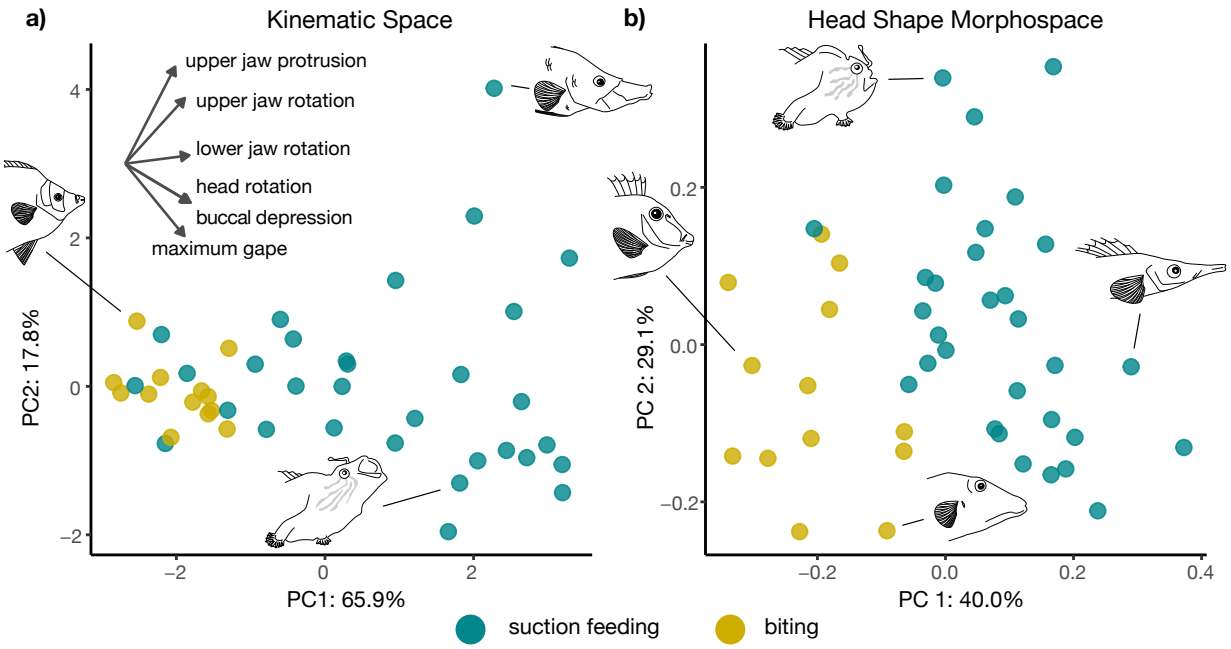

Fig. 3. Distribution of biting and suction feeding fishes in kinematic and morphological space. a) Principal component axes (PCs) 1 and 2 from a PCA of six kinematic components. Points represent species' means. Note that suction feeders occupy much larger ranges than biters on PCs 1 and 2. Vectors in upper left inset represent PC loadings of kinematic components. Illustrated species at maximum gape posture, clockwise, starting from left: *Chaetodon lunula; Epibulus insidiator; Antennarius hispidus*. b) Morphospace of head shapes based on landmark morphometric data. Within the space defined by PCs 1 and 2, the two feeding modes have minimal overlap in shape. Illustrated head shapes (closed mouth posture) of selected species, clockwise, starting from left: *Naso elegans; Antennarius hispidus; Oxycirrhites typus; Canthigaster bennetti*.

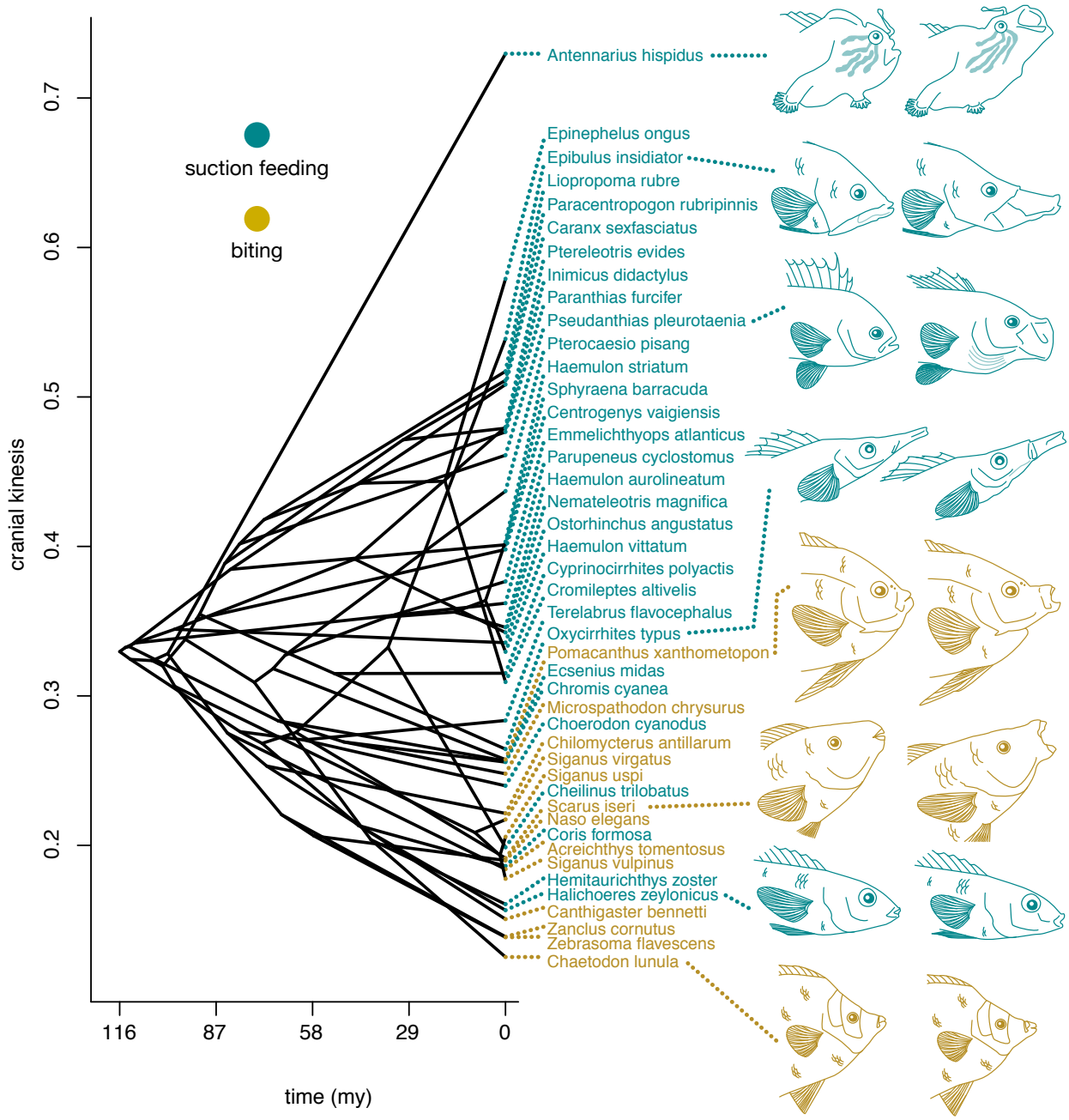

Fig. 4. The evolutionary history of overall cranial kinesis among fishes. The y-axis is total cranial kinesis measured during suction-feeding strikes. Selected species have been drawn in starting and maximum gape postures to illustrate the range of overall cranial kinesis found in our dataset. Illustrated fishes, as well as species names, have been

colored by feeding mode. Internal branches and nodes were estimated using maximum-likelihood with the phenogram function in phytools (Revell 2012).

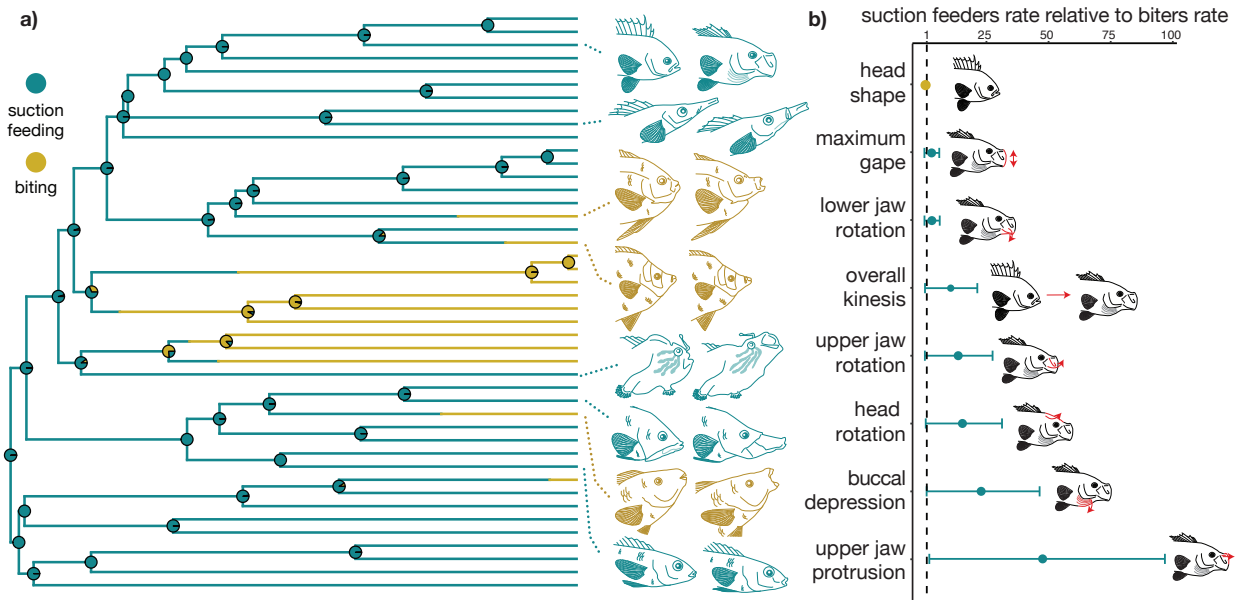

Fig. 5. Results of macroevolutionary models in a Brownian Motion and Ornstein-Uhlenbeck model-fitting framework. a) Sample stochastic character map of feeding mode history, with pie charts at each node indicating the frequencies of each state, across 1,000 stochastic character maps. b) Rate ratios of suction feeding species to biting species for multi-rate, multi-optima Ornstein-Uhlenbeck (OUMV) models for each trait except head shape, where multi-rate Brownian Motion (BMS) estimated the rate. Bars indicate 95% confidence intervals. Blue coloration indicates observations where suction rates are faster than biting rates. Gold coloring indicates that biters have a faster rate. The dashed line, at 1, marks where the rates of evolution of suction feeders and biters are equal.

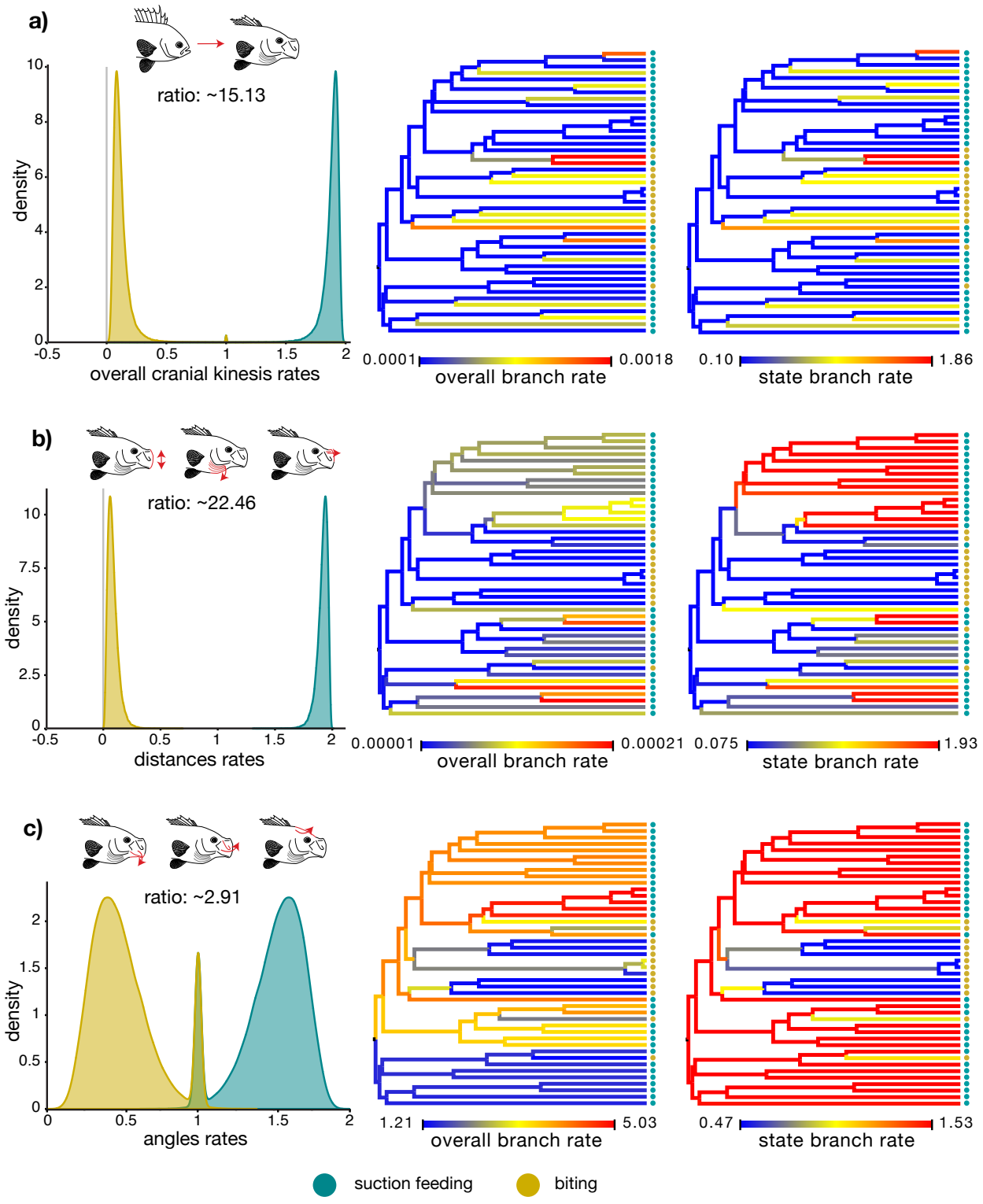

Fig. 6. Results of macroevolutionary model-fitting with a Bayesian, multivariate, state-dependent, relaxed clock model of Brownian Motion across 3 models, showing

substantial support for independent rates for each feeding mode state. Left, the posterior density distributions of the rates for each group colored by feeding mode. Center, overall per-branch rate estimates are mapped onto the phylogeny. Right, rate variation that is attributed to the discrete state are mapped onto the phylogeny. Center and right, on branches warmer colors indicate higher rates and cooler colors, lower rates. To the right of tree tips, circles indicate the feeding mode state for each species. a) Model-fitting on overall cranial kinesis showed strong support for distinct rates between groups, with most of the rate variation explained by the feeding mode state. b) The three distance-based traits showed strong support for distinct rates between groups but a more moderate effect of background rate evolution, seen in the increased disparity between the overall rates and the rate variation attributed to the discrete trait. c) The three angle-based traits, while still strongly supporting two discrete rate classes, show a peak indicating a lower probability of identical rates between groups. Notably, the relationship between branch rate and feeding mode state is very pronounced in angle state-dependent rates, as suction feeders uniformly have higher rate than biters.

Table 1. Best-fitting evolutionary models from Ornstein-Uhlenbeck model fitting.

Trait	Model	AICc	AICc diff.	% best model	σ^2 ratio	Alpha	Θ_{biters}	$\Theta_{suction}$
Maximum gape	OUM	-131.59	0.62	93.3	1.00	0.01	0.03	0.13
	OUMV	-131.87	0.34	97.7	2.99	0.02	0.04	0.12
Head rotation	BMS	316.95	1.78	74.9	6.46	-	-	-
	OUMV	315.37	0.23	96.2	15.35	0.03	1.06	17.31
Buccal depression	BMS	-224.53	0.04	99.5	20.15	-	-	-
	OUMV	-223.31	1.28	95.0	22.73	0.01	0.01	0.03
Kinesis	OUMV	-63.03	0.07	95.8	10.52	0.05	0.13	0.34
Lower jaw rotation	OUM	380.56	1.05	80.8	1.00	0.02	19.34	46.00
	OUMV	379.93	0.50	85.4	3.07	0.06	22.87	45.61
Upper jaw rotation	OUMV	372.25	0.01	99.4	13.62	0.02	11.38	38.54
Upper jaw protrusion	OUMV	-172.82	0.01	97.0	47.40	0.13	0.01	0.05

Notes: We fit single-rate Brownian Motion, “BM1”; multi-rate Brownian Motion, “BMS”; single rate, single optimum Ornstein-Uhlenbeck, “OU1”; multi-optimum, single rate Ornstein-Uhlenbeck, “OUM”, and multi-rate, multi-peak Ornstein-Uhlenbeck, “OUMV”. We display multiple models in the cases where more than one model was considered ‘equally likely’ by AICc. The sum of “total percent best model” for a single trait may exceed 100% in cases where more than one model was consistently identified as best- or equally-well-fitting. ‘σ^2 ratio’ is the ratio of σ^2 estimated in suction feeders relative to biters, under the best fitting model.

CHAPTER 2

THE RISE OF BITING DURING THE CENOZOIC FUELED REEF FISH BODY SHAPE DIVERSIFICATION

INTRODUCTION

Reef habitats are renowned for high biodiversity (Alfaro et al. 2007; Cowman and Bellwood 2011; Brandl and Bellwood 2014; Floeter et al. 2018; Hemingson et al. 2021). Often, this pattern is attributed to the structural complexity of reefs, as complex habitats provide increased opportunity for microhabitat-related adaptations and niche partitioning (MacArthur and MacArthur 1961; Schoener 1974; Price et al. 2015). Among reef fishes, many major drivers of phenotypic and ecological diversity have been recognized at a range of phylogenetic scales (Wainwright and Bellwood 2002; Goatley et al. 2010; Borstein et al. 2019; Gajdzik et al. 2019; Hemingson et al. 2019), but we still lack a clear understanding of the processes and mechanisms that have made reef fish faunas the most diverse in modern oceans.

One striking axis of diversity that distinguishes reef fish communities from those in other marine habitats is the variety of feeding modes used to capture prey. Fishes can employ a direct biting mechanism to remove attached prey from hard substrates or can use suction feeding, which relies on the density and viscosity of an aquatic medium to pull in water and prey via rapid expansion of the head. Suction feeding, which is most effectively used to capture mobile prey (Lauder 1980a, 1980b; Muller et al. 1982; Sanford and Wainwright 2002; Westneat 2006; Van Wassenbergh et al. 2009), is both ancestral for teleost fishes (Lauder 1980c) and well-represented on modern reefs (Mihalitsis and Bellwood 2019). However, direct biting feeding mechanisms characterize many iconic reef fish groups, including parrotfishes, butterflyfishes, surgeonfishes, and triggerfishes. The evolution of biting has allowed fishes to exploit a variety of benthic prey that are firmly attached to reef surfaces and thus resist suction, including molluscs, echinoderms,

cnidarians, sponges, algae, and other primary producers (Motta 1988; Bellwood and Choat 1990; Purcell and Bellwood 1993; Konow et al. 2008; Copus and Gibb 2013; Clements et al. 2017). The ecosystem importance of this functional breakthrough in trophic habits is perhaps best represented by the many benthic biting herbivores and detritivores (Randall 1967; Hobson 1974; Kotrschal 1988; Bellwood et al. 2014b; Clements et al. 2017; Nicholson and Clements 2021) that play a central role in energy transfer through reefs and regulating the composition of benthic communities (Williams and Polunin 2001; Bellwood et al. 2006; Hughes et al. 2007, 2013; Teichert et al. 2020).

Benthic biting has been a major facet of the trophic diversity of reef fishes since at least the Eocene. Herbivores were well established in the Monte Bolca lagerstätte (~ 50 Ma), marking the first evidence that teleosts could graze upon the reef surface and signaling a major shift in reef community functions (Bellwood 2003; Friedman 2010; Bellwood et al. 2014a). These herbivores appear to have risen to dominance within reef ecosystems globally through expansion and colonization following the split of the Tethys Sea and the increased availability of reef flat habitats in the late Cenozoic (Friedman 2010; Bellwood et al. 2017; Siqueira et al. 2019a, 2019b, 2020), though the implications of biting for phenotypic diversification of reef fishes remain unknown (Friedman 2010). Use of a biting feeding mode prior to the Eocene appears to be primarily the domain of non-teleost fishes. As long ago as the Devonian, lungfishes and some arthrodire placoderms captured and crushed hard prey with their jaws (Campbell and Barwick 1990; Anderson 2008, 2009; Long 2011). Several lineages of early-branching ray-finned fishes used biting for prey capture throughout the Mesozoic, including pycnodonts, macrosemiids, and semionotids (Nursall 1996; Tintori 1998; Bellwood 2003; Bellwood

and Hoey 2004); of these, pycnodonts persisted until the Eocene (Nursall 1996). The striking lack of biting teleosts prior to the Eocene (Bellwood 2003) may be due to a 20-million year gap in major deposits of spiny-rayed (Acanthomorph) fishes from the late Campanian (~75 Ma) to the late Paleocene (~55 Ma) (Patterson 1993), during which biting by teleost fishes most likely proliferated to its Eocene prominence. The ambiguity regarding the origins of the expansion of biting among teleosts and its role in morphological diversification presents an opportunity for comparative phylogenetics to provide insight into the history of modern reef fishes.

In this study, we explored the evolutionary history of benthic biting feeding mechanisms in reef fishes and the impact this novelty had on their phenotypic diversification. We compared benthic biting with three other feeding modes: suction feeding, an intermediate group using a mix of both suction and biting, and an uncommon feeding mode we refer to as “ram biting.” To determine how the prevalence of benthic biting has changed through time, we reconstructed the history of feeding modes among reef-dwelling teleosts using stochastic mapping on a time-calibrated phylogeny. We then measured the effect of feeding mode on rates of body shape evolution across a broad sample of 1,530 species of reef fishes spanning 111 families of extant teleosts. If biting feeding modes have been a significant stimulus to the diversification of modern reef fishes, we expect to see differences in body shape occupation of morphospace and phenotypic diversification when comparing biters to fish that employ other feeding modes. Our results provide insight into the evolutionary mechanisms underlying the vast phenotypic and ecological diversity of reef fishes.

MATERIALS & METHODS

Morphological trait data. Body shape data were drawn from a previously published collection of measurements we made from museum specimens of teleost fishes (Price et al. 2019, 2020; Friedman et al. 2020a, 2020b). Wherever possible, species values were computed as averages of measurements from 3 adult specimens. The dataset consisted of 8 linear measurements spanning three dimensions: standard length and jaw length; mouth, body, and caudal peduncle width; and head, body, and caudal peduncle depth. We used the R package 'rFishBase' (Boettiger et al. 2012b) to identify 1,530 species from the larger body shape dataset that were both marine and reef-associated according to FishBase (Froese and Pauly 2018), and extracted these species for use in our analyses. These 1,530 species spanned 486 genera and 111 families, nearly one-quarter of all extant teleost fish families (Dataset S2).

Body shape is a key aspect of morphology that interacts functionally with feeding mode. Though feeding mechanisms have long been linked to evolution of the feeding apparatus, recent research suggests that motions of the body are integral to successful prey capture across feeding mechanisms. Suction-based prey capture is only effective within ~1 mouth diameter of the jaws (Day et al. 2005) and so suction feeders must swim towards their prey; these forward swimming motions are the major axis of variation among suction kinematics (Longo et al. 2016), and muscles of the body power the rapid motions of the cranium that produce suction (Camp et al. 2015). For herbivores and other attached-prey feeders, motions of the body and fins are crucial to prey capture as they can be the dominant cause of the forces that detach prey items from the substrate (Perevolotsky et al. 2020).

We conducted most statistical analyses in the R computing environment v 4.0.2 (87). Measurements were size-corrected using the preferred method from previous comparisons of size correction with this dataset (Price et al. 2019), log shape ratios (Claude 2013; Klingenberg 2016). We created a "size" variable as the geometric mean of standard length, body depth, and body width for each species. Then, we calculated scaled trait values as the ratio of each trait and the new size variable and took the log of those values.

Feeding mode categorizations. We categorized fishes into feeding modes based on the prey that each species feeds on, using a combination of the primary literature, our own field and lab-based observations, and FishBase (Froese and Pauly 2018) (see Dataset S1). We used the functional characteristics of the prey to infer the likely feeding mode required to capture that prey item (further details are provided in Appendix 2).

"Suction feeders" were categorized as species where >90% of the prey were free-swimming or otherwise non-attached (including, but not limited to fishes, many crustaceans, errant polychaetes, and zooplankton). Examples of suction feeders include most grunts (Haemulidae), groupers (Serranidae), and jacks (Carangidae).

A "biter" was a species for whom >50% of the prey require direct contact with the jaws for acquisition, in order to graze, scrape, or dislodge the item from a substrate (e.g., many molluscs, hard and soft corals, sponges, algae, hydroids, bryozoans, detritus, and some echinoderms). Examples of biters include parrotfishes (Scarinae), most angelfishes (Pomacanthidae), most surgeonfishes (Acanthuridae), porcupinefishes (Diodontidae), and most triggerfishes (Balistidae). Not all biters are herbivores, feeding on plant material, or detritivores, feeding on detritus; instead, some benthic biters consume higher

proportions of metazoan prey such as sponges, corals, molluscs, echinoderms, or fish scales. We used data on prey type to describe whether biters were "herbivores/detritivores" or not by categorizing a species as an herbivore/detritivore if 50% or more of its attached prey were plant material and/or detritus.

In classifying feeding modes, we discretized a naturally continuous trait. To accommodate this uncertainty, we added a third category, "mixed biting and suction", for species for which between 10-50% of their prey were attached prey items that require direct biting actions to capture, and the remainder of their diet were prey that would likely be captured using suction. For example, we classified many wrasses (Labridae), most porgies (Sparidae), and some pufferfishes (Tetraodontidae) as "mixed" feeders that rely on both suction and biting.

Our final category was "ram biters", which were categorized as species that use direct biting actions of the jaws but minimal suction to capture evasive or free-swimming prey (Norton 1991, 1995; Norton and Brainerd 1993; Ferry et al. 2015). This feeding mode was only possible to designate in cases where the literature contained information on the mechanism of prey capture, or we had personal observations. Most ram biters are piscivorous, including moray eels (Muraenidae), barracudas (Sphyraenidae), and many lizardfishes (Synodontidae).

Phylogeny of teleost fishes. In order to align the time calibration closely with community consensus of divergence times (Near et al. 2012; Alfaro et al. 2018; Hughes et al. 2018), we calibrated a pruned phylogram of our 1,530 species (Rabosky et al. 2018) by aligning it with a smaller, recent phylogeny based on genomic ultraconserved elements for which divergence times had been estimated with fossils (Alfaro et al. 2018). We used the R

package ‘geiger’ v 2.0.7 (Harmon et al. 2008; Eastman et al. 2013; Pennell et al. 2014) to “congruify” these trees by identifying nodes shared between both trees, and a penalized likelihood program (treePL) to estimate divergence times across the rest of the phylogeny’s nodes using the shared nodes as starting calibrations (Sanderson 2002; Smith and O’Meara 2012; Maurin 2020).

Models of discrete and continuous character variation. To reconstruct the history of feeding modes along the phylogeny, we used ‘phytools’ v 0.7-80 to generate a distribution of 100 stochastic character maps (104, 105; further details in Appendix 2). We generated a distribution of character maps to account for uncertainty in the timing and number of feeding mode transitions throughout the evolutionary history of teleost fishes. While using a distribution allows us to alleviate some uncertainty, the reconstructions are confined to the information in our sampled dataset of 1,530 species. It is possible that biases among unobserved speciation and extinction events may also influence our trait reconstructions.

We used a Principal Component Analysis (PCA) on the correlation matrix of all eight body shape variables to visualize body shape variation in our dataset. We conducted phylogenetic ANOVAs and MANOVA to examine the effect of feeding mode on average body shape in the R package ‘geomorph’ v 3.3.1 (Adams and Otárola-Castillo 2013; Adams et al. 2018).

We used random forest models to understand which body shape traits were most powerful in discriminating between feeding mode groups. Random forest models are a machine-learning method of categorization using decision trees that uses combinations of continuous variables (body shape data) to categorize species by feeding mode group (Breiman 2001). We used cforest in the R package ‘party’ v 1.3-5 (Hothorn et al. 2006,

2015) to fit random forest models using conditional inference trees, which are more robust to interactions between the continuous variables. We trained the model on a subset of 70% of the data (sampled randomly and without replacement) and then fit the model on the remaining 30% of the dataset, generating a distribution of 5,000 decision trees. We estimated the importance of each continuous variable across the distribution of decision trees as the mean decrease in categorization accuracy when that variable is excluded from the analysis (further details in Appendix 2).

We used 'geomorph' to compute multivariate and univariate morphological variance for each of the four feeding mode groups. To further compare morphospace occupation among feeding mode groups, we generated hypervolumes using the R package 'hypervolume' v.3.0.0 (Blonder et al. 2014, 2018) which each contained the 6-dimensional morphospace that a given set of species occupied. We used the first 6 axes of a PCA on the correlation matrix, which together accounted for 98.5% of the variance in the data. Hypervolumes were generated for species in each feeding mode group and for sets of species not in each group (e.g., comparing all "suction feeders" to all species not coded as "suction feeders"). We compared overlap of the hypervolumes in order to estimate how much of the morphospace occupied by each feeding mode group was unique. To assess how similar our comparisons were to random groupings of our data, we simulated a null distribution of hypervolumes by permuting group assignments among our species data and compared the percentile of unique space occupation of our data to the distribution of permuted hypervolumes (more details in Appendix 2).

We used MuSSCRat (implemented in RevBayes v. 1.0.10; Höhna et al. 2016; May and Moore 2019) to compare rates of body shape evolution between feeding mode

groups (O'Meara et al. 2006). MuSSCRat is a Bayesian model of multivariate Brownian motion that estimates the effect of a discrete character (feeding mode) on rates of continuous-character evolution (body shape evolution), while controlling for "background" variation in rates. We used an uncorrelated log-normal clock to place an independent parameter on each branch to model background-rate variation that is not due to the discrete trait of interest (similar to the UCLN relaxed-clock model for molecular evolution; 116). The MCMC ran for 200,000 generations. We used Tracer v 1.7.1 (Rambaut et al. 2018) to verify convergence of the MCMC and the package 'RevGadgets' v 0.1.0 in R to visualize and plot results (Tribble et al. 2021).

RESULTS

Evolutionary history of feeding modes. We classified 1,530 species of reef fishes by feeding mechanism. 335 (22%) were classified as biters; 277 (18%) were mixed suction and biting feeders; 830 (54%) were suction feeders; and 88 (6%) were ram biters (Dataset S1). We also classified biters and mixed feeders by whether they prey primarily upon algae and detritus ("herbivores/detritivores") or take a larger portion of animal material such as sponges, corals, or echinoderms. In total, 58% of dedicated biters were herbivores/detritivores, 17% of "mixed" feeders were herbivores/detritivores, and combined, 39% of biters and mixed feeders were herbivores/detritivores.

We used stochastic character mapping to reconstruct the history of feeding mode over the phylogeny. A distribution of 100 stochastic character maps had a mean of 244.5 transitions between feeding modes across reef-dwelling teleosts, with strongly asymmetrical transitions between states (Fig. 1, and Figs. S1-S2). The mean total time

on the phylogeny spent in each state varied dramatically among feeding mode groups (Table 1).

Stochastic character maps indicated a major transformation since the early Cenozoic in the representation of all three non-suction modes (Fig. 1). Prior to the end-Cretaceous, suction feeding was used by at least 96% of teleost lineages that include species on modern reefs, with the three non-suction modes accounting for only about 2.8% of all branches at the K/Pg boundary. Since that time, the proportion of lineages using biting modes has grown to its peak in the present at 40%. Beginning in the early Cenozoic, a steady rise was observed in the proportion of lineages that use the three non-suction modes of feeding, especially the dedicated attached prey biting category, which clearly accelerated in representation over the past 30 My.

Morphological disparity and occupation of shape space. We explored how feeding mode affects the morphological diversity of reef fishes, estimating three-dimensional body shape with 8 linear measurements of length, depth, and width of the head, body, jaws, and caudal peduncle. When visualizing body shape diversity with a scatterplot of principal components 1 and 2, most species in our dataset were concentrated in an oval-shaped region of morphospace distributed in the upper half of PC1 and across PC2. A low-density spur spanned the majority of PC1, composed of eels and other elongate species, such as pipefishes and needlefishes. Standard length, body depth, and head depth were the major axes of diversity, dominating PC1, which accounted for 43.1% of the total variation, with smaller roles for caudal peduncle depth and width (Fig. 2, Table S1). PC1 defined an axis with elongate, slender bodies with shallow heads on one side and deeper, shorter bodies and deeper heads on the other. PC2, which contained 26.8% of the variation, was

dominated by width and jaw traits: body width, lower jaw length, and mouth width. PCs 3 and 4, which each contained ~10% of the variation in the data, were made up of fish width and caudal peduncle traits; and lower jaw length, caudal peduncle width, and fish width; respectively.

All eight body shape traits differed between feeding mode categories in phylogenetic ANOVAs at $\alpha = 0.05$, and all traits except maximum fish width at $\alpha = 0.01$ (Fig. S3, Table S2). All traits had low explanatory power and small effect sizes, except lower jaw length, where feeding mode explained 6% of the variation in the data. Similarly, in a phylogenetic MANOVA, including all eight body shape traits, there was a significant effect of feeding mode on body shape ($p < 0.0001$), explaining 2.8% of the overall variance in body shape and an effect size of 5.98. Random forest model fitting identified lower jaw length as the most important trait for discriminating between feeding mode groups, with over 3-fold higher importance in correctly categorizing species than any other trait (Table S3). We found a trend among feeding mode groups along a gradient of prey evasiveness, where ram biters had elongate, slender bodies with large jaws, and species using biting had shorter, deeper heads and bodies, with short jaws. Suction feeders typically had intermediate body shapes between ram biters and benthic biters, but with substantial variation.

To analytically compare which feeding mode groups had the most variation in body shape, we used multivariate disparity analyses. Body shape disparity was highest in ram biters, followed by suction feeders, then biters and mixed biting and suction feeders (Table 1). This pattern was generally repeated among univariate disparity analyses with the notable exceptions of maximum body depth and mouth width, where ram biters had

the lowest disparity, and maximum fish width, where there was very little variation between groups (Table S4).

We used hypervolumes to compare the multidimensional morphospace occupation by feeding mode groups. Hypervolumes composed of the first 6 dimensions of a principal components analysis revealed modest differences in the amount of unique shape space occupied by feeding mode groups when each was compared to a group containing all other species. However, no comparisons were more extreme than 95% of a 'null' distribution of hypervolumes randomly generated from our data (Table S5). Notably, 19% of the space occupied by a composite group of all species using any form of attached prey biting, formed by combining the biting group and the mixed biting and suction group, was unique when compared to a group composed of ram biters and suction feeders (Table S5; Fig. S4).

Evolutionary models of body shape diversity. Feeding mode had a strong effect on the multivariate rate of body shape evolution (across all 8 body shape traits; posterior probability of state-dependence = 1.0; Fig. 3). Attached-prey biters evolved traits 1.5-fold faster than species that use mixed suction and biting, 1.7-fold faster than suction feeders, and 1.9-fold faster than ram biters (Table 1). The substantial variation in background rate of body shape evolution uncovered and accounted for in these models is not surprising, given the vast amounts of evolutionary time and taxonomic breadth encompassed by our dataset; Fig. S5, Appendix 2).

DISCUSSION

Our results reveal that the end-Cretaceous mass extinction preceded a sustained growth in the preponderance of teleost reef fish lineages that use biting for prey capture. The timing indicated in our reconstruction suggests that the prominence of herbivorous teleosts in the middle Eocene fossil record (Bellwood 2003; Friedman 2010; Goatley et al. 2010; Bellwood et al. 2014a) resulted from a rapid escalation of biting feeding modes among reef fishes, as the frequency of biting had only begun to increase among teleosts in the previous 15 My. These Eocene fossil teleosts show the shortened lower jaws that characterize benthic biters (Westneat 1994; Wainwright and Bellwood 2002), a novel invasion of functional morphospace specialized for feeding on attached prey (Bellwood 2003). This rise in benthic biting overlaps with the emergence in the Paleogene and Neogene of lineages that are foundational to modern coral reefs, such as scleractinian corals and crustose coralline algae, and which are major substrates for the feeding activities of benthic biting reef fish (Wood 1998; Kiessling 2008). Coupled with these novel functional abilities in marine fishes, the evolution of modern reefs in the early Cenozoic appears to have facilitated a dramatic shift in the distribution of feeding modes used by reef teleosts. We find that the ecological composition of modern reef fish faunas is a relatively recent state and is very different from the historical distribution of feeding modes: the ancestors of modern reef fishes used almost exclusively suction prior to the Cenozoic, but on today's reefs, fully 40% of species use some degree of biting to capture their prey. Furthermore, these benthic feeders are a major driver of reef fish phenotypic diversification as they show substantially elevated rates of body shape evolution when compared to suction feeders despite reduced disparity (Fig. 2, Fig. 3, Table 1). Taken

together, these results suggest that reef biters, which uniquely exploit the flora and fauna that compete for and attach to hard substrates on modern reefs, capitalized on mechanical modifications of the teeth and jaws to diversify around the novel ecological opportunities represented by this resource.

It appears that the expansion of biting in the early Cenozoic took advantage of already-shifting reef communities. Reefs during the early Cretaceous were formed by groups of rudist bivalves, bryozoans, corals, and some algae (Scott 1981, 1988; Wood 1995, 1998), and there is little evidence from the fossil record to suggest that teleosts fed on these substrates (Wood 1998; Bellwood 2003; Bellwood et al. 2014a). However, by the late Cretaceous, a transition was underway to reef structures dominated by grazing-resilient forms of algae and corals that are directly fed on by modern reef fishes and provide substrate for attachment of many other benthic prey (Wood 1995, 1998). The transition to reef structures that succeed despite breakage and excavation, which preceded the expansion of biting in fishes, may have been driven by recently evolved herbivorous urchins and deep-boring limpets (Wood 1998). Thus, ecological shifts towards grazing-resilient structures in response to invertebrate grazers may have made reef conditions increasingly favorable for biters and able to support larger communities of high-efficiency attached prey feeders (Wood 1998), such that when fishes began to use biting and evolved functional features adapted for benthic feeding, like shortened jaws and flexible teeth (Tedman 1980; Bellwood 2003; Bellwood et al. 2014a, 2014b), they were extremely successful and were able to diversify within this broad adaptive zone. This pattern could contribute to the previously observed increase in morphological and species diversification of acanthomorph fishes in the early- to mid-Cenozoic

(Ghezelayagh et al. 2021). A similar ecological mechanism may explain the dramatic rise of dedicated biting in the last 30 My (Fig. 1), where colonization of highly productive reef flat habitats may have offered new opportunities for intense attached prey feeding by fishes (Bellwood et al. 2018); the novelty of reef flats appears to have also stimulated herbivore speciation in this period (Siqueira et al. 2020).

Our results demonstrate that biting feeding mechanisms elevate body shape diversification. While we find that dedicated biters evolve body shape most rapidly, we also observe subtly increased rates of body shape evolution of mixed feeders that use both suction and biting (~1.15x faster than dedicated suction feeders). The pairing of a reduced reliance on biting in “mixed” feeders with a minor rate shift suggests that the magnitude of the role of biting in a fish’s feeding repertoire may correlate with the magnitude of increase in evolutionary rate. While reliance on a biting feeding mechanism is not common in the marine realm outside of reef habitats, our results generalize across 111 families of teleost fishes and extend findings from other studies that a biting lineage, the parrotfishes, has the highest rates of evolution of functional morphological traits (Price et al. 2010; Gajdzik et al. 2019), though this effect is not uniform between and within families, as other ecological factors may affect body shape evolution of species (Fig. 3). However, previous studies have found significant but small effects of major habitat transitions on fish body shape diversification (Friedman et al. 2020a; Martinez et al. 2021) that contrast with the significant and stronger results from our phylogenetic MANOVA, suggesting that feeding mode has a relatively strong influence on body shape and its evolution when compared to the effects of other ecological traits.

Among reef fishes, herbivores have been found to evolve functional traits most rapidly, alongside top predators (Borstein et al. 2019). Our results suggest that this effect extends to all fishes that feed by biting benthic prey, as only 39% of species across both our biting and 'mixed biting and suction feeders' fed specifically on plant material or detritus. Evolution of biting prey capture mechanisms allowed access to a group of novel trophic niches for fishes (Bellwood et al. 2014b) involving a diversity of prey types with distinct functional properties. This group includes several lineages that feed on turfs, leafy algae, detritus, and benthic microbial communities that must be scraped, browsed, or yanked off the substrate (Jones 1968; Perevolotsky et al. 2020); predators of colonial cnidarians that either scrape the coral surfaces (e.g. many butterflyfishes) or bite off pieces of the colony, complete with bits of the skeleton (e.g. some filefishes and pufferfishes); species that scrape encrusted dead coral to feed on the mix of turf algae, detritus and cyanobacteria that resides on and within the skeleton (e.g., parrotfishes) (Bellwood and Choat 1990; Clements et al. 2017; Nicholson and Clements 2021; Pombo-Ayora and Tavera 2021); and even species that grab and extract more mobile invertebrate prey, including urchins and bivalve molluscs, from holdfasts (e.g. some triggerfishes and wrasses). These different prey impose diverse functional requirements on the prey capture apparatus (Huby et al. 2019), providing opportunity for functional and morphological diversification. Reliance on biting for prey capture often results in a highly modified feeding apparatus; indeed, jaw length was the strongest variable in differentiating between feeding mode groups, with biters having shorter jaws on average (Fig. S3). Many biters have evolved substantial novelties that increase access or processing of attached prey such as a pharyngeal mill (Gobalet 1989), an intramandibular

joint within the oral jaws (Konow et al. 2008; Gibb et al. 2015), or elongated teeth, an innovation that improves access to loosely attached algae and detritus (Bellwood et al. 2014b). Such novelties may also promote morphological diversification (Simpson 1944; Schluter 2000; Dornburg et al. 2011; Rabosky 2017; Larouche et al. 2020; Burress and Muñoz 2021).

Biters densely populate a region of shape space characterized by shorter jaws and laterally compressed bodies (Fig. 2), consistent with observations that biters have shortened jaws for improved force transmission during prey capture (Westneat 1994; Bellwood 2003) and predictions that they use a deep body shape for agile maneuvering among the complex reef substrate (Blake 2004). Biting species with the most extreme body shapes in this region lie fully outside the range shown by suction feeding species (Fig. S4). However, the dynamic body shape evolution of attached prey feeders also led to occupation of morphospace that is shared with fishes using other feeding mechanisms, indicating that feeding mode is not a rigid predictor of body shape. The relatively recent proliferation of biting among reef fishes and the elevated rates of biters' body shape evolution suggest that the emergence of biting in the Cenozoic exposed a range of underexploited feeding niches with consequences for both feeding and locomotor functional morphology. We propose that this novel landscape of diverse feeding opportunities, made possible by adept biting, stimulated jaw and body shape evolution.

Our results demonstrate the relative recency of feeding mode diversity among teleost fishes on reefs, dominated by the emergence of the major ecological group of benthic biters that play a prominent role in modern ecosystem processes. We reconstruct the evolution of mechanisms of feeding on attached prey, finding a steady increase in the

proportions of reef fishes using biting throughout the Cenozoic. Coupled with evolutionary model-fitting results showing that biters have elevated rates of morphological diversification, our results suggest that ecological changes surrounding the end-Cretaceous mass extinction event set the stage for the diversification of benthic biters, which uniquely took advantage of new, more grazing-resilient reefs in the Cenozoic. A major role for feeding on attached prey appears to be one key to the spectacular diversity of modern reef fishes.

Coauthors. Sarah T. Friedman, Edward D. Burress, Christopher M. Martinez, Olivier Larouche, Samantha A. Price, Peter C. Wainwright

Chapter Acknowledgments. We thank Michael May for his help implementing the MuSSCRat model and Benjamin Blonder for providing useful insight on the implementation of hypervolumes. We appreciate helpful comments on this manuscript from Michael Turelli and Michael May. The staff and curators at the National Museum of Natural History, particularly Kris Murphy, are gratefully acknowledged for welcoming and supporting us during the collection of these data. We thank the many undergraduates of the Fish Shapes team for their assistance with data collection. Finally, we are grateful to the Wainwright Lab, particularly Alexus Roberts and Jennifer Hodge, for their support and useful discussions throughout the writing of this manuscript.

Funding. This work was supported by the National Science Foundation grant no. DEB-1556953 to S.A.P & P.C.W. K.A.C. was supported by an American Dissertation Fellowship from the American Association of University Women, the Achievement

Rewards for College Scientists Foundation, and the Center for Population Biology at University of California, Davis.

FIGURES & TABLES

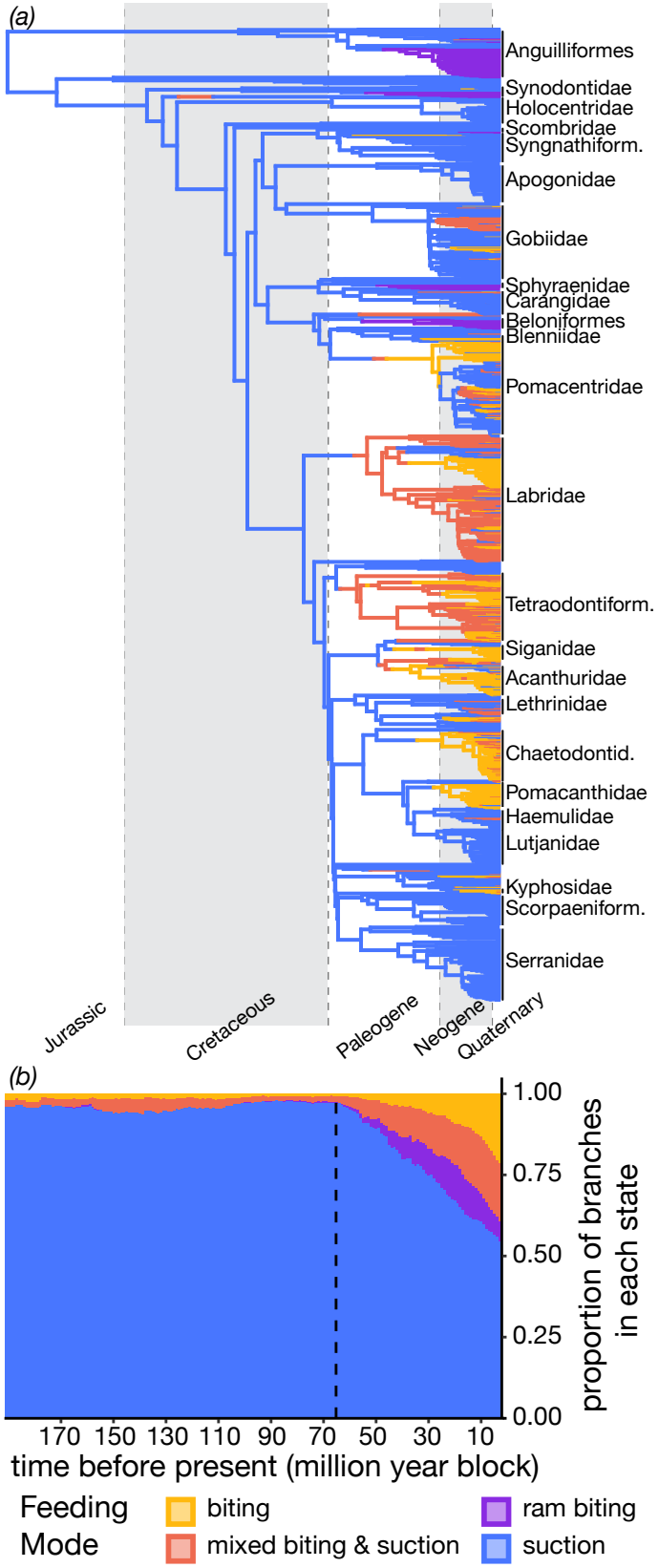

Fig. 1. a) An ancestral state reconstruction of feeding mode using stochastic character mapping in reef-dwelling teleost fishes. Branches are colored by feeding mode, with selected major lineages labeled to the right. Background bars (white and grey) indicate geologic time period. b) A barplot showing the proportion of branches at million-year intervals in each feeding mode state, averaged across 100 stochastic character maps. Proportion of branches in each feeding mode is on the y-axis, with bars along the x-axis at million-year intervals starting 192 million years ago (left) and progressing rightwards towards the present. Dashed line indicates the time of the end-Cretaceous mass extinction event 66 million years ago. Note the dramatic increase of biting and mixed feeding modes following the mass extinction event.

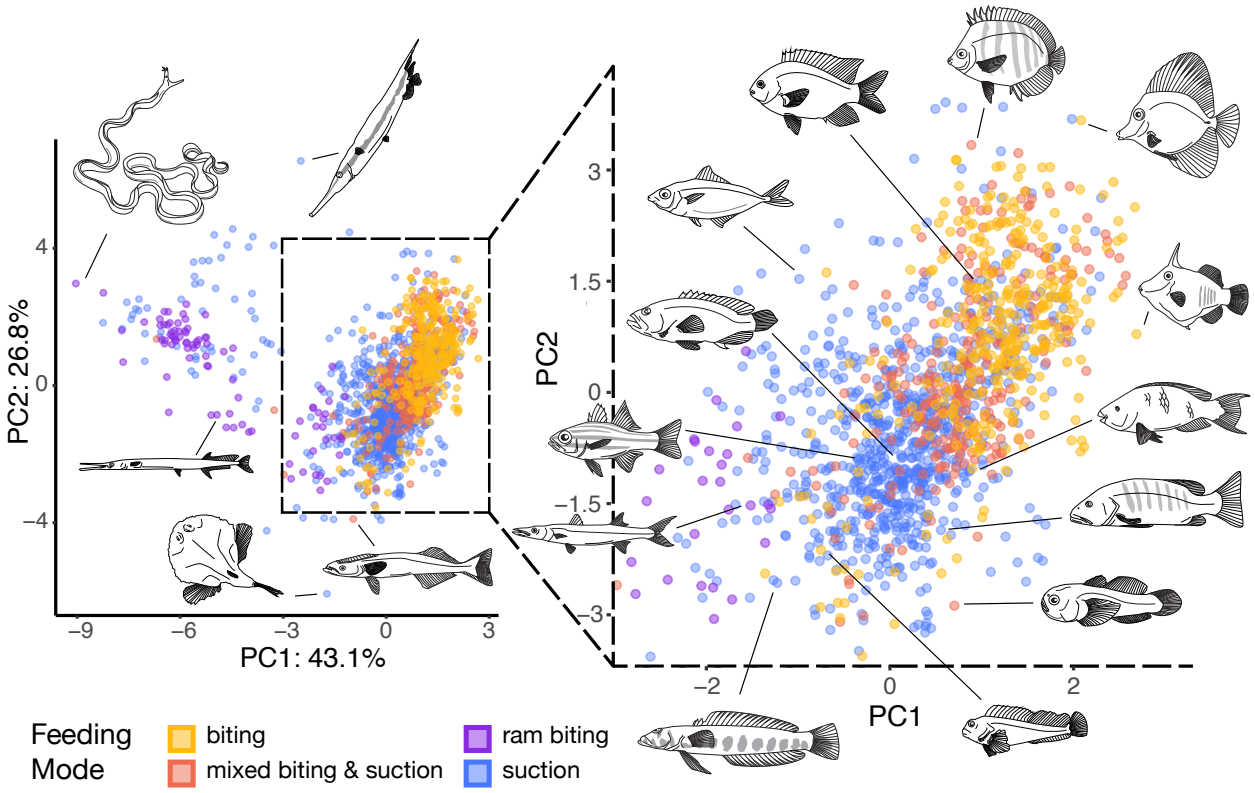

Fig. 2. A plot of 1,530 reef fish species on Principal Components 1 and 2 based on eight body shape traits, with an inset on the right of a high-density region. Points represent species averages, and each species is colored by feeding mode. Several fishes are drawn to illustrate shapes of fishes at different regions of morphospace. Main plot (left), clockwise from with upper right: *Aeoliscus strigatus, Remora remora, Halieutichthys aculeatus, Tylosaurus acus, Rhinomuraena quaesita*. Inset (right), starting with upper right: *Zebrasoma scopas, Amanses scopas, Scarus guacamaia, Lutjanus cyanopterus, Paragobiodon modestus, Hypsoblennius hentz, Parapercis millepunctata, Sphyraena jello, Ostorhinchus holotaenia, Cephalopholis cruentata, Equulites stercorarius, Stegastes obreptus, Chaetodon multicinctus*. Fish images drawn by K. Corn.

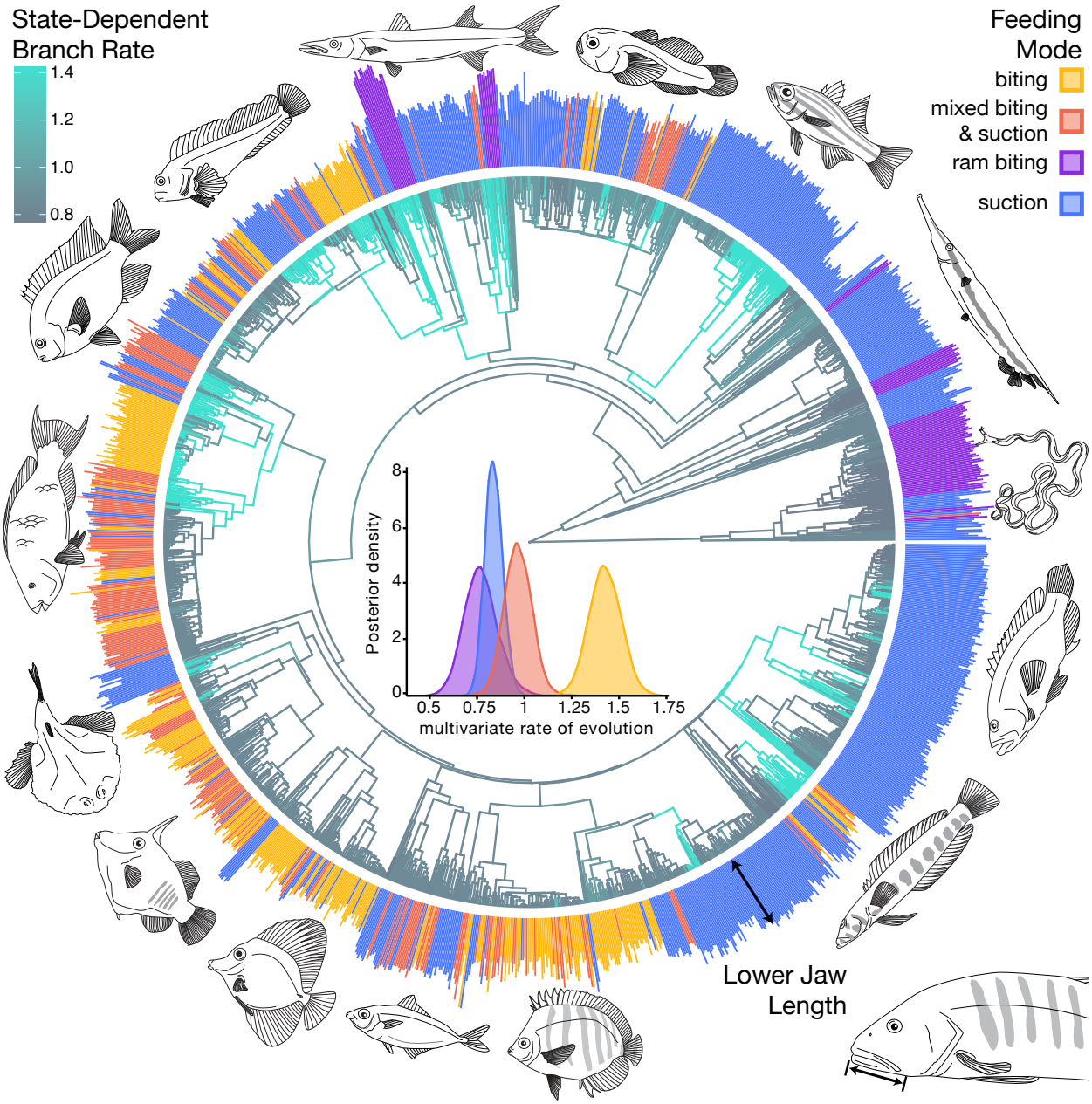

Fig. 3. Results from model-fitting for rate of body shape evolution. Center, distribution of multivariate, state-dependent rates, colored by feeding mode. Branch colors on the phylogeny indicate per-branch state-dependent rates of evolution, with grey indicating a lower rate and teal indicating a higher rate. Outer ring, bars are colored by feeding mode, and length of bars represents lower jaw length. Selected fishes have been drawn and placed near their clade on the phylogeny; clockwise from inset at bottom right: *Lutjanus*

cyanopterus (inset)*, Chaetodon multicinctus, Equulites stercorarius, Zebrasoma scopas, Amanses scopas, Halieutichthys aculeatus, Scarus guacamaia, Stegastes obreptus, Hypsoblennius hentz, Sphyraena jello, Paragobiodon modestus, Ostorhinchus holotaenia, Aeoliscus strigatus, Rhinomuraena quaesita, Cephalopholis cruentata, Parapercis millepunctata*. Fish images drawn by K. Corn.

Table 1. Comparison of results of multivariate disparity, stochastic character mapping, and evolutionary rate analyses among feeding mode groups.

Feeding group	Disparity[1]	Time on tree[2]	Rate[3]
Biting	0.103	12.1%	1.426
Mixed suction & biting	0.121	14.4%	0.966
Ram biting	0.324	7.4%	0.77
Suction	0.189	66.0%	0.838

[1]Disparity represents multivariate disparity across all eight body shape traits.
[2]Time on tree represents the proportion of the total branch length on the phylogeny reconstructed to be in each state using stochastic character mapping, averaged across 100 reconstructions.
[3]Rates are calculated as the state-dependent rate of multivariate evolution, which excludes background evolution on each branch.

CHAPTER 3

FASTER BODY SHAPE EVOLUTION AT THE EDGES OF FISH MORPHOSPACE

INTRODUCTION

Extreme or exaggerated morphologies, such as the elongated horn of the rhinoceros beetle, are iconic examples of the unusual or bizarre spaces to which evolution can take species. Often, these morphologies are a consequence of a mismatch in morphological scaling, where the extreme trait changes size at a different rate than the rest of the body (Emlen and Nijhout 2000; Emlen et al. 2012; Shingleton and Frankino 2013). Typical animals with 'extreme morphologies' have scaled just a single aspect of morphology to an exaggerated form, and the rest of their body has a common shape that is not very disparate from their relatives or their form without such a structure (Emlen 2001). Many examples of extreme morphologies are driven by sexual selection, frequently as honest signals of health and fitness, and thus are present in just a single sex (Darwin 1871; Emlen 2001; Irschick et al. 2007). But some taxa have evolved extreme body shapes, where the extreme form is not just an exaggerated feature alongside an otherwise proportionately scaled body but is the shape of the entire body.

Defining an extreme body shape is non-trivial, as it requires comprehensive knowledge of the distribution of body shapes within that clade. The recently developed morphospace of teleost fishes provides an opportunity to do so, and shows that nearly all teleost species lie in a single, dense oval in shape space (Price et al. 2019, Fig. 1). This oval, or "ridge," encompasses considerable body form diversity, ranging from deep-bodied, laterally compressed fishes like butterflyfishes to nearly cylindrical bodies like many catfishes. Just ~10% of fish species lie outside this oval-shaped region of shape space, including fishes with some of the most striking shapes and life histories. These species have substantially altered the classic body form along many different axes of

morphology; for example, goosefishes are strongly dorsoventrally compressed; snipe eels are extremely thin and elongate, with bodies as much as 161 times as long as they are deep; and batfishes are short and deep, with bodies that are deeper than they are long. The mechanisms underlying the evolution of these extreme shapes are not clear. There are abundant links between morphology and ecology ("ecomorphology"; Wainwright and Reilly 1994), such as the relationship between body shape and swimming mechanism (Webb 1984; Dornburg et al. 2011; Di Santo et al. 2021) or body shape and prey capture mechanism (e.g., Cooper and Westneat 2009; McCord and Westneat 2016). The apparent pervasiveness of these links in the literature makes it puzzling how fish lineages would evolve body shapes so disparate from a ridge in morphospace that contains a wide range of shapes with strong functional associations with the lifestyles that fishes typically have. Yet it is possible that novel ecological and functional opportunities available to fishes with extremely different forms facilitates more dynamic evolution of body shapes at the extremes of morphospace.

In this study, we explored the evolution of extreme body shapes among the largest vertebrate radiation, teleost fishes. We used the largest available dataset of three-dimensional body shape to estimate extremeness of fish shapes for 5,940 species from 392 families of teleosts. After reconstructing the history of body shape evolution, we estimated the average fish shape, then integrated these morphological data with ecological data for the species in our dataset. We measured whether position in morphospace (as the difference from the average shape) affects the rate of evolution of body shapes, and whether ecological traits spanning habitat, migration, and trophic status promoted the evolution of extreme morphologies. If extreme body shapes represent a

departure from body shapes that are well suited for the lifestyles that most fishes live, we expect body shape evolution to be faster among fishes with common shapes. However, if there is novel ecological opportunity available to fishes with extreme forms, we expect evolution to be more dynamic at the extremes of morphospace.

MATERIALS & METHODS

Phylogeny. We used the largest available time-calibrated phylogeny of ray-finned fishes to accommodate the effect of shared ancestry between species (Rabosky et al. 2018). We pruned the phylogeny to the 5,940 species in our morphological dataset using the package *ape* v 5.6-2 (Paradis et al. 2004) in the statistical programming environment R v 4.1.3 (R Core Team 2022). We used base R in conjunction with the *tidyverse* data handling framework to manage data (Wickham et al. 2019); and *ggplot2* v 3.3.5 and *cowplot* v 1.1.1 for data visualization (Wickham 2016; Wilke 2021).

Body shape data. We used a previously published dataset of body shapes for 5,940 extant species of teleost fishes spanning 392 families (Price et al. 2019, 2020). These data comprise eight linear measurements capturing body shape in three dimensions: standard body and jaw length; head, body, and caudal peduncle depth; and body, jaw, and caudal peduncle width. Species values were calculated as the average of three adult specimens wherever possible. We used log shape ratios for each species to scale measurements by size among species (Claude 2013; Klingenberg 2016), which was the favored method of size correction in a previous study on this dataset (Price et al. 2019).

We visualized the distribution of fishes in morphospace using a Principal

Components Analysis (PCA) on the covariance matrix of all 5,940 extant species using the *stats* package v 4.1.3. To understand the history of body shapes in this space, we projected ancestral shapes for nodes into the morphospace of extant species by reconstructing ancestral states for each PC axis using Brownian Motion in the R package *phytools* v 1.0-1 (Revell 2012). These reconstructions did not incorporate correlations between dimensions, as ancestral states for species along each PC axis were reconstructed independently.

We estimated the 8-dimensional centroid of extant fish shapes as the weighted average of species' shapes, computed by taking the mean of each of the 8 PC axes. This centroid can be thought of as the mean fish shape, weighted by the relative contribution of each aspect of morphology to the variation among species. As a metric of extremeness, we measured the distance of each point from the centroid in 8 dimensions; a greater distance from the centroid indicates a more extreme shape, and a species with a smaller distance from the centroid has a shape closer to the average (or a "more common shape"). Using the distances of each node and tip from the centroid, we estimated the length of each branch on the phylogenetic tree in 8 dimensions of morphospace and whether the branch was traveling towards the centroid (ending node/tip closer to the centroid than starting node) or away from the centroid (starting node closer to the centroid than ending node/tip).

Evolutionary rates. We estimated rates of evolution in two ways. First, we computed point estimates of rates at each internal node using phylogenetic independent contrasts in *ape* v 5.6-2 (Felsenstein 1985; Paradis et al. 2004). We computed contrasts separately for each morphological trait, then averaged the 8 contrasts for each node to get a mean

estimate of evolutionary rate across all traits at that node. We refer to these as “rates” or “contrasts.” Second, we manually estimated rates of evolution through morphospace for each branch as the ratio of the length of the branch in 8 dimensions of PC space and the length of the branch in millions of years. We refer to these as “branch rates” or “per-branch rates” of evolution.

We chose to focus our rate measurements on estimates of Brownian rate, rather than use Ornstein-Uhlenbeck (OU) models, a common alternative (O’Meara 2012; Huey et al. 2019). Our rationale for this choice was two-fold; first, given the inherent multidimensionality of our data (e.g., shape in 8 dimensions), the univariate nature of most implementations of OU models would miss out on a large portion of the diversity among the species in our dataset. For example, seahorses and pipefishes occupy a region of shape space characterized by extreme elongation, a small jaw, and a moderately sized caudal peduncle; these species would be indistinguishable from either other elongate species, like eels, or other small-jawed and moderate-caudal peduncled species, like butterflyfishes, were we to use a univariate metric of body shape; thus missing out on what appears to be a nearly unique radiation into a novel region of morphospace. Second, most OU model-fitting frameworks are best suited to recovering a small number of peaks (Boettiger et al. 2012a). Given the incredible taxonomic and ecological diversity among our data, we feel that the few peaks we would be likely to recover would be a gross oversimplification of the complexity of body shape evolution among fishes and would be misleading with regards to the true patterns of diversification among body shapes.

Ecological traits. We used the package *rfishbase* v 4.0.0 (Boettiger et al. 2012b) to access ecological data about the species in our dataset. We downloaded information

about food items (at the lowest level of resolution, I); migration status, which we re-coded as a binary trait ("migratory" or "non-migratory"); depth habitat, which we re-coded as a discrete trait with 3 states ("epipelagic", "mesopelagic", and "bathy-/abyssopelagic") following Martinez et al. (2021); reef habitation, which we estimated as a composite trait from the fishbase categorizations for 'DemersPelag', reef flats, and reefs; intertidal habitation, which we estimated as a binary trait compositely from the fishbase categorizations for the intertidal, littoral zone, and tidepools; cave habitation, which we estimated as a binary trait compositely from the fishbase categorizations for 'Cave', 'Caves', 'CaveAnchialine', and 'Cave2'; as well as habitation of streams, lakes, mangroves, estuaries, and swamps/marshes. We also downloaded information about trophic level as a continuous trait using the fishbase categorization for trophic level based on food items.

Linear model fitting. We fit ordinary least squares models in the *stats* package to compare the relationship between variables. We estimated the effect of distance from the centroid on contrasts (a rate-by-state test); and we estimated the effect of the distance of the starting node of a given branch on its branch rate; and the total length of the branch in 8 dimensions of PC space. We fit an ANOVA to determine whether the directionality of branches with regards to the centroid affected the rate of evolution. Branch rates, distance from centroid of nodes and tips, and length of the branch in 8 dimensions of PC space were log10-transformed for statistical analyses to fit the assumption of normality among continuous variables.

We used phylogenetic least squares (PGLS) models to estimate the relationships between traits and species' distances from the centroid while incorporating the effects of

shared evolutionary history, fit in *geomorph* (Adams and Otárola-Castillo 2013).

We used a series of PGLS models described below to estimate the effects of various ecological traits on the distance from the centroid of each species. Significance for each PGLS model was estimated by permuting the data across the tips of the phylogeny 10,000 times. We fit separate models with four types of ecological data, for which we had data for varying numbers of species.

1. "Salinity" model, measuring the effect of marine-freshwater habitation, for which we had data for 5749 species.
2. "Migration" model, measuring the effect of migratory status, for which we had data for 1,493 species.
3. "Trophic" model, measuring the effect of continuous trophic level, for which we had data for 3,253 species.
4. "Food" model, measuring the effect of discrete food categories used as prey ("FoodI"), for which we had data for 3,324 species.
5. "Habitat" model, comparing the effect of depth zone, reef habitation, intertidal habitation, streams habitation, cave habitation, mangroves habitation, swamp/marsh habitation, lake habitation, and estuary habitation; for which we had data for 2,591 species. For this model, we used backwards stepwise regression using p-values to identify the combination of habitat traits with the most meaningful effect on the distance from centroid of each species.

Stochastic character mapping. We reconstructed the history of "extremeness" among fish lineages using stochastic character maps implemented in *phytools* (Huelsenbeck et al. 2003; Bollback 2006; Revell 2012). "Extremeness" was discretized by labeling the top

10% of fishes when ranked by decreasing distance from the centroid as “extreme” fishes, and all others as “not extreme.” We generated a distribution of 100 stochastic character maps to account for uncertainty in our reconstructions, and estimated the ratio of transitions to and from extreme shapes.

In order to determine whether our stochastic character maps represented a pattern that was meaningfully different than a Brownian Motion process on our tree, we generated a “null” distribution by simulating 100 datasets under Brownian Motion. For each dataset, we simulated 8 independent traits under a constant rate for 5,940 species using the phylogeny of our species in *phytools*, then rotated the dataset in a PCA and computed both the centroid of points in all 8 dimensions of PC space and the distance of each simulated species from the centroid in 8 dimensions of PC space. We then characterized “extremeness” in the dataset using the same criteria as for our true data and reconstructed the history of extremeness in each simulated dataset using a distribution of 100 stochastic character maps. We took the ratio of transition rates between extreme body forms and non-extreme body forms for the averages for each of the distribution of 100 null datasets and compared it to our true data (see Appendix 3 for more details).

RESULTS

Body shapes of fishes. Principal components analysis of our data largely agree with previous analyses of fishes (Claverie and Wainwright 2014; Price et al. 2019); with major axes of shape variation among species being body length, width, and depth (Table S1). Over 90% of all species in the dataset were concentrated in a ‘ridge’ along PC2, with an

extended, less dense ‘spur’ of species spanning PC1 (Fig. 1, Fig 2a). PC1, which contained 43% of the variation among species, was dominated by standard length, body depth, and caudal peduncle depth and width; with elongate, slender species with small caudal peduncles high on this axis. In contrast, PC2 contained 23% of the variation among species and represented an axis of both body and jaw width, jaw length, and body depth; with longer and wider jawed and shallower-bodied fishes high on this axis, while laterally compressed, deep-bodied fishes with small jaws appeared low on this axis.

The centroid of all fishes lay in the middle of the dense cluster of fishes along PC2, shifted slightly towards the edge of the cluster higher along PC1 (Fig. 2a). The closest species to the centroid in our dataset, and therefore the closest fish to the “average” body shape of fishes, was *Malacoctenus triangulatus*, the saddled blenny. The distribution of fishes when ordered by distance from the centroid was similar to their positioning on PCs 1-2, but did not match perfectly due to variation in positioning on PCs 3-8. Distance from the centroid was not concentrated along the phylogeny, but instead was relatively dispersed (Fig. 2b).

Reconstructed ancestral shapes. Ancestral states, or estimated states of nodes, reflected the general distribution of extant species, which is expected when reconstructing ancestral states with Brownian motion (Martins and Hansen 1997; Polly 2001).

Linear model fitting. Ordinary least squares models found that shapes farther from the centroid have higher rates of body shape evolution (Table 1, Fig. 2c). Nodes had higher standardized phylogenetic independent contrasts with increased distance from the centroid. Branches that began farther from the centroid traversed more morphological space, and had higher branch rates, than branches that started close to the centroid. We

found that branches traveling away from the centroid had slightly higher branch rates than those traveling towards the centroid, suggesting that elevated rates of evolution at the extremes of morphospace are not due to rapid "pull" of shapes back towards the centroid (Table 1, Fig. 2d). We also found that species farther from the centroid spent more of their path history traveling away from the centroid than species closer to the centroid (Table 1).

Ecology. We found a range of habitat traits that were disproportionately represented in the extremes of morphospace (Fig. 4; Tables 2, S3). Among habitat traits, habitation of the deep sea, caves, and reefs had significant effects on the distance from centroid of species. Other habitats, such as swamps/marshes, and lakes had few to no fishes with extreme forms, though there was some presence of species with extreme shapes in estuaries, the intertidal zone, and mangroves.

In contrast, though not statistically significant, migration appeared to be under-represented among fishes with extreme shapes. A gradient of high to low trophic level (where low values indicate a position lower in the food chain and increased reliance on herbivory or detritivory) better described the range of fishes within the oval of common shapes (Fig. 4) than the diversity of extreme fishes, but was statistically significant across all data (Table 2). Likewise, food group had a significant effect on distance from centroid (Table 2). Fishes with extreme forms appeared under-represented outside of the ocean, though not statistically so (Table 2).

Stochastic character mapping. We recovered an average of 176 transitions between "extreme shapes" and "non-extreme" shapes across the distribution of 100 stochastic character maps (Fig. 3a). Transitions were highly asymmetric, with an average of 140

transitions from non-extreme shapes to extreme body shapes, and 37 transitions from extreme shapes to non-extreme shapes; lineages were 3.8-fold more likely to transition from being non-extreme to being extreme than from extreme shapes back to non-extreme shapes.

This asymmetry was reflected in the transition rates recovered for data simulated using Brownian Motion on our phylogeny, but with a far higher number of transitions in both directions recovered from the simulations (Fig. 3c,d, Fig. S1). Across 100 simulated datasets and 100 stochastic character maps for each dataset, there was an average of 309 transitions between states, a 1.75-fold increase over our data. Simulated data had an average of 230 transitions from non-extreme shapes to extreme body shapes, and 79 transitions from extreme shapes to non-extreme shapes; a 2.98-fold higher chance of evolving an extreme shape from a non-extreme shape than the reverse. In total, our measured data had fewer transitions between states than 100% of the simulated datasets; fewer transitions from extreme states to non-extreme states by nearly half than the fewest among the distribution of simulated data (36.8 transitions in our data to 49.5 transitions in the simulated dataset with the fewest transitions in this direction); and fewer transitions from non-extreme states to extreme states than all but 4% of the simulated data sets.

DISCUSSION

Our results reveal that the position of fish in morphospace has a substantial effect on the tempo and mode of body shape evolution. The acceleration of rates of body shape

evolution with increasing distance from the average shape suggests that the evolution of extreme shapes involves the release of constraints that limit typical fish shapes. These constraints may be biomechanical, ecological, or developmental. Shifts in any or a combination of these realms could promote extreme morphologies, via mechanisms like extreme trait values as a consequence of increased integration among traits (Claverie and Patek 2013; Goswami et al. 2014; Klingenberg 2014), or axial elongation due to mutations to *Hox* genes (Krumlauf 1994; Burke et al. 1995; Woltering et al. 2009; Di-Poï et al. 2010). Our data suggest that the evolution of an extreme shape is likely due to changes in these or other mechanisms that are difficult to achieve. Though most fishes have body shapes that are highly effective for the things that fishes typically do, many fishes with extreme body shapes may have invaded novel adaptive zones, such as challenging hydrodynamic environments with functional or ecological pressures that promoted the evolution of extreme morphologies. The evolution of extreme body shapes in fishes appears to be largely a consequence of major disruptions in the evolutionary and developmental mechanisms promoting body shape evolution.

The transformations in body shape required to achieve an extreme shape appear to be relatively rare, as extreme body shapes were evolved just half as often as predicted by simulated Brownian evolution; we recover just ~140 transitions to extreme shapes across 5,940 species (Fig. 3). Such major changes in body shapes may be successful only in specific ecological or evolutionary conditions despite being highly successful in those scenarios (Wainwright & Price 2016). Evidence based on the time scale of evolution of phenotypic disparity suggests that disparity accumulates in burst-like shifts in adaptive zone on the scale of millions of years (Simpson 1944; Estes and Arnold 2007; Uyeda et

al. 2011), perhaps due to the rarity of matches between morphological innovations and novel adaptive zones that allow their success. The fishes in our data may be examples of successful matches between evolving an innovative body shape and a large-scale shift in adaptive zone that allows it to flourish, and the rarity we observe may be an indicator of the uncommon nature of such a successful opportunity. It appears that transitions to extreme body shapes are not just a consequence of random evolution, but instead may represent rare transitions in adaptive zone that result in dramatic increases in disparity.

Such novel adaptive zones appear to include major changes to the lifestyles of most extreme fishes. Groups of fishes that are strongly represented in extreme regions of shape space include goosefishes (Lophiidae), which lie on the seafloor and ambush prey with exceptionally wide mouths (Steimle et al. 1999); flatfishes (Pleuronectiformes), which perform much the same strategy for prey capture, but have moved both eyes to the same side of the head to more effectively lie on their sides and bury in the sand (Gibson 2005); seahorses, pipefishes, and their relatives (Syngnathiformes), which have a diverse range of novel habitat and locomotory strategies, including swimming vertically in the water column or hanging onto substrate via a prehensile tail (Gill 1905; Aronson 1983; Foster and Vincent 2004); and the amazingly diverse deep sea fishes, which have modified their caudal region dramatically, likely to suit constant but low-intensity swimming with a less muscularized body (Pelster 1997). Such strange and unusual life histories are a marked contrast to the lifestyles of most fishes that have common shapes.

Ecological correlates of extreme shapes

Habitats with novel hydrodynamic conditions in the ocean may provide conditions that stimulate the rapid diversification of extreme morphologies into novel adaptive zones.

Overall, we found that extreme shapes were over-represented in habitats that impose difficult hydrodynamic or ecological conditions upon their inhabitants, such as the deep sea, reefs, and caves (Table 2, Fig. 4, Fig. S2). Some of these zones are characterized by intense interaction with the substrate, consistent with past analysis of marine fishes demonstrating that substrate-association promotes morphological diversification, perhaps as a release from the functional requirements of swimming (Friedman et al. 2020a). Indeed, the most swimming-intensive ecological trait in our dataset, migration, appears to be under-associated with extreme forms (Fig. 4E, Fig. S2), though not statistically significantly so (Table 2). The reduced frequency of migration among extreme fishes suggests that the migration to spawn among Anguillid eels, some of which migrate from Europe or North America to the Sargasso Sea to mate, is truly remarkable.

Though the deep sea and reef habitats have been recognized as a source of body shape diversification (Price et al. 2011, 2013; Gilbert et al. 2021; Martinez et al. 2021, but see Frédérich et al. 2016; Evans et al. 2019b), our results suggest that caves have been historically overlooked as sources of extreme morphological disparity. The deep sea may promote the evolution of slow, physiologically efficient swimming modes performed well by body forms that we recover as highly extreme, such as extreme elongation and a small caudal peduncle (Martinez et al. 2021). Caves are known for convergently producing unusual or bizarre morphologies, such as absent or reduced eyes or pelvic girdles capable of tetrapod-like ‘walking’ (Wilkens et al. 1989; Flammang et al. 2016; Hart et al. 2020; Crawford et al. 2022), and this pattern appears to extend to extremeness of body shapes that can be evolved by cave fishes. Reefs are often recovered as a source of morphological diversification, and we find that reef habitation both promotes the evolution

of extreme forms as well as diversity among non-extreme shapes (Fig. 4B). Some common shapes that are evolved by reef fishes may vary based on prey type. Most morphologically extreme fishes typically feed, likely using suction, on the other fish and nekton that are common prey for most fishes. But, feeding on attached prey and reef habitation are each often associated with morphological modifications for deep, narrow body shapes specialized for maneuvering around complex substrates (Webb 1984; Larouche et al. 2020), and laterally compressed shapes appear to be common enough to be part of the range of typical body shapes in fishes despite being fairly different from the average fish shape. Differentiation in trophic status towards feeding on attached prey such as plants occurs primarily within the ridge of common shapes; a similar pattern is clear when trophic level is measured as a continuous trait (Figs. 4D, S2).

Potential mechanisms underlying the diversification of extreme shapes

Shifts in the regulation or structure of *Hox* genes are a compelling mechanism for the evolution of novel body plans in fishes. Variation in *Hox* expression throughout the body is strongly associated with body plan regionalization across animals (Krumlauf 1994; Burke et al. 1995; Averof and Patel 1997; Martin et al. 2016). Some extreme fishes in our dataset have evidence of a role for variation in body regionalization in becoming extreme, as different groups of eels elongate different regions of their body (Mehta et al. 2010; Ward and Mehta 2014). There is some evidence for a direct link between flexibility of the suite of *Hox* genes and the evolution of extreme forms in fishes, as fully duplicated set of *Hox* genes, likely retained from the genome duplication at the base of the teleost radiation, may provide the genetic blueprint for the whole-body morphological transformation some eel larvae undergo that results in extreme elongation (Henkel et al. 2012a, 2012b).

However, it is unlikely that alterations to body plan patterning in the genome are the sole mechanism underlying the evolution of extreme shapes. Though genomic correlations are highly effective at creating suites of morphologies that evolve together, adequate natural selection can pull apart even closely linked traits (Beldade et al. 2002).

An alternative mechanism that could contribute to accelerated evolution of body shapes in regions of extreme shape space is shifting in modularity among regions of the body. An increase in the number of modules can provide more opportunities for diversification by reducing the potential trade-offs that could arise from evolving traits together; and changes in modularity are known to elevate morphological evolution in fishes (Larouche et al. 2018; Evans et al. 2019a). The variation in degree of elongation among regions of the body in eels (Mehta et al. 2010; Ward and Mehta 2014) suggests that increased modularity has allowed elevated diversification of elongate body shapes. Or, decreases in the number of modules by integrating traits can drag morphologies to extreme forms, sometimes via selection on just one of those traits (Goswami et al. 2014). We see this pattern in other regions of extreme morphospace, where an increase in integration among skull traits has driven the rapid evolution of flatfishes (Evans et al. 2021), suggesting that differences in patterns of changes in integration and modularity among parts of the body may allow access to different extreme shapes.

Conclusions

Taken together, our data suggest that the evolution of extreme shapes is a result of rapid evolution following relatively rare invasions of extreme shape space. This rapid evolution is associated with some hydrodynamically challenging environments, which may facilitate uncommon matches between innovative life histories or morphologies and the

environments in which they can succeed. Fishes evolving extreme morphologies may be doing so via release of the constraints that typically limit body shapes, perhaps due to shifts in the genetics of body plan patterning or to changes to the modules among fishes. Rather than being an evolutionary sink, departing from the range of typical fish body shapes may simply be an alternate path to success in novel environments.

Coauthors. Sarah T. Friedman, Samantha A. Price, Peter C. Wainwright

Chapter Acknowledgements. We are grateful to the many members of the Fish Shapes team who helped us collect data at the National Museum of Natural History, and to the museum staff, particularly Kris Murphy, for their support of our team. We appreciate thought-provoking discussions with Artyom Kopp, and helpful statistical suggestions from Ed Burress and Rachel Crawford. Finally, we are grateful to the Wainwright Lab for their support and helpful conversations.

Funding. This work was supported by the National Science Foundation grant no. DEB-1556953 to S.A.P & P.C.W. K.A.C. was supported by an American Dissertation Fellowship from the American Association of University Women, a fellowship from the Achievement Rewards for College Scientists Foundation, and the Center for Population Biology at University of California, Davis.

FIGURES & TABLES

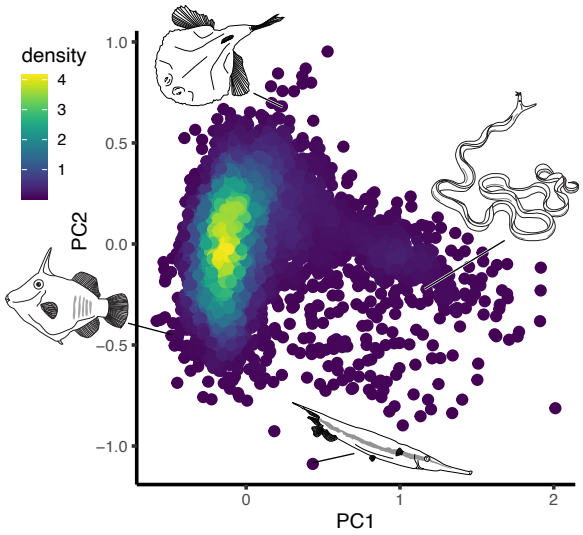

Fig. 1. Scatterplot of 5,940 extant species, rotated in a Principal Components Analysis of 8 morphological traits. Every point represents a species, and points have been colored by the local density of points surrounding it. Selected fishes have been highlighted to show the range of shapes in different regions of the PCA. Clockwise from top: *Halieutichthys aculeatus, Rhinomuraena quaesita, Aeoliscus strigatus, Amanses scopas.*

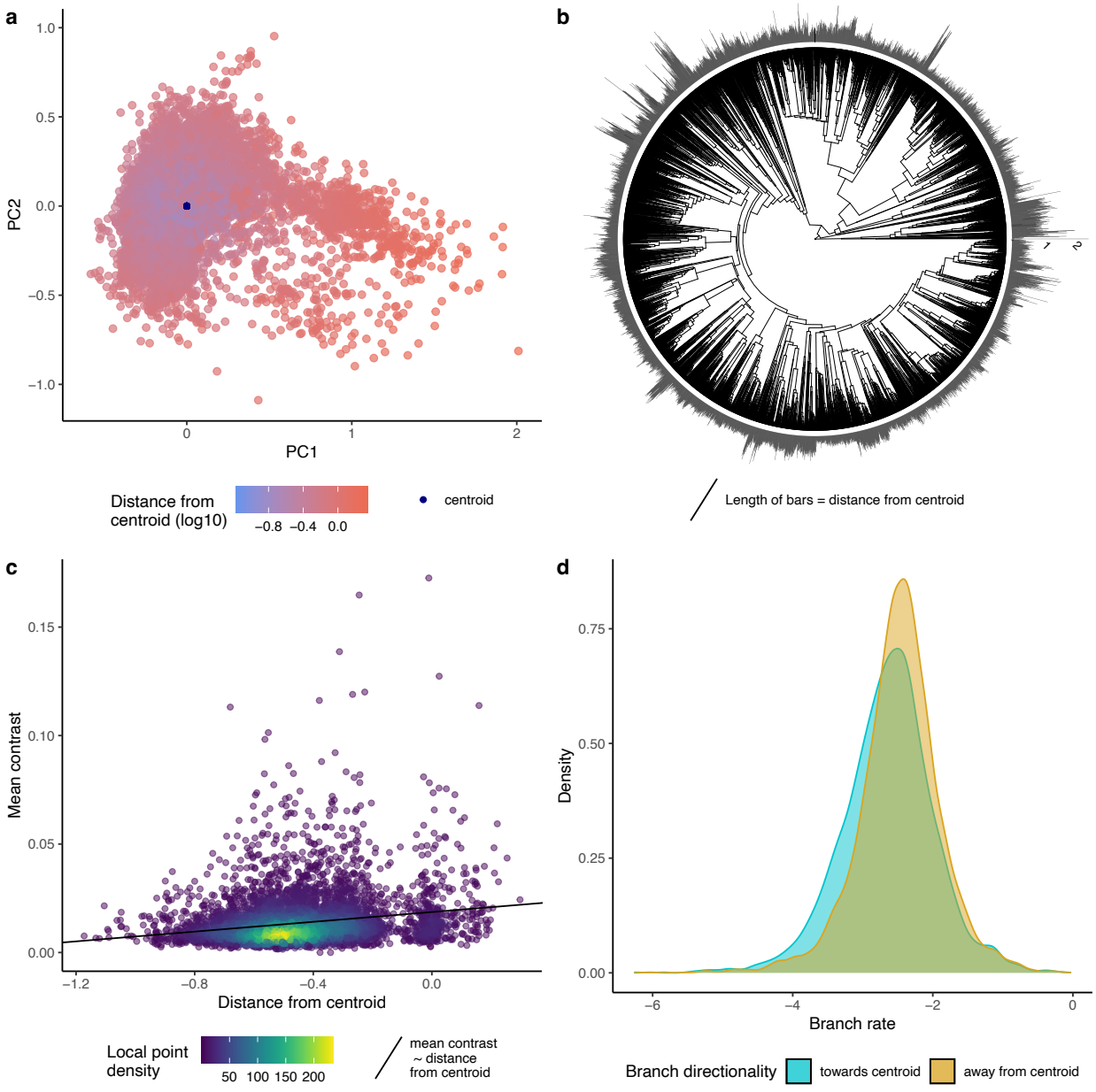

Fig. 2. a) Principal components analysis of 5,940 extant species, colored by the distance of each point from the centroid in 8 dimensions. Centroid is in navy. b) Phylogeny of all 5,940 species, with bars representing the distance in morphospace of each species from the centroid. c) Distance from centroid of each node, plotted against mean trait contrast. Each point represents a node. Points are colored by local point density on this plot. d)

Distribution of branch directionality demonstrating that branches traveling away from the average shape (the centroid) have higher rates than those traveling towards the centroid.

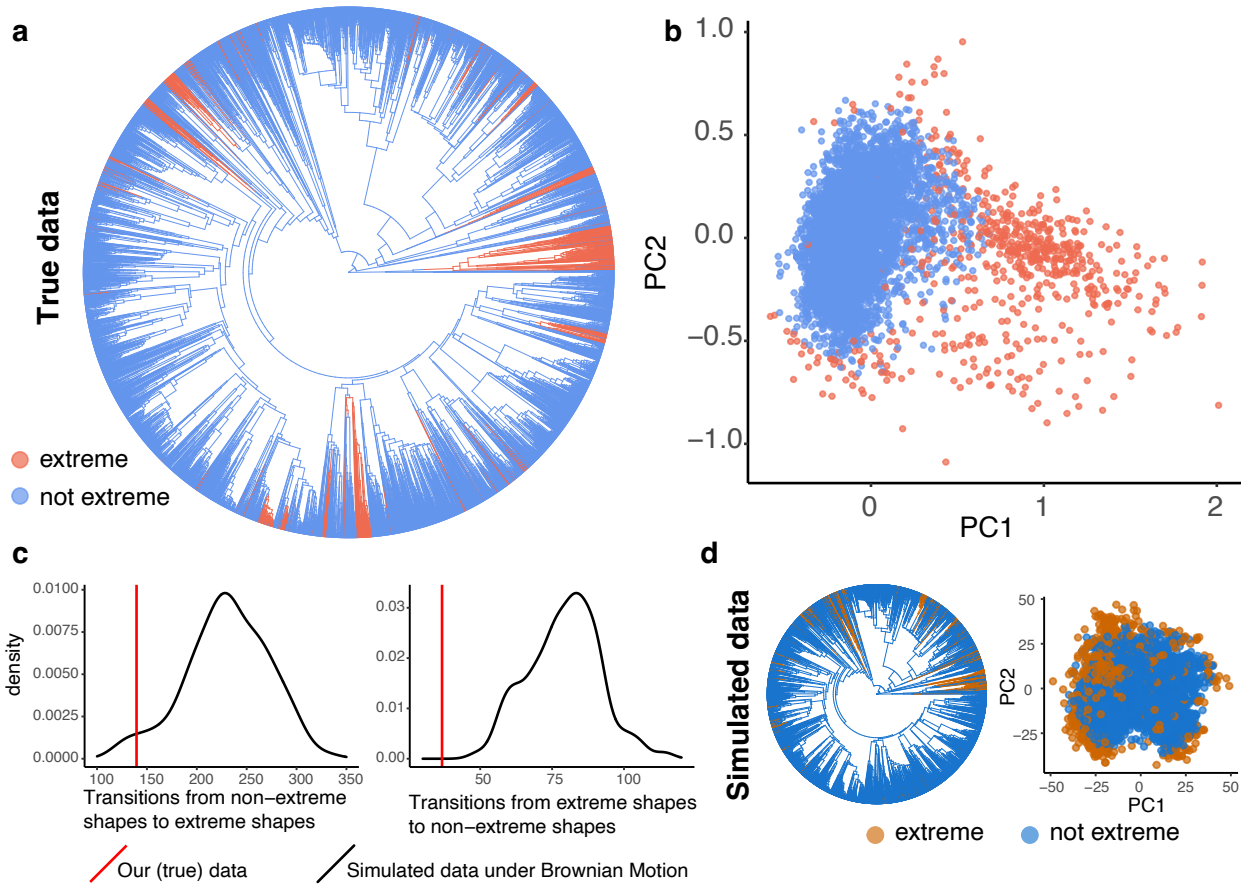

Fig. 3. Data and selected results from simulated character histories. a) A sample stochastic character map generated from our true data demonstrating a reconstruction of "extremeness" among lineages. b) PCs 1 and 2 of fishes coded as "extreme" using this metric, where the top 10% of fishes when ranked by decreasing distance from the centroid (in 8 dimensions) were labeled "extreme." c) Comparisons of average numbers of transitions between states between our true data and the distribution of simulated datasets. d) A sample stochastic character map and PCA displaying a dataset generated under Brownian Motion. Notably, the shape of the data is very different than in our true PCA, and the "extreme" taxa are much more evenly distributed across the PCA.

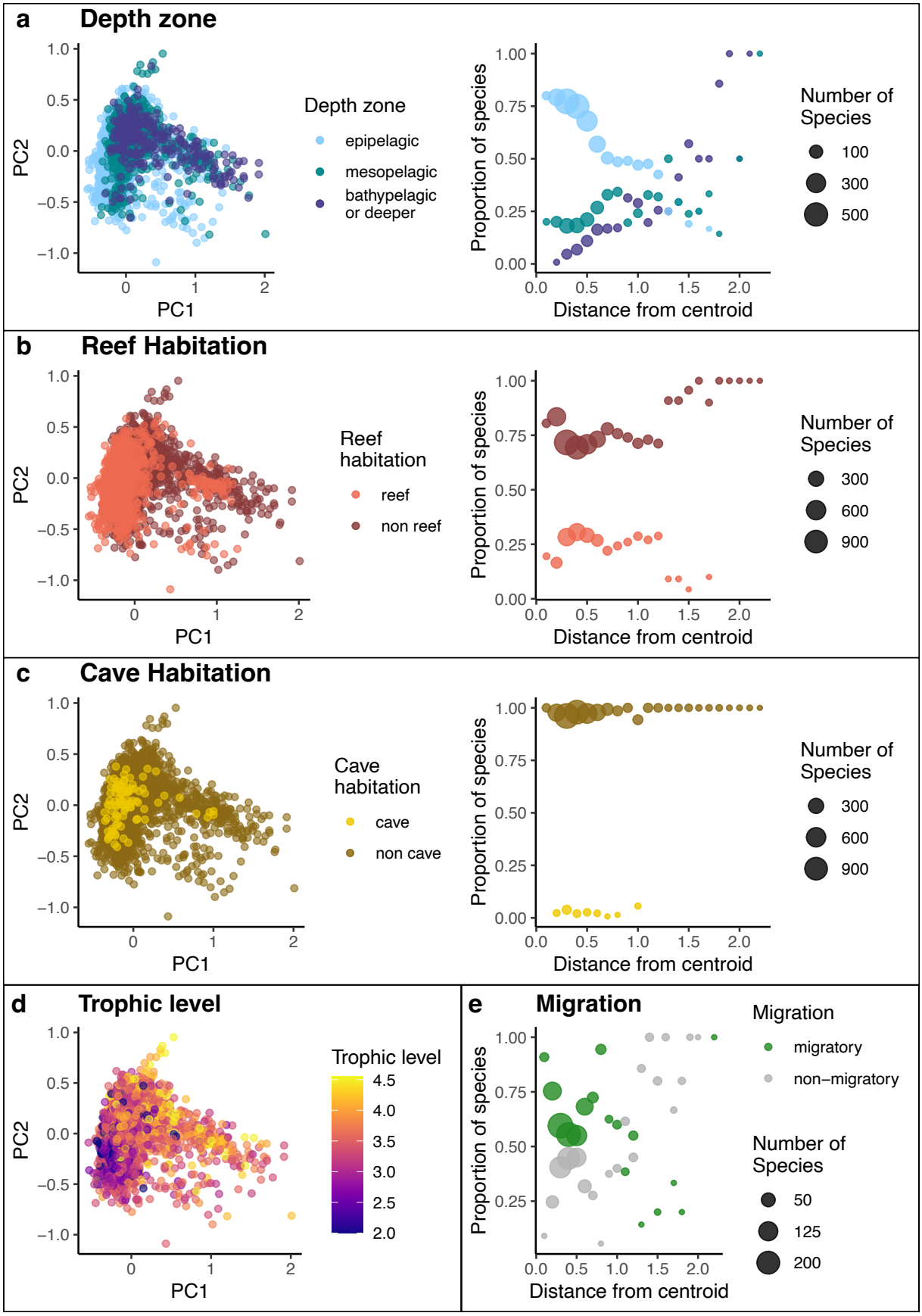
a
Depth zone
PC2
PC1
Depth zone
epipelagic
mesopelagic
bathypelagic or deeper
Proportion of species
Distance from centroid
Number of Species
100
300
500
b
Reef Habitation
Reef habitation
reef
non reef
300
600
900
c
Cave Habitation
Cave habitation
cave
non cave
300
600
900
d
Trophic level
Trophic level
4.5
4.0
3.5
3.0
2.5
2.0
e
Migration
migratory
non−migratory
50
125
200

Fig. 4. Distribution of selected ecological traits among species; all three statistically significant habitat traits, trophic level, and migration status. Left column, distribution in principal components space of species in various ecological groups, with points colored by ecological grouping. Right, plots of the proportion of species in different trophic groups by distance from centroid. Distance from centroid was split into 22 equally sized bins, and the proportion of bins in each ecological category was calculated. Points represent the proportion of bins in a given ecological state in each 'distance from centroid' bin, with the size of the point representing the total number of species in that state in the bin. a) Variation in phenotype due to depth zone. Notably, though the total number of species is much lower with increasing distance from the centroid, nearly all species that are farthest from the centroid are in mesopelagic or bathypelagic zones. b) Approximately a quarter of fishes with moderately extreme shapes inhabit reefs, suggesting that reefs encourage both diversity among common shapes but also promote extreme shapes. c) Cave fishes are over-represented in extreme regions of shape space. d) Trophic level best distinguishes variation among body shapes along the ridge of common shapes. e) Though not statistically significant, there is a substantial visually obvious decrease in the frequency of migration far from the centroid.

Table 1. Results of ordinary least squares model fitting.

Regression	Intercept	Slope	d.f.	Adj. R-sq	p-value
Mean trait contrast ~ Distance of node from centroid	0.019	0.011	1, 5937	0.039	< 2.2e-16
Branch rate ~ Branch directionality to or from the centroid	-2.48	-0.16	1, 11876	0.014	< 2.2e-16
Branch rate ~ Distance of the start of the branch from the centroid	-2.29	0.53	1, 11876	0.030	< 2.2e-16
Length of PC space traversed by branch ~ Distance of the start of the branch from the centroid	-1.50	0.48	1, 11876	0.022	< 2.2e-16

Table 2. Results of phylogenetic least squares model fitting.

Regression	d.f.	Adj. R-sq	p-value	Z-score
Distance from centroid ~ Trophic level	1, 3251	0.01338	9.999e-05	4.3197
Distance from centroid ~ Food (categorical)	1, 3318	0.00565	0.008299	2.47
Distance from centroid ~ Marine habitation	1, 5746	0.00004	0.8956	-1.2516
Distance from centroid ~ Migration	1, 1491	0.00001	0.8985	- 1.3386
Distance from centroid ~	Total: 2590			
Depth zone	2	0.01276	9.999e-05	4.1946
+ Reef habitation	1	0.00257	0.0121	2.1128
+ Cave habitation	1	0.00214	0.0199	1.9433

LITERATURE CITED

Adams D.C. 2014. Quantifying and comparing phylogenetic evolutionary rates for shape and other high-dimensional phenotypic data. Syst. Biol. 63:166–177.

Adams D.C., Collyer M.L. 2018. Multivariate Phylogenetic Comparative Methods: Evaluations, Comparisons, and Recommendations. Syst. Biol. 67:14–31.

Adams D.C., Collyer M.L. 2019. Phylogenetic Comparative Methods and the Evolution of Multivariate Phenotypes. Annu. Rev. Ecol. Evol. Syst. 50:405–425.

Adams D.C., Collyer M.L., Kaliontzopoulou A. 2018. Geomorph: Software for geometric morphometric analyses.

Adams D.C., Otárola-Castillo E. 2013. Geomorph: An r package for the collection and analysis of geometric morphometric shape data. Methods Ecol. Evol. 4:393–399.

Alfaro M.E., Faircloth B.C., Harrington R.C., Sorenson L., Friedman M.A., Thacker C.E., Oliveros C.H., Černý D., Near T.J. 2018. Explosive diversification of marine fishes at the Cretaceous-Palaeogene boundary. Nat. Ecol. Evol. 2:688–696.

Alfaro M.E., Santini F., Brock C.D. 2007. Do reefs drive diversification in marine teleosts? Evidence from the pufferfish and their allies (Order Tetraodontiformes). Evolution. 61:2104–2126.

Anderson P.S.L. 2008. Shape variation between arthrodire morphotypes indicates possible feeding niches. J. Vertebr. Paleontol. 28:961–969.

Anderson P.S.L. 2009. Biomechanics, functional patterns, and disparity in Late Devonian arthrodires. Paleobiology. 35:321–342.

Anker G.C. 1974. Morphology and kinetics of the head of the stickleback, Gasterosteus aculeatus. Trans. Zool. Soc. London. 32:311–416.

Aronson R.B. 1983. Foraging Behavior of the West Atlantic Trumpetfish, Aulostomus Maculatus: Use of Large, Herbivorous Reef Fishes as Camouflage. Bull. Mar. Sci. - Miami-. 33:7.

Averof M., Patel N.H. 1997. Crustacean appendage evolution associated with changes in Hox gene expression. Nature. 388:682–686.

Beaulieu J.M., Jhwueng D.C., Boettiger C., O'Meara B.C. 2012. Modeling stabilizing selection: Expanding the Ornstein-Uhlenbeck model of adaptive evolution. Evolution. 66:2369–2383.

Beldade P., Koops K., Brakefield P.M. 2002. Developmental constraints versus flexibility in morphological evolution. Nature. 416:844–847.

Bellwood D.R. 2003. Origins and escalation of herbivory in fishes: a functional perspective. Paleobiology. 29:71–83.

Bellwood D.R., Choat J.H. 1990. A functional analysis of grazing in parrotfishes (family Scaridae): the ecological implications. Environ. Biol. Fishes. 28:189–214.

Bellwood D.R., Goatley C.H.R., Bellwood O. 2017. The evolution of fishes and corals on reefs: Form, function and interdependence. Biol. Rev. 92:878–901.

Bellwood D.R., Goatley C.H.R., Brandl S.J., Bellwood O. 2014a. Fifty million years of herbivory on coral reefs: fossils, fish and functional innovations. Proc. R. Soc. B Biol. Sci. 281:20133046.

Bellwood D.R., Hoey A.S. 2004. Feeding in Mesozoic fishes: a functional perspective. Mesozoic fishes 3.:639–649.

Bellwood D.R., Hoey A.S., Bellwood O., Goatley C.H.R. 2014b. Evolution of long-toothed fishes and the changing nature of fish–benthos interactions on coral reefs. Nat. Commun. 5:1–6.

Bellwood D.R., Hughes T.P., Hoey A.S. 2006. Sleeping functional group drives coral-reef recovery. Curr. Biol. 16:2434–2439.

Bellwood D.R., Tebbett S.B., Bellwood O., Mihalitsis M., Morais R.A., Streit R.P., Fulton C.J. 2018. The role of the reef flat in coral reef trophodynamics: Past, present, and future. Ecol. Evol. 8:4108–4119.

Bemis W.E., Lauder G. V. 1986. Morphology and function of the feeding apparatus of the lungfish, Lepidosiren paradoxa (Dipnoi). J. Morphol. 187:81–108.

Bennett A.F., Lenski R.E. 2007. An experimental test of evolutionary trade-offs during temperature adaptation. Proc. Natl. Acad. Sci. 104:8649–8654.

Bishop K.L., Wainwright P.C., Holzman R.A. 2008. Anterior-to-posterior wave of buccal expansion in suction feeding fishes is critical for optimizing fluid flow velocity profile. J. R. Soc. Interface. 5:1309–16.

Blake R.W. 2004. Fish functional design and swimming performance. J. Fish Biol. 65:1193–1222.

Blonder B., Lamanna C., Violle C., Enquist B.J. 2014. The n-dimensional hypervolume. Glob. Ecol. Biogeogr. 23:595–609.

Blonder B., Morrow C.B., Maitner B., Harris D.J., Lamanna C., Violle C., Enquist B.J., Kerkhoff A.J. 2018. New approaches for delineating n-dimensional hypervolumes. Methods Ecol. Evol. 9:305–319.

Boettiger C., Coop G., Ralph P. 2012a. Is your phylogeny informative? Evolution. 66:2240–2251.

Boettiger C., Temple Lang D., Wainwright P.C. 2012b. rfishbase: Exploring, manipulating and visualizing FishBase data from R. J. Fish Biol. 81:2030–2039.

Bollback J.P. 2006. SIMMAP: Stochastic character mapping of discrete traits on phylogenies. BMC Bioinformatics. 7.

Borstein S.R., Fordyce J.A., O'Meara B.C., Wainwright P.C., McGee M.D. 2019. Reef fish functional traits evolve fastest at trophic extremes. Nat. Ecol. Evol. 3:191–199.

Brandl S., Bellwood D.R. 2014. Pair--formation in coral reef fishes: An ecological perspective. Oceanogr. Mar. Biol. 52:1–80.

Breiman L. 2001. Random forests. Mach. Learn. 45:5–32.

Burke A.C., Nelson C.E., Morgan B.A., Tabin C. 1995. Hox genes and the evolution of vertebrate axial morphology. Development. 121:333–346.

Burress E.D., Muñoz M.M. 2021. Ecological Opportunity from Innovation, not Islands, Drove the Anole Lizard Adaptive Radiation. Syst. Biol. 71:93–104.

Camp A.L., Roberts T.J., Brainerd E.L. 2015. Swimming muscles power suction feeding in largemouth bass. Proc. Natl. Acad. Sci. 112:8690–8695.

Campbell K.S.W., Barwick R.E. 1990. Paleozoic dipnoan phylogeny: Functional complexes and evolution without parsimony. Paleobiology. 16:143–169.

Claude J. 2013. Log-shape ratios, Procrustes superimposition, elliptic Fourier analysis: Three worked examples in R. Hystrix. 24.

Claverie T., Patek S.N. 2013. Modularity and rates of evolutionary change in a power-amplified prey capture system. Evolution. 67:3191–3207.

Claverie T., Wainwright P.C. 2014. A Morphospace for Reef Fishes: Elongation Is the Dominant Axis of Body Shape Evolution. PLoS ONE. 9:e112732.

Clements K.D., German D.P., Piché J., Tribollet A., Choat J.H. 2017. Integrating ecological roles and trophic diversification on coral reefs: Multiple lines of evidence identify parrotfishes as microphages. Biol. J. Linn. Soc. 120:729–751.

Cooper N., Thomas G.H., Venditti C., Meade A., Freckleton R.P. 2016. A cautionary note on the use of Ornstein Uhlenbeck models in macroevolutionary studies. Biol. J. Linn. Soc. 118:64–77.

Cooper W.J., Westneat M.W. 2009. Form and function of damselfish skulls: Rapid and repeated evolution into a limited number of trophic niches. BMC Evol. Biol. 9:1–17.

Copus J.M., Gibb A.C. 2013. A forceful upper jaw facilitates picking-based prey capture: Biomechanics of feeding in a butterflyfish, Chaetodon trichrous. Zoology. 116:336–347.

Cornic A. 1987. Poissons de l'Ile Maurice. Ile Maurice: Stanley Rose Hill.

Cowman P.F., Bellwood D.R. 2011. Coral reefs as drivers of cladogenesis: Expanding coral reefs, cryptic extinction events, and the development of biodiversity hotspots. J. Evol. Biol. 24:2543–2562.

Craig M.T. 2007. Preliminary observations on the life history of the white-streaked grouper, Epinephelus ongus, from Okinawa, Japan. Ichthyol. Res. 54:81–84.

Crawford C.H., Webber-Schultz A., Hart P.B., Randall Z.S., Cerrato-Morales C., Kellogg A.B., Amplo H.E., Suvarnaraksha A., Page L.M., Chakrabarty P., Flammang B.E. 2022. They like to move it (move it): walking kinematics of balitorid loaches of Thailand. J. Exp. Biol. 225:jeb242906.

Dagg A.I. 1973. Gaits in mammals. Mamm. Rev. 3:135–154.

Darwin C. 1871. The descent of man, and selection in relation to sex. Princeton, NJ: Princeton University Press.

Day S.W., Higham T.E., Cheer A.Y., Wainwright P.C. 2005. Spatial and temporal patterns of water flow generated by suction-feeding bluegill sunfish Lepomis macrochirus resolved by Particle Image Velocimetry. J. Exp. Biol. 208:2661–2671.

Denton J.S.S., Adams D.C. 2015. A new phylogenetic test for comparing multiple high-dimensional evolutionary rates suggests interplay of evolutionary rates and modularity in lanternfishes (Myctophiformes; Myctophidae). Evolution. 69:2425–2440.

Di Santo V., Goerig E., Wainwright D.K., Akanyeti O., Liao J.C., Castro-Santos T., Lauder G.V. 2021. Convergence of undulatory swimming kinematics across a diversity of fishes. Proc. Natl. Acad. Sci. 118:e2113206118.

Di-Poï N., Montoya-Burgos J.I., Miller H., Pourquié O., Milinkovitch M.C., Duboule D. 2010. Changes in Hox genes' structure and function during the evolution of the squamate body plan. Nature. 464:99–103.

Dornburg A., Sidlauskas B.L., Santini F., Sorenson L., Near T.J., Alfaro M.E. 2011. The influence of an innovative locomotor strategy on the phenotypic diversification of triggerfish (family: Balistidae). Evolution. 65:1912–1926.

Drummond A.J., Ho S.Y.W., Phillips M.J., Rambaut A. 2006. Relaxed phylogenetics and dating with confidence. PLoS Biol. 4:699–710.

Eastman J.M., Harmon L.J., Tank D.C. 2013. Congruification: Support for time scaling large phylogenetic trees. Methods Ecol. Evol. 4:688–691.

Elshoud-Oldenhave M.J.W. 1979. Prey Capture in the Pike-Perch, Stizostedion lucioperca (Teleostei, Percidae): A Structural and Functional Analysis. Zoomorphologie. 32:1–32.

Emlen D.J. 2001. Costs and the Diversification of Exaggerated Animal Structures. Science. 291:1534–1536.

Emlen D.J., Nijhout H.F. 2000. The Development and Evolution of Exaggerated Morphologies in Insects. Annu. Rev. Entomol. 45:661–708.

Emlen D.J., Warren I.A., Johns A., Dworkin I., Lavine L.C. 2012. A Mechanism of Extreme Growth and Reliable Signaling in Sexually Selected Ornaments and Weapons. Science. 337:860–864.

Estes S., Arnold S.J. 2007. Resolving the paradox of stasis: Models with stabilizing selection explain evolutionary divergence on all timescales. Am. Nat. 169:227–244.

Evans K.M., Larouche O., Watson S.J., Farina S.C., Habegger M.L., Friedman M.A. 2021. Integration drives rapid phenotypic evolution in flatfishes. Proc. Natl. Acad. Sci. U. S. A. 118:1–10.

Evans K.M., Vidal-García M., Tagliacollo V.A., Taylor S.J., Fenolio D.B. 2019a. Bony Patchwork: Mosaic Patterns of Evolution in the Skull of Electric Fishes (Apteronotidae: Gymnotiformes). Integr. Comp. Biol.:1–12.

Evans K.M., Williams K.L., Westneat M.W. 2019b. Do Coral Reefs Promote Morphological Diversification? Exploration of Habitat Effects on Labrid Pharyngeal Jaw Evolution in the Era of Big Data. Integr. Comp. Biol. icz103:1–31.

Farina S.C., Knope M.L., Corn K.A., Summers A.P., Bemis W.E. 2019. Functional coupling in the evolution of suction feeding and gill ventilation of sculpins (Perciformes: Cottoidei). Integr. Comp. Biol. 59:394–409.

Feilich K.L., López-Fernández H. 2019. When does form reflect function? Acknowledging and supporting ecomorphological assumptions. Integr. Comp. Biol.:1–13.

Felsenstein J. 1985. Phylogenies and the Comparative Method. Am. Nat. 125:1–15.

Ferry L.A., Konow N., Gibb A.C. 2012. Are kissing gourami specialized for substrate-feeding? Prey capture kinematics of Helostoma temminckii and other Anabantoid fishes. J. Exp. Zool. A. 317:571–579.

Ferry L.A., Paig-Tran E.W.M., Gibb A.C. 2015. Suction, ram, and biting: Deviations and limitations to the capture of aquatic prey. Integr. Comp. Biol. 55:97–109.

Ferry-Graham L.A., Konow N. 2010. The intramandibular joint in Girella: A mechanism for increased force production? J. Morphol. 271:271–279.

Ferry-Graham L.A., Wainwright P.C., Bellwood D.R. 2001. Prey capture in long-jawed butterflyfishes (Chaetodontidae): The functional basis of novel feeding habits. J. Exp. Mar. Bio. Ecol. 256:167–184.

Flammang B.E., Suvarnaraksha A., Markiewicz J., Soares D. 2016. Tetrapod-like pelvic girdle in a walking cavefish. Sci. Rep. 6:23711.

Floeter S.R., Bender M.G., Siqueira A.C., Cowman P.F. 2018. Phylogenetic perspectives on reef fish functional traits. Biol. Rev. 93:131–151.

Foster S.J., Vincent A.C.J. 2004. Life history and ecology of seahorses: implications for conservation and management. J. Fish Biol. 65:1–61.

Frédérich B., Marramà G., Carnevale G., Santini F. 2016. Non-reef environments impact the diversification of extant jacks, remoras and allies (Carangoidei, Percomorpha). Proc. R. Soc. B Biol. Sci. 283:20161556.

Friedman M.A. 2010. Explosive morphological diversification of spiny-finned teleost fishes in the aftermath of the end-Cretaceous extinction. Proc. R. Soc. B Biol. Sci. 277:1675–1683.

Friedman S.T., Corn K.A., Larouche O., Martinez C.M., Price S.A., Wainwright P.C. 2020a. Body shape diversification along the benthic-pelagic axis in marine fishes. Proc. R. Soc. B Biol. Sci.

Friedman S.T., Price S.A., Corn K.A., Larouche O., Martinez C.M., Wainwright P.C. 2020b. Data from: Body shape diversification along the benthic-pelagic axis in marine fishes. :Dryad, Dataset.

Friel J.P., Wainwright P.C. 1997. A model system of structural duplication: homologies of adductor mandibulae muscles in Tetraodontiform fishes. Syst. Biol. 46:441.

Froese R., Pauly D. 2018. Fishbase. www.fishbase.org.

Futuyma D.J., Moreno G. 1988. The Evolution of Ecological Specialization. Annu. Rev. Ecol. Syst. 19:207–233.

Gajdzik L., Aguilar-Medrano R., Frédérich B. 2019. Diversification and functional evolution of reef fish feeding guilds. Ecol. Lett. 22:572–582.

Gatesy S.M., Middleton K.M. 1997. Bipedalism, flight, and the evolution of theropod locomotor diversity. J. Vertebr. Paleontol. 17:308–329.

Ghezelayagh A., Harrington R.C., Burress E.D., Campbell M.A., Buckner J.C., Chakrabarty P., Glass J.R., McCraney W.T., Unmack P.J., Thacker C.E., Alfaro M.E., Friedman S.T., Ludt W.B., Cowman P.F., Friedman M.A., Price S.A., Dornburg A., Faircloth B.C., Wainwright P.C., Near T.J. 2021. Prolonged morphological expansion of spiny-rayed fishes following the end-Cretaceous. bioRxiv.

Gibb A.C., Ferry-Graham L.A. 2005. Cranial movements during suction feeding in teleost fishes: Are they modified to enhance suction production? Zoology. 108:141–153.

Gibb A.C., Staab K.L., Moran C., Ferry L.A. 2015. The teleost intramandibular joint: A mechanism that allows fish to obtain prey unavailable to suction feeders. Integr. Comp. Biol. 55:85–96.

Gibson R.N., editor. 2005. Flatfishes: biology and exploitation. Chichester, West Sussex ; Hoboken, NJ: John Wiley & Sons Inc.

Gilbert M.C., Conith A.J., Lerose C.S., Moyer J.K., Huskey S.H., Albertson R.C. 2021. Extreme Morphology, Functional Trade-offs, and Evolutionary Dynamics in a Clade of Open-Ocean Fishes (Perciformes: Bramidae). Integr. Org. Biol. 3.

Gill T. 1905. The life history of the sea-horses (Hippocampids). Proc. Natl. Acad. Sci.

Gillis G.B., Lauder G. V. 1995. Kinematics of feeding in bluegill sunfish: Is there a general distinction between aquatic capture and transport behaviors? J. Exp. Biol. 198:709–720.

Goatley C.H.R., Bellwood D.R., Bellwood O. 2010. Fishes on coral reefs: changing roles over the past 240 million years. Paleobiology. 36:415–427.

Gobalet K.W. 1989. Morphology of the parrotfish pharyngeal jaw apparatus. Am. Zool. 29:319–331.

Gosline W.A. 1987. Jaw structures and movements in higher teleostean fishes. Japanese J. Ichthyol. 34:21–32.

Goswami A., Smaers J.B., Soligo C., Polly P.D. 2014. The macroevolutionary consequences of phenotypic integration: from development to deep time. Philos. Trans. R. Soc. Lond. B. Biol. Sci. 369:20130254.

Grobecker D.B., Pietsch T.W. 1979. High-speed cinematographic evidence for ultrafast feeding in antennariid anglerfishes. Science. 205:1161–1162.

Gunz P., Mitteroecker P. 2013. Semilandmarks: A method for quantifying curves and surfaces. Hystrix. 24:103–109.

Hallgrímsson B., Jamniczky H., Young N.M., Rolian C., Parsons T.E., Boughner J.C., Marcucio R.S. 2009. Deciphering the palimpsest: Studying the relationship between morphological integration and phenotypic covariation. Evol. Biol. 36:355–376.

Harmon L.J., Weir J.T., Brock C.D., Glor R.E., Challenger W. 2008. GEIGER: Investigating evolutionary radiations. Bioinformatics. 24:129–131.

Hart P.B., Niemiller M.L., Burress E.D., Armbruster J.W., Ludt W.B., Chakrabarty P. 2020. Cave-adapted evolution in the North American amblyopsid fishes inferred using phylogenomics and geometric morphometrics. Evolution. 74:936–949.

Hemingson C.R., Cowman P.F., Hodge J.R., Bellwood D.R. 2019. Colour pattern divergence in reef fish species is rapid and driven by both range overlap and symmetry. Ecol. Lett. 22:190–199.

Hemingson C.R., Siqueira A.C., Cowman P.F., Bellwood D.R. 2021. Drivers of eyespot evolution in coral reef fishes. Evolution. 75:903–914.

Henkel C.V., Burgerhout E., de Wijze D.L., Dirks R.P., Minegishi Y., Jansen H.J., Spaink H.P., Dufour S., Weltzien F.-A., Tsukamoto K., van den Thillart G.E.E.J.M. 2012a. Primitive Duplicate Hox Clusters in the European Eel's Genome. PLoS ONE. 7:e32231.

Henkel C.V., Dirks R.P., de Wijze D.L., Minegishi Y., Aoyama J., Jansen H.J., Turner B., Knudsen B., Bundgaard M., Hvam K.L., Boetzer M., Pirovano W., Weltzien F.-A., Dufour S., Tsukamoto K., Spaink H.P., van den Thillart G.E.E.J.M. 2012b. First draft genome sequence of the Japanese eel, Anguilla japonica. Gene. 511:195–201.

Hiatt R.W., Strasburg D.W. 1960. Ecological Relationships of the Fish Fauna on Coral Reefs of the Marshall Islands. Ecol. Monogr. 30:65–127.

Hildebrand M. 1989. The quadrupedal gaits of vertebrates. Bioscience. 39:766–775.

Ho L.S.T., Ané C. 2014. Intrinsic inference difficulties for trait evolution with Ornstein-Uhlenbeck models. Methods Ecol. Evol. 5:1133–1146.

Hobson E.S. 1974. Feeding relationship of teleostean fishes on coral reefs in Kona, Hawaii. Fish. Bull. 72:915–1031.

Höhna S., Landis M.J., Heath T.A., Boussau B., Lartillot N., Moore B.R., Huelsenbeck J.P., Ronquist F. 2016. RevBayes: Bayesian phylogenetic inference using graphical models and an interactive model-specification language. Syst. Biol. 65:726–736.

Holzman R.A., Collar D.C., Price S.A., Hulsey C.D., Thomson R.C., Wainwright P.C. 2012. Biomechanical trade-offs bias rates of evolution in the feeding apparatus of fishes. Proc. R. Soc. B Biol. Sci. 279:1287–1292.

Holzman R.A., Day S.W., Mehta R.S., Wainwright P.C. 2008. Jaw protrusion enhances forces exerted on prey by suction feeding fishes. J. R. Soc. Interface. 5:1445–1457.

Hothorn T., Hornik K., Strobl C., Zeileis A. 2015. party: A laboratory for recursive partytioning. R Packag. version 0.9-0, URL http//CRAN. R-project. org.:37.

Hothorn T., Hornik K., Zeileis A. 2006. Unbiased recursive partitioning: A conditional inference framework. J. Comput. Graph. Stat. 15:651–674.

Huby A., Lowie A., Herrel A., Vigouroux R., Frédérich B., Raick X., Kurchevski G., Godinho A.L., Parmentier E. 2019. Functional diversity in biters: the evolutionary

morphology of the oral jaw system in pacus, piranhas and relatives (Teleostei: Serrasalmidae). Biol. J. Linn. Soc. 127:722–741.

Huelsenbeck J.P., Nielsen R., Bollback J.P. 2003. Stochastic mapping of morphological characters. Syst. Biol. 52:131–158.

Huey R.B., Garland T., Turelli M. 2019. Revisiting a Key Innovation in Evolutionary Biology: Felsenstein's "Phylogenies and the Comparative Method." Am. Nat. 193:703055.

Hughes L.C., Ortí G., Huang Y., Sun Y., Baldwin C.C., Thompson A.W., Arcila D., Betancur-R R., Li C., Becker L., Bellora N., Zhao X., Li X., Wang M., Fang C., Xie B., Zhou Z., Huang H., Chen S., Venkatesh B., Shi Q. 2018. Comprehensive phylogeny of ray-finned fishes (Actinopterygii) based on transcriptomic and genomic data. Proc. Natl. Acad. Sci.:201719358.

Hughes T.P., Linares C., Dakos V., van de Leemput I.A., van Nes E.H. 2013. Living dangerously on borrowed time during slow, unrecognized regime shifts. Trends Ecol. Evol. 28:149–155.

Hughes T.P., Rodrigues M.J., Bellwood D.R., Ceccarelli D., Hoegh-Guldberg O., McCook L., Moltschaniwskyj N., Pratchett M.S., Steneck R.S., Willis B. 2007. Phase Shifts, herbivory, and the resilience of coral reefs to climate change. Curr. Biol. 17:360–365.

Huttegger S.M., Mitteroecker P. 2011. Invariance and Meaningfulness in Phenotype spaces. Evol. Biol. 38:335–351.

Irschick D.J., Herrel A., Vanhooydonck B., Damme R.V. 2007. A functional approach to sexual selection. Funct. Ecol. 21:621–626.

Jacobs C., Holzman R.A. 2018. Conserved spatio-temporal patterns of suction-feeding flows across aquatic vertebrates: a comparative flow visualization study. J. Exp. Biol.:jeb.174912.

Jones R.S. 1968. Ecological relationships in Hawaiian and Johnston Island Acanthuridae (Surgeonfishes). Micronesica. 4:309–361.

Kendall D.G. 1984. Shape-manifolds, procrustean metrics, and complex projective spaces. Bull L. Math Soc. 16:81–121.

Kiessling W. 2008. Sampling-standardized expansion and collapse of reef building in the Phanerozoic. Foss. Rec. 11:7–18.

Klingenberg C.P. 2014. Studying morphological integration and modularity at multiple levels: concepts and analysis. Philos. Trans. R. Soc. B Biol. Sci. 369:20130249.

Klingenberg C.P. 2016. Size, shape, and form: concepts of allometry in geometric morphometrics. Dev. Genes Evol. 226:113–137.

Koehl M.A.R. 1997. When does morphology matter? Annu. Rev. Ecol. Syst. 27:501–542.

Konow N., Bellwood D.R. 2005. Prey-capture in Pomacanthus semicirculatus (Teleostei, Pomacanthidae): functional implications of intramandibular joints in marine angelfishes. J. Exp. Biol. 208:1421–1433.

Konow N., Bellwood D.R., Wainwright P.C., Kerr A.M. 2008. Evolution of novel jaw joints promote trophic diversity in coral reef fishes. Biol. J. Linn. Soc. 93:545–555.

Kotrschal K. 1988. Evolutionary patterns in tropical marine reef fish feeding. J. Zool. Syst. Evol. Res. 26:51–64.

Krumlauf R. 1994. Hox genes in vertebrate development. Cell. 78:191–201.

Larouche O., Benton B., Corn K.A., Friedman S.T., Gross D., Iwan M., Kessler B., Martinez C.M., Rodriguez S., Whelpley H., Wainwright P.C., Price S.A. 2020. Reef-associated fishes have more maneuverable body shapes at a macroevolutionary scale. Coral Reefs.

Larouche O., Hodge J.R., Alencar L.R. V, Camper B., Adams D.S., Zapfe K., Friedman S.T., Wainwright P.C., Price S.A. 2020. Do key innovations unlock diversification? A case-study on the morphological and ecological impact of pharyngognathy in acanthomorph fishes. Curr. Zool. 66:575–588.

Larouche O., Zelditch M.L., Cloutier R. 2018. Modularity promotes morphological divergence in ray-finned fishes. Sci. Rep. 8:1–6.

Lauder G. V. 1980a. Hydrodynamics of prey capture by teleost fishes. In: Schneck D.J., editor. Biofluid mechanics. New York, NY: Springer. p. 161–181.

Lauder G. V. 1980b. The suction feeding mechanism in sunfishes (Lepomis spp.): an experimental analysis. J. Exp. Biol. 88:49–72.

Lauder G. V. 1980c. Evolution of the feeding mechanism in primitive actinopterygian fishes: A functional anatomical analysis of Polypterus, Lepisosteus, and Amia. J. Morphol. 163:283–317.

Lauder G. V. 1985. Aquatic feeding in lower vertebrates. In: Hildebrand M., editor. Functional Vertebrate Morphology. Cambridge, MA: Harvard University Press. p. 185–229.

Liem K.F. 1978. Modulatory multiplicity in the functional repertoire of the feeding mechanism in cichlid fishes. I. Piscivores. J. Morphol. 158:323–360.

Liem K.F. 1979. Modulatory multiplicity in the feeding mechanism in cichlid fishes, as exemplified by the invertebrate pickers of Lake Tanganyika. J. Zool. 189:93–125.

Liem K.F. 1980. Adaptive significance of intra-and interspecific differences in the feeding repertoires of cichlid fishes. Amer. Zool. 20:295–314.

Long J.A. 2011. Strangers in the Bite: Dipnomorphans. The Rise of Fishes: 500 Million Years of Evolution. BALTIMORE: The Johns Hopkins University Press. p. 187–207.

Longo S.J., McGee M.D., Oufiero C.E., Waltzek T.B., Wainwright P.C. 2016. Body ram, not suction, is the primary axis of suction-feeding diversity in spiny-rayed fishes. J. Exp. Biol. 219:119–128.

MacArthur R.H., MacArthur J.W. 1961. On bird species diversity. Ecology. 42:594–598.

Mackey B., Vanderploeg K., Ferry L.A. 2014. Variation in prey capture mechanics in the swordtail, Xiphophorus helleri in response to food type. J. Arizona-Nevada Acad. Sci. 45:59–63.

Martin A., Serano J.M., Jarvis E., Bruce H.S., Wang J., Ray S., Barker C.A., Connell L.C.O., Patel N.H. 2016. CRISPR/Cas9 Mutagenesis Reveals Versatile Roles of Hox Genes in Crustacean Limb Specification and Evolution. Curr. Biol.:14–26.

Martinez C.M., Friedman S.T., Corn K.A., Larouche O., Price S.A., Wainwright P.C. 2021. The deep sea is a hot spot of fish body shape evolution. Ecol. Lett. 24:1788–1799.

Martinez C.M., McGee M.D., Borstein S.R., Wainwright P.C. 2018. Feeding ecology underlies the evolution of cichlid jaw mobility. Evolution. 72:1645–1655.

Martinez C.M., Wainwright P.C. 2019. Extending the geometric approach for studying biomechanical motions. Integr. Comp. Biol. 59:684–695.

Martins E.P., Hansen T.F. 1997. Phylogenies and the comparative method: A general approach to incorporating phylogenetic information into the analysis of interspecific data. Am. Nat. 153:448.

Maurin K.J.L. 2020. An empirical guide for producing a dated phylogeny with treePL in a maximum likelihood framework. arXiv.:1–11.

May M.R., Moore B.R. 2019. A Bayesian approach for inferring the impact of a discrete character on rates of continuous-character evolution in the presence of background-rate variation. Syst. Biol. 69:530–544.

McCord C.L., Westneat M.W. 2016. Evolutionary patterns of shape and functional diversification in the skull and jaw musculature of triggerfishes (Teleostei: Balistidae). J. Morphol. 277:737–752.

McGee M.D., Faircloth B.C., Borstein S.R., Zheng J., Hulsey C.D., Wainwright P.C., Alfaro M.E. 2016. Replicated divergence in cichlid radiations mirrors a major vertebrate innovation. Proc R Soc B. 283:20151413.

McKaye K.R., Marsh A. 1983. Food switching by two specialized algae-scraping cichlid fishes in Lake Malawi, Africa. Oecologia. 56:245–248.

Mehta R.S., Ward A.B., Alfaro M.E., Wainwright P.C. 2010. Elongation of the Body in Eels. Integr. Comp. Biol. 50:1091–1105.

Mihalitsis M., Bellwood D.R. 2019. Morphological and functional diversity of piscivorous fishes on coral reefs. Coral Reefs. 38:945–954.

Mosauer W. 1932. On the Locomotion of Snakes. Science. 76:583–585.

Motta P.J. 1988. Functional morphology of the feeding apparatus of ten species of Pacific butterflyfishes (Perciformes, Chaetodontidae): an ecomorphological approach. Environ. Biol. Fishes. 22:39–67.

Muller M., Osse J.W.M., Verhagen J.H.G. 1982. A quantitative hydrodynamical model of suction feeding in fish. J. Theor. Biol. 95:49–79.

Muñoz M.M., Anderson P.S.L., Patek S.N. 2017. Mechanical sensitivity and the dynamics of evolutionary rate shifts in biomechanical systems. Proc. R. Soc. B Biol. Sci. 284:20162325.

Muñoz M.M., Hu Y., Anderson P.S.L., Patek S.N. 2018. Strong biomechanical relationships bias the tempo and mode of morphological evolution. Elife. 7:5607–5610.

Myers R.F. 1991. Micronesian Reef Fishes. Barrigada, Guam: Coral Graphics.

Near T.J., Eytan R.I., Dornburg A., Kuhn K.L., Moore J.A., Davis M.P., Wainwright P.C., Friedman M.A., Smith W.L. 2012. Resolution of ray-finned fish phylogeny and timing of diversification. Proc. Natl. Acad. Sci. 109:13698–13703.

Nicholson G.M., Clements K.D. 2021. Ecomorphological divergence and trophic resource partitioning in 15 syntopic Indo-Pacific parrotfishes (Labridae: Scarini). Biol. J. Linn. Soc.:1–22.

Niklas K.J. 1994. Morphological evolution through complex domains of fitness. Proc. Natl. Acad. Sci. U. S. A. 91:6772–6779.

Norton S.F. 1991. Capture success and diet of cottid Ffshes: The role of predator morphology and attack kinematics. Ecology. 72:1807–1819.

Norton S.F. 1995. A functional approach to ecomorphological patterns in cottid fishes. Environ. Biol. Fishes. 44:61–78.

Norton S.F., Brainerd E.L. 1993. Convergence in the feeding mechanics of ecomorphologically similar species in the Centrarchidae and Cichlidae. J. Exp. Biol. 176:11–29.

Nursall J.R. 1996. Distribution and ecology of pycnodont fishes. Mesozoic Fishes - Syst. Paleoecol.:115–124.

O'Meara B.C. 2012. Evolutionary Inferences from Phylogenies: A Review of Methods. Annu. Rev. Ecol. Evol. Syst. 43:267–285.

O'Meara B.C., Ané C., Sanderson M.J., Wainwright P.C. 2006. Testing for Different Rates of Continuous Trait Evolution Using Likelihood. Evolution. 60:922.

Olsen A.M., Hernandez L.P., Camp A.L., Brainerd E.L. 2019. Channel catfish use higher coordination to capture prey than to swallow. Proc. R. Soc. B Biol. Sci. 286.

Ormond R.F.G. 1980. Aggressive mimicry and other interspecific feeding associations among Red Sea coral reef predators. J. Zool. 191:247–262.

Oufiero C.E., Holzman R.A., Young F.A., Wainwright P.C. 2012. New insights from serranid fishes on the role of trade-offs in suction-feeding diversification. J. Exp. Biol. 215:3845–3855.

Paradis E., Claude J., Strimmer K. 2004. APE: Analyses of phylogenetics and evolution in R language. Bioinformatics. 20:289–290.

Patterson C. 1993. An overview of the early fossil record of acanthomorphs. Bull. Mar. Sci. 52:29–59.

Pelster B. 1997. Buoyancy at depth. Deep-sea fishes: Fish physiology. Academic Press. p. 195–237.

Pennell M.W., Eastman J.M., Slater G.J., Brown J.W., Uyeda J.C., Fitzjohn R.G., Alfaro M.E., Harmon L.J. 2014. Geiger v2.0: An expanded suite of methods for fitting macroevolutionary models to phylogenetic trees. Bioinformatics. 30:2216–2218.

Perevolotsky T., Martin C.H., Rivlin A., Holzman R.A. 2020. Work that body: fin and body movements determine herbivore feeding performance within the natural reef environment. Proceedings. Biol. Sci. 287:20201903.

Polly P.D. 2001. Paleontology and the Comparative Method: Ancestral Node Reconstructions versus Observed Node Values. Am. Nat.:14.

Polly P.D. 2020. Functional Tradeoffs Carry Phenotypes Across the Valley of the Shadow of Death. Integr. Comp. Biol.:1–15.

Polly P.D., Stayton C.T., Dumont E.R., Pierce S.E., Rayfield E.J., Angielczyk K.D. 2016. Combining geometric morphometrics and finite element analysis with evolutionary modeling: towards a synthesis. J. Vertebr. Paleontol. 36.

Pombo-Ayora L., Tavera J. 2021. Are feeding modes concealing morphofunctional diversity? The case of the New World parrotfishes. Front. Mar. Sci. 8.

Price S.A., Claverie T., Near T.J., Wainwright P.C. 2015. Phylogenetic insights into the history and diversification of fishes on reefs. Coral Reefs. 34:997–1009.

Price S.A., Friedman S.T., Corn K.A., Martinez C.M., Larouche O., Wainwright P.C. 2019. Building a body shape morphospace of teleostean fishes. Integr. Comp. Biol. 59:716–730.

Price S.A., Holzman R.A., Near T.J., Wainwright P.C. 2011. Coral reefs promote the evolution of morphological diversity and ecological novelty in labrid fishes. Ecol. Lett. 14:462–469.

Price S.A., Larouche O., Friedman S.T., Corn K.A., Wainwright P.C., Martinez C.M. 2020. A CURE for a major challenge in phenomics: a practical guide to implementing a quantitative specimen-based undergraduate research experience. Integr. Org. Biol.

Price S.A., Tavera J.J., Near T.J., Wainwright P.C. 2013. Elevated rates of morphological and functional diversification in reef-dwelling haemulid fishes. Evolution. 67:417–428.

Price S.A., Wainwright P.C., Bellwood D.R., Kazancioglu E., Collar D.C., Near T.J. 2010. Functional innovations and morphological diversification in parrotfish. Evolution. 64:3057–3068.

Purcell S.W., Bellwood D.R. 1993. A functional analysis of food procurement in two surgeonfish species, Acanthurus nigrofuscus and Ctenochaetus striatus (Acanthuridae). Environ. Biol. Fishes. 37:139–159.

R Core Team. 2019. R: A Language and Environment for Statistical Computing.

R Core Team. 2022. R: A Language and Environment for Statistical Computing.

Rabosky D.L. 2017. Phylogenetic tests for evolutionary innovation: The problematic link between key innovations and exceptional diversification. Philos. Trans. R. Soc. B Biol. Sci. 372:1–8.

Rabosky D.L., Chang J., Title P.O., Cowman P.F., Sallan L., Friedman M., Kaschner K., Garilao C., Near T.J., Coll M., Alfaro M.E. 2018. An inverse latitudinal gradient in speciation rate for marine fishes. Nature. 559:392–395.

Rambaut A., Drummond A.J., Xie D., Baele G., Suchard M.A. 2018. Posterior summarization in Bayesian phylogenetics using Tracer 1.7. Syst. Biol. 67:901–904.

Randall J.E. 1967. Food habits of reef fishes of the West Indies. Stud. Trop. Oceanogr. 5:665–847.

Randall J.E., Allen G.R., Steene R.C. 1997. Fishes of the Great Barrier Reef and Coral Sea. Honolulu, HI: University of Hawaii Press.

Revell L.J. 2012. phytools: An R package for phylogenetic comparative biology (and other things). Methods Ecol. Evol. 3:217–223.

Revell L.J. 2013. A comment on the use of stochastic character maps to estimate evolutionary rate variation in a continuously valued trait. Syst. Biol. 62:339–345.

Rohlf F.J. 2015. The tps series of software. Hystrix. 26:1–4.

Rohlf F.J., Slice D. 1990. Extensions of the Procrustes method for the optimal superimposition of landmarks. Syst. Zool. 39:40.

Rupp M.F., Hulsey C.D. 2014. Influence of substrate orientation on feeding kinematics and performance of algae-grazing Lake Malawi cichlid fishes. J. Exp. Biol. 217:3057–3066.

Sanderson M.J. 2002. Estimating absolute rates of molecular evolution and divergence times: A penalized likelihood approach. Mol. Biol. Evol. 19:101–109.

Sanford C.P., Wainwright P.C. 2002. Use of sonomicrometry demonstrates the link between prey capture kinematics and suction pressure in largemouth bass. J. Exp. Biol. 205:3445–57.

Schaefer S.A., Lauder G. V. 1996. Testing Historical Hypotheses of Morphological Change: Biomechanical Decoupling in Loricarioid Catfishes. Evolution. 50:1661–1675.

Schaeffer B., Rosen D.E. 1961. Major adaptive levels in the evolution of the actinopterygian feeding mechanism. Am. Zool. 1:187–204.

Schluter D. 2000. The Ecology of Adaptive Radiation. New York: Oxford University Press.

Schoener T.W. 1974. Resource partitioning in ecological communities. Science. 185:27–39.

Scott R.W. 1981. Biotic relations in early Cretaceous coral-algal-rudist reefs, Arizona. J. Paleontol. 55:463–478.

Scott R.W. 1988. Evolution of late Jurassic and Early Cretaceous reef biotas. Palaios. 3:184–193.

Shingleton A.W., Frankino W.A. 2013. New perspectives on the evolution of exaggerated traits. BioEssays. 35:100–107.

Simpson G.G. 1944. Tempo and mode in evolution. New York, NY: Columbia University Press.

Siqueira A.C., Bellwood D.R., Cowman P.F. 2019a. The evolution of traits and functions in herbivorous coral reef fishes through space and time. Proc. R. Soc. B Biol. Sci. 286:20182672.

Siqueira A.C., Bellwood D.R., Cowman P.F. 2019b. Historical biogeography of herbivorous coral reef fishes: The formation of an Atlantic fauna. J. Biogeogr. 46:1611–1624.

Siqueira A.C., Morais R.A., Bellwood D.R., Cowman P.F. 2020. Trophic innovations fuel reef fish diversification. Nat. Commun. 11:1–11.

Smith S.A., O'Meara B.C. 2012. TreePL: Divergence time estimation using penalized likelihood for large phylogenies. Bioinformatics. 28:2689–2690.

Staab K.L., Holzman R.A., Hernandez L.P., Wainwright P.C. 2012. Independently evolved upper jaw protrusion mechanisms show convergent hydrodynamic function in teleost fishes. J. Exp. Biol. 215:1456–1463.

Stayton C.T. 2015. The definition, recognition, and interpretation of convergent evolution, and two new measures for quantifying and assessing the significance of convergence. Evolution. 69:2140–2153.

Stayton C.T. 2019. Performance in three shell functions predicts the phenotypic distribution of hard-shelled turtles. Evolution. 73:720–734.

Steimle F.W., Morse W.W., Johnson D.L. 1999. Goosefish, Lophius americanus, Life History and Habitat Characteristics. .

Tedman R.A. 1980. Comparative study of the cranial morphology of the Labrids Choerodon venustus and Labroides dimidiatus and the Scarid Scarus fasciatus (Pisces: Perciformes) II. Cranial myology and feeding mechanisms. Mar. Freshw. Res. 31:351–372.

Teichert S., Steinbauer M., Kiessling W. 2020. A possible link between coral reef success, crustose coralline algae and the evolution of herbivory. Sci. Rep. 10:1–12.

Tintori A. 1998. Fish biodiversity in the marine norian (late triassic) of northern Italy: The first neopterygian radiation. Ital. J. Zool. 65:193–198.

Tribble C.M., Freyman W.A., Landis M.J., Lim Y., Barido-Sottani J., Kopperud B.T., Ohna S.H.¨, May M.R. 2021. RevGadgets: an R Package for visualizing Bayesian phylogenetic analyses from RevBayes. bioRxiv.:2021.05.10.443470.

Uyeda J.C., Hansen T.F., Arnold S.J., Pienaar J. 2011. The million-year wait for macroevolutionary bursts. Proc. Natl. Acad. Sci. 108:15908–15913.

Van Wassenbergh S., Herrel A., Adriaens D., Aerts P. 2007. No trade-off between biting and suction feeding performance in clariid catfishes. J. Exp. Biol. 210:27–36.

Van Wassenbergh S., Lieben T., Herrel A., Huysentruyt F., Geerinckx T., Adriaens D., Aerts P. 2009. Kinematics of benthic suction feeding in Callichthyidae and Mochokidae, with functional implications for the evolution of food scraping in catfishes. J. Exp. Biol. 212:116–125.

Vial C., Ojeda F.P. 1990. Cephalic anatomy of the herbivorous fish Girella laevifrons (Osteichthyes: Kyphosidae): mechanical considerations of its trophic function. Rev. Chil. Hist. Nat. 63:247–260.

Wainwright P.C. 2007. Functional Versus Morphological Diversity in Macroevolution. Annu. Rev. Ecol. Evol. Syst. 38:381–401.

Wainwright P.C., Bellwood D.R. 2002. Ecomorphology of feeding in coral reef fishes. In: Sale P.F., editor. Coral Reef Fishes: Dynamics and Diversity in a Complex Ecosystem. London, UK: Academic Press. p. 33–55.

Wainwright P.C., Price S.A. 2016. The Impact of Organismal Innovation on Functional and Ecological Diversification. Integr. Comp. Biol. 56:479–488.

Wainwright P.C., Reilly S.M. 1994. Ecological morphology: Integrative organismal biology. Chicago, IL: University of Chicago Press.

Wainwright P.C., Richard B.A. 1995. Predicting patterns of prey use from morphology of fishes. Environ. Biol. Fishes. 44:97–113.

Walker J.A. 2007. A general model of functional constraints on phenotypic evolution. Am. Nat. 170:681–689.

Ward A.B., Mehta R.S. 2014. Differential occupation of axial morphospace. Zoology. 117:70–76.

Webb P.W. 1984. Body Form, Locomotion, and Foraging in Aquatic Vertebrates. Am. Zool. 24:107–120.

Westneat M.W. 1994. Transmission of force and velocity in the feeding mechanisms of labrid fishes (Teleostei, Perciformes). Zoomorphology. 114:103–118.

Westneat M.W. 1995. Feeding, function, and phylogeny: Analysis of historical biomechanics in Labrid fishes using comparative methods. Syst. Biol. 44:361–383.

Westneat M.W. 2003. A biomechanical model for analysis of muscle force, power output and lower jaw motion in fishes. J. Theor. Biol. 223:269–281.

Westneat M.W. 2006. Skull biomechanics and suction feeding in fishes. In: Shadwick R.E., Lauder G. V., editors. Fish Physiology Series: Fish Biomechanics. San Diego, CA: Academic Press. p. 29–75.

Wickham H. 2016. ggplot2: elegant graphics for data. Springer.

Wickham H., Averick M., Bryan J., Chang W., McGowan L., François R., Grolemund G., Hayes A., Henry L., Hester J., Kuhn M., Pedersen T., Miller E., Bache S., Müller K., Ooms J., Robinson D., Seidel D., Spinu V., Takahashi K., Vaughan D., Wilke C., Woo K., Yutani H. 2019. Welcome to the Tidyverse. J. Open Source Softw. 4:1686.

Wilke C. 2021. cowplot: streamlined plot theme and plot annotations for ‘ggplot2’ .

Wilkens H., Strecker U., Yager J. 1989. Eye reduction and phylogenetic age in ophidiiform cave fish. Z Zool Syst Evol.-Forsch. 27:126–134.

Williams I.D., Polunin N.V.C. 2001. Large-scale associations between macroalgal cover and grazer biomass on mid-depth reefs in the Caribbean. Coral Reefs. 19:358–366.

Wilson D.S., Yoshimura J. 1994. On the Coexistence of Specialists and Generalists. Am. Nat. 144:692–707.

Woltering J.M., Vonk F.J., Müller H., Bardine N., Tuduce I.L., de Bakker M.A.G., Knöchel W., Sirbu I.O., Durston A.J., Richardson M.K. 2009. Axial patterning in snakes and caecilians: Evidence for an alternative interpretation of the Hox code. Dev. Biol. 332:82–89.

Wood R. 1995. The changing biology of reef-building. Palaios. 10:517–529.

Wood R. 1998. The ecological evolution of reefs. Annu. Rev. Ecol. Syst. 29:179–206.

APPENDIX 1

SUPPLEMENTAL MATERIALS FOR CHAPTER 1

A MULTIFUNCTION TRADE-OFF HAS CONTRASTING EFFECTS ON THE EVOLUTION OF FORM AND FUNCTION

SUPPLEMENTAL METHODS

Dataset construction. Fishes were classified as “suction feeders” if their primary mode of prey capture uses suction. We classified a “biting” feeding mode as one where the fish uses suction as well as direct biting actions. A direct biting action was designated as one where the fish’s closing jaws make contact with the prey item to either grip it or scrape it from a holdfast. The number of strikes in our analyses for each species ranged from 2-9, with a median of 3. The number of individuals filmed for each species ranged from 1-3, with a median of 1 individual per species. All fishes were filmed feeding on minimally- or non-evasive prey and care was taken to induce high-effort strikes, where the fishes achieved a fully opened mouth. Protocols for animal care and experiments were approved by the University of California, Davis Institutional Animal Care and Use Committee (protocol #20475).

Landmark data. Landmarks were chosen to capture the highest proportion possible of the motion of the fish’s head during suction feeding strikes. Sliding semi-landmarks were designed to track changes in curvature along the ventral margin of the fish’s head. Semi-landmarks were necessary in order to capture shape change along a structure with few features that could be identified to discrete, fixed points. In this case, they captured the curvature of the hyoid of the fish with eight equidistant semi-landmarks that were bounded on either end by fixed points at the insertion of the pelvic fin and at the base of the rostral tip of the dentary (Fig. S1). We measured kinematic components as the maximum value of each trait throughout the strike, regardless of whether that value occurred at peak gape. Measurements are depicted in Fig. S2.

Evolutionary model simulations. To test the ability of our tree topology and character distribution to distinguish between different Brownian Motion or Ornstein-Uhlenbeck evolutionary models, we ran simulations in the R package *OUwie* (Beaulieu et al. 2012). We simulated data using our tree and discrete trait topology under each model that we fit in our analysis (single-rate Brownian Motion, BM1; multi-rate Brownian Motion, BMS; single-rate, single-optimum Ornstein-Uhlenbeck, OU1; single-rate, multi-optimum Ornstein-Uhlenbeck, OUM; multi-rate, multi-optimum Ornstein-Uhlenbeck, OUMV). First, we generated a distribution of 100 stochastic character maps of the discrete trait history using *phytools* (Revell 2012). Then, we simulated a dataset under each of the 5 models on each discrete trait history. We compared the fit of all 5 BM and OU models on each of the simulated datasets to see whether we could recover the model under which the traits had been simulated as the best-fit model.

Bayesian evolutionary model prior robustness. To measure the effect of the prior we specified on the number of rate shifts, we ran alternative models with priors of 1, 5, and 10 rate shifts and compared its effect on posterior estimates of key parameters. The 1 and 10 shift prior models on the linear distance dataset MCMCs ran for 750,000 generations and the 5 shift prior model MCMC ran for 500,000 generations. The angles dataset MCMCs ran for 1 million generations. The overall kinesis dataset ran for 2 million generations and we ran an additional MCMC for the 10 shift prior for 3 million generations (see Results). All models ran with a with a 10% burn-in.

SUPPLEMENTAL RESULTS

Evolutionary model simulations. Simulations suggested that we had moderately high ability to distinguish between evolutionary models, which may explain the similar fits of the OUMV model with either BMS or OUM models with our observed dataset. Most models that we fit were well- or moderately- able to be distinguished from other models, or were selected as the best model with one or more other models having comparable fits. 88% of the time, simulations run under BM1 were best-fit by BM1 alone or BM1 fit similarly as 1 or more other models. The other proportions of the time in which the simulated model was recovered as the best-fit were as follows: 44% BMS, 98% OU1, 92% OUM, and 78% OUMV.

Bayesian evolutionary model prior robustness. We found that the estimated parameters were largely consistent across the three priors on the number of rate shifts in the angles and distances dataset (Figure S5). As expected, the posterior number of rate shifts in the continuous characters increased with the prior, but the posterior number of states changes and the rate ratio between the states were consistent across different priors. However, in the overall cranial kinesis data, we found some variation in the rate ratios between the states based on the prior on the number of rate shifts. It appears that the 1-shift prior model found a peak in parameter space where the rates of evolution between groups are different, but with higher rates of evolution in biters. It is likely that the 1-shift prior model has gotten stuck in an area of low likelihood, but with just one predicted shift, has few opportunities to traverse parameter space in search of another likelihood region. The 10-shift prior produced contrasting results across different runs, with a model run for 2 million generations mirroring the 1-shift results and a model run for

3 million generations mirroring the 5-shift results, indicating that there may be a local likelihood peak where the models support a faster rate in biters. However, with more generations of the MCMC, the model found a peak with suction feeders faster. This pattern may reflect issues outlined in Moore et al. (2016) where the prior on the number of rate shifts may constrain or overly influence the posterior, or highlight the benefit of running the MCMCs for additional generations.

SUPPLEMENTAL FIGURES & TABLES

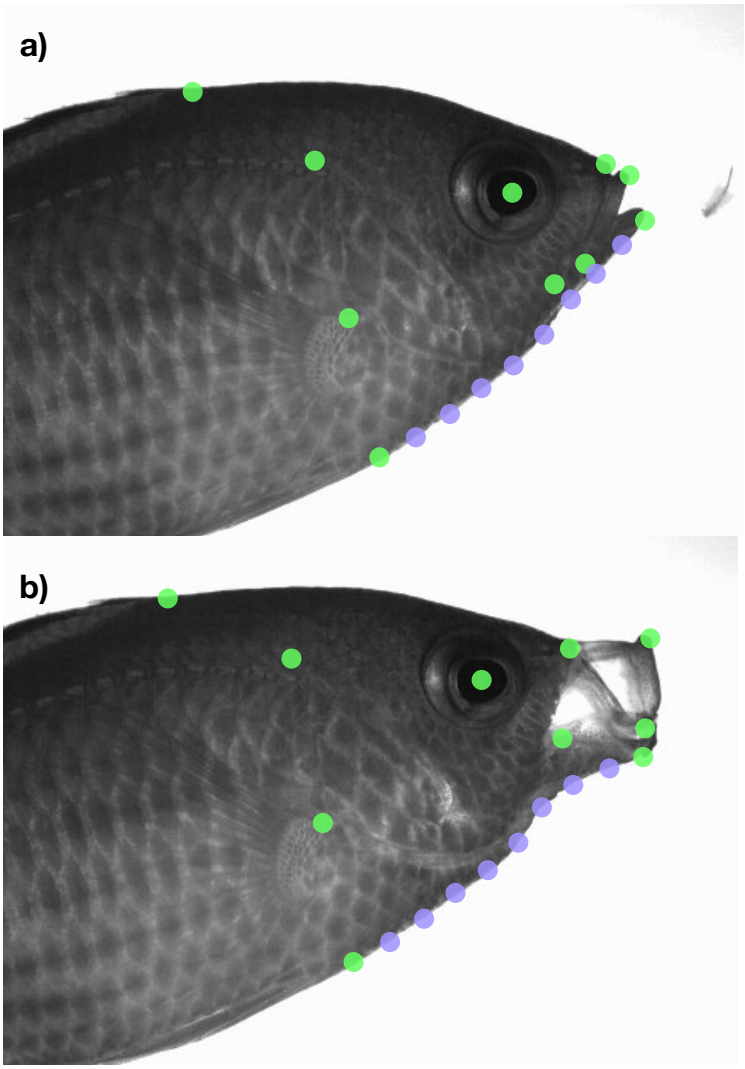

Fig. S1. Landmarks on a fish at a) strike initiation and b) maximum gape. Ten green points indicate fixed landmarks. Purple points indicate the eight sliding semi-landmarks.

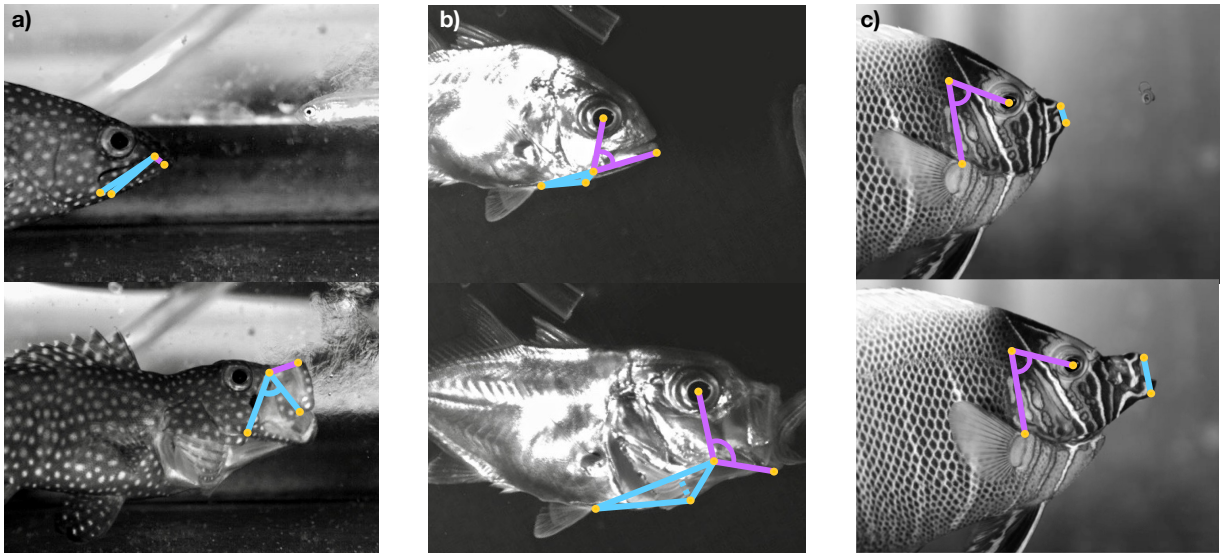

Fig. S2. Angles and distances used to measure kinematic components. a) Blue indicates angle of maxillary rotation; purple displays premaxillary protrusion. b) Blue shows measurement of hyoid depression, as height of triangle; purple is angle of lower jaw depression. c) Blue indicates gape measurement; purple depicts angle of cranial elevation.

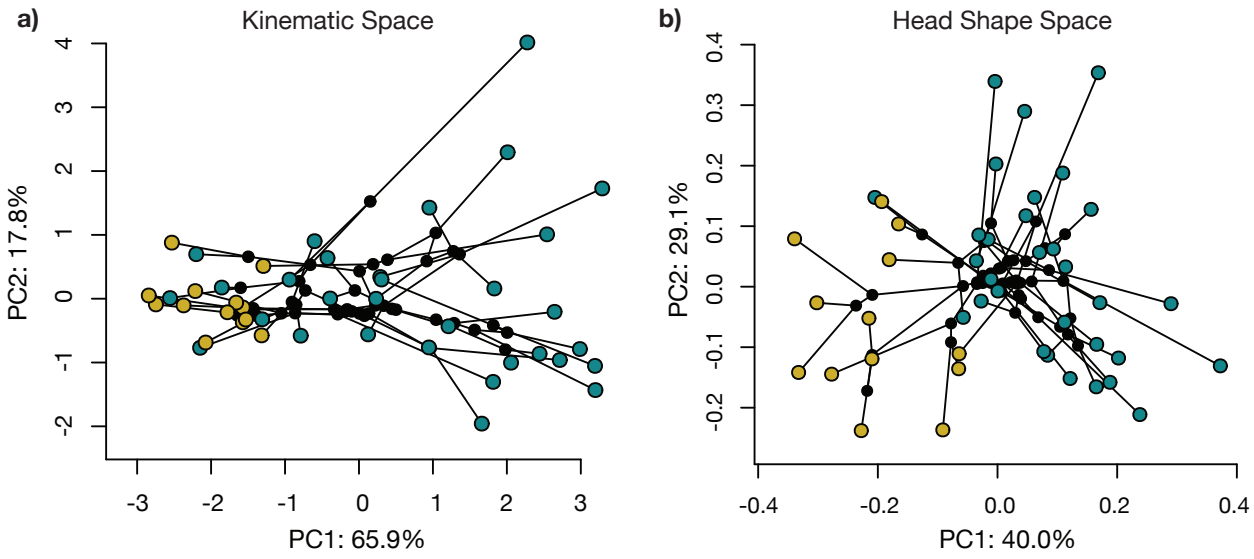

Fig. S3. Plots of principle component axes 1 and 2 with lines displaying phylogenetic relationships between observations, species (depicted without phylogeny in Fig. 3). a), kinematic space occupation. b), cranial shape morphospace occupation. Notably, the kinematic PCA shows a relatively moderate effect of phylogenetic signal. In contrast, the head shape PCA shows a substantial effect of relatedness in the biting group and weaker effect in suction feeders.

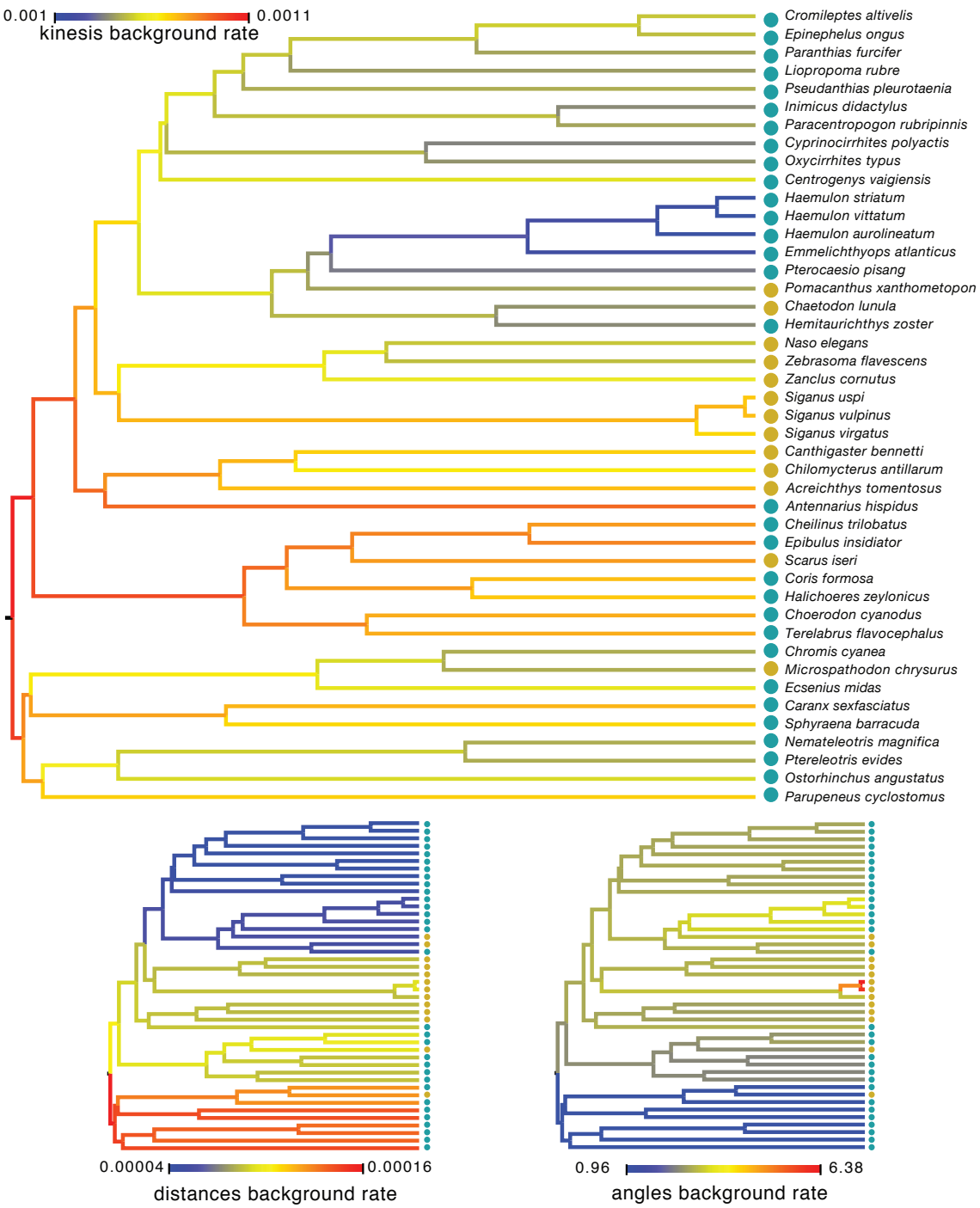

Fig. S4. Background rate of evolution mapped onto the phylogenetic tree for each kinematic trait dataset from Bayesian relaxed clock, state-dependent, multivariate models of evolution. Rates of evolution shown are rate variation that could not be attributed to the discrete trait.

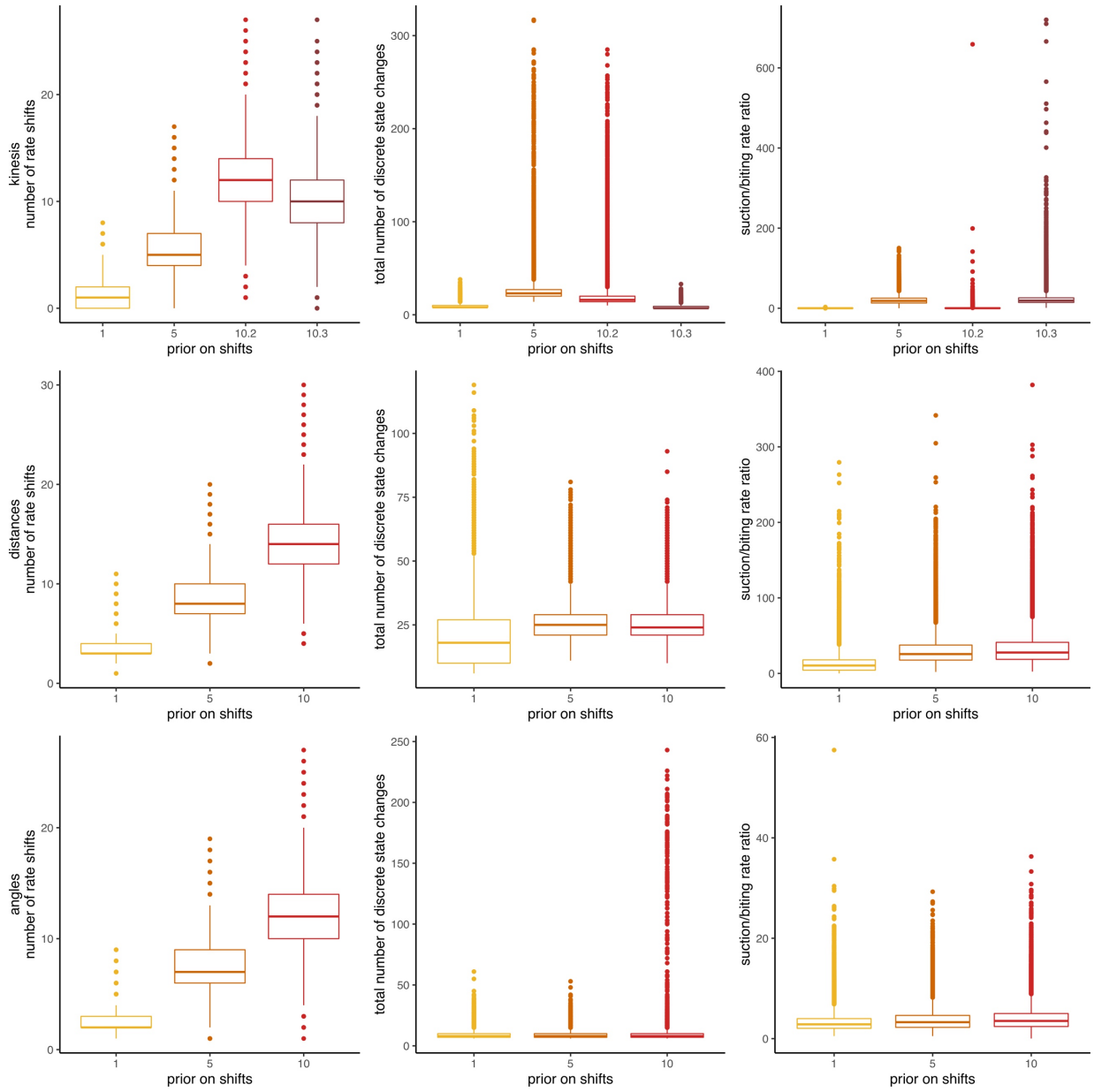

Fig. S5. Effects of the prior on the number of rate shifts on parameter estimates for Bayesian relaxed-clock, multivariate, state-dependent models of evolution. We find generally consistent parameter results at each value of the prior on the number of rate shifts for distances and angles, but varied effects of the prior on models of overall cranial kinesis. In models of kinesis, “10.2” is a 10-shift-prior model run for 2 million generations of the MCMC, and “10.3” is a 10-shift-prior model run for 3 million generations.

Table S1. List of species used in this study with feeding mode designation.

Species	Family	Feeding mode
Acreichthys tomentosus	Monacanthidae	biting
Antennarius hispidus	Antennariidae	suction feeding
Canthigaster bennetti	Tetraodontidae	biting
Caranx sexfasciatus	Carangidae	suction feeding
Centrogenys vaigiensis	Centrogenidae	suction feeding
Chaetodon lunula	Chaetodontidae	biting
Cheilinus trilobatus	Labridae	suction feeding
Chilomycterus antillarum	Diodontidae	biting
Choerodon cyanodus	Labridae	suction feeding
Chromis cyanea	Pomacentridae	suction feeding
Coris formosa	Labridae	suction feeding
Cromileptes altivelis	Serranidae	suction feeding
Cyprinocirrhites polyactis	Cirrhitidae	suction feeding
Emmelichthyops atlanticus	Haemulidae	suction feeding
Epibulus insidiator	Labridae	suction feeding
Epinephelus ongus	Serranidae	suction feeding
Escenius midas	Blenniidae	suction feeding
Haemulon aurolineatum	Haemulidae	suction feeding
Haemulon striatum	Haemulidae	suction feeding
Haemulon vittatum	Haemulidae	suction feeding
Halichoeres zeylonicus	Labridae	suction feeding
Hemitaurichthys zoster	Chaetodontidae	suction feeding
Inimicus didactylus	Synanceiidae	suction feeding
Liopropoma rubre	Serranidae	suction feeding
Microspathodon chrysurus	Pomacentridae	biting
Naso elegans	Acanthuridae	biting

Nemateleotris magnifica	Microdesmidae	suction feeding
Ostorhinchus angustatus	Apogonidae	suction feeding
Oxycirrhites typus	Cirrhitidae	suction feeding
Paracentropogon rubripinnis	Tetrarogidae	suction feeding
Paranthias furcifer	Serranidae	suction feeding
Parupeneus cyclostomus	Mullidae	suction feeding
Pomacanthus xanthometopon	Pomacanthidae	biting
Pseudanthias pleurotaenia	Anthiinae	suction feeding
Ptereleotris evides	Microdesmidae	suction feeding
Pterocaesio pisang	Lutjanidae	suction feeding
Scarus iseri	Scaridae	biting
Siganus uspi	Siganidae	biting
Siganus virgatus	Siganidae	biting
Siganus vulpinus	Siganidae	biting
Sphyraena barracuda	Sphyraenidae	suction feeding
Terelabrus flavocephalus	Labridae	suction feeding
Zanclus cornutus	Zanclidae	biting
Zebrasoma flavescens	Acanthuridae	biting

Table S2. Morphological disparity analyses.

Trait	Biters Variance	Suction Variance	Variance ratio	p-value
kinesis	0.0016	0.018	10.93	0.02
upper jaw protrusion	1.85e-04	2.01e-03	10.87	0.11
maximum gape	9.37e-04	3.06e-03	3.27	0.04
upper jaw rotation	39.85	379.03	9.51	0.01
lower jaw rotation	104.29	348.21	3.34	0.02
head rotation	4.71	107.92	22.91	0.00
buccal depression	1.68e-05	5.68e-04	33.89	0.01

Table S3. Results from phylogenetic ANOVAs.

Regression	d.f.	p-value	F-value
overall cranial kinesis ~ feeding mode	1,42	$p < 0.01$	8.63
upper jaw protrusion ~ feeding mode	1,42	$p < 0.05$	4.97
upper jaw rotation ~ feeding mode	1,42	$p < 0.01$	7.46
buccal depression ~ feeding mode	1,42	$p < 0.05$	6.62
head rotation ~ feeding mode	1,42	$p < 0.01$	8.81
lower jaw rotation ~ feeding mode	1,42	$p = 0.15$	2.09
maximum gape ~ feeding mode	1,42	$p < 0.05$	4.72

Table S4. Loadings from a principal component analysis.

component	PC1	PC2	PC3	PC4	PC5	PC6
upper jaw protrusion	0.30	0.66	0.37	-0.11	0.15	-0.42
maximum gape	0.37	-0.46	-0.26	-0.10	0.68	-0.19
upper jaw rotation	0.35	0.47	-0.42	0.45	0.24	0.43
lower jaw rotation	0.39	0.08	-0.45	-0.65	-0.43	0.13
buccal depression	0.40	-0.23	-0.14	0.55	-0.50	-0.47
head rotation	0.40	-0.24	0.53	0.10	-0.14	0.59
cumulative variance explained	0.66	0.84	0.90	0.95	0.98	1.00

APPENDIX 1 REFERENCES

Beaulieu J.M., Jhwueng D.C., Boettiger C., O'Meara B.C. 2012. Modeling stabilizing selection: Expanding the Ornstein-Uhlenbeck model of adaptive evolution. Evolution. 66:2369–2383.

Moore B.R., Höhna S., May M.R., Rannala B., Huelsenbeck J.P. 2016. Critically evaluating the theory and performance of Bayesian analysis of macroevolutionary mixtures. Proc. Natl. Acad. Sci. 113:201518659.

Revell L.J. 2012. phytools: An R package for phylogenetic comparative biology (and other things). Methods Ecol. Evol. 3:217–223.

APPENDIX 2

SUPPLEMENTARY INFORMATION FOR CHAPTER 2

THE RISE OF BITING IN THE CENOZOIC FUELED REEF FISH BODY SHAPE DIVERSIFICATION

SUPPLEMENTAL METHODS

Feeding mode categorizations. We used a hierarchical process to categorize prey proportions: where volumetric data of consumer stomach contents were available, then proportions of volume were used. If volumetric data were not available but individual counts of prey items from stomach contents were available, then proportions of the total number of prey were used. If only lists of prey taxa found in gut contents were available, then we used the proportion of taxa on which the species feeds listed to estimate proportions of prey. In this case, prey items at the end of a long list of taxa were considered less important than prey items at the beginning of the list.

History of feeding modes. We used *make.simmap* to reconstruct ancestral character states using the R package 'phytools' (Revell 2012). We set the function to fit a continuous-time Markov model for the evolution of feeding modes using a fixed value of the Q matrix (Huelsenbeck et al. 2003; Bollback 2006), and we estimated the stationary distribution (pi) from the Q matrix, which was used as the prior on the root frequency.

Random forest models. We used 7 continuous variables in each decision tree. We selected this number after iterating random forest model-fitting over different numbers of variables (ranging from 1-7), each across 5,000 decision trees, and comparing predicted group membership accuracy across the different numbers of variables used for the decision trees. We used a conditional implementation of *varimp* in the 'party' R package to estimate variable importance. In the conditional implementation, the importance of each trait is computed by permuting other variables whose covariance with the variable of interest exceeds a user-specified threshold (0.2 in our model) (Hothorn et al. 2004, 2006; Strobl et al. 2007, 2008).

Hypervolumes. We used six PC axes to generate hypervolumes as hypervolumes are best run on orthogonal data axes (Blonder et al. 2018) and constructed hypervolumes using the R package 'hypervolume' (Blonder et al. 2014; 2018). Each hypervolume was computed by generating a gaussian density kernel containing 95% of points from the original group of data. To assess how extreme our data were compared to a random distribution of hyervolumes, we permuted group assignments among original species data and re-computed all hypervolumes and all hypervolume comparisons. We ran 10,000 iterations of the permuted hypervolumes and comparisons between them, then compared the proportion of our comparisons between hypervolumes that were more extreme than comparisons between the distribution of analagous hypervolumes. We estimated whether our data were more extreme than the 'null' distribution in a 2-tailed fashion, such that our data could be more extreme than the distribution of permuted hypervolumes by occupying either more or less unique space than 95% of the distribution.

Evolutionary rate models. We set a log-normal prior on each branch's background rate. We placed a log-uniform prior at 1×10^{-10} on the rate of transitions between states ("lambda"). To ensure that model fitting was not affected strongly by the transition rate prior, we also fit models with higher (1×10^{-7}) and lower (1×10^{-13}) priors on lambda. Both alternative prior models ran for 150,000 generations of the MCMC.

SUPPLEMENTAL RESULTS

History of feeding mode. Stochastic character mapping recovered asymmetrical transitions between states (Fig. S2), with many transitions between attached prey biting and mixed feeding; fewer but still numerous transitions between mixed feeding and

suction feeding; some transitions between attached prey biting and suction feeding; and few transitions from suction to ram biting. We recovered almost no transitions from ram biting to any other state, and zero transitions from ram biting to either attached prey biting or mixed suction and biting.

Evolutionary rate models. A Bayesian, state-dependent, relaxed-clock model of evolutionary rate estimated 214 transitions between feeding mode states. We uncovered substantial variation in background rate across the history of body shape, as the standard deviation of the background rate parameter was relatively large (1.41). Alternative prior testing on lambda, the rate of transitions between states, revealed minimal effects of the prior (Fig. S6). There was little difference across alternative priors in any of three relevant metrics: 1) the estimated number of transitions between states, 2) the posterior estimate of lambda, or 3) the resulting ratio of rate estimates between groups of interest.

SUPPLEMENTAL FIGURES & TABLES

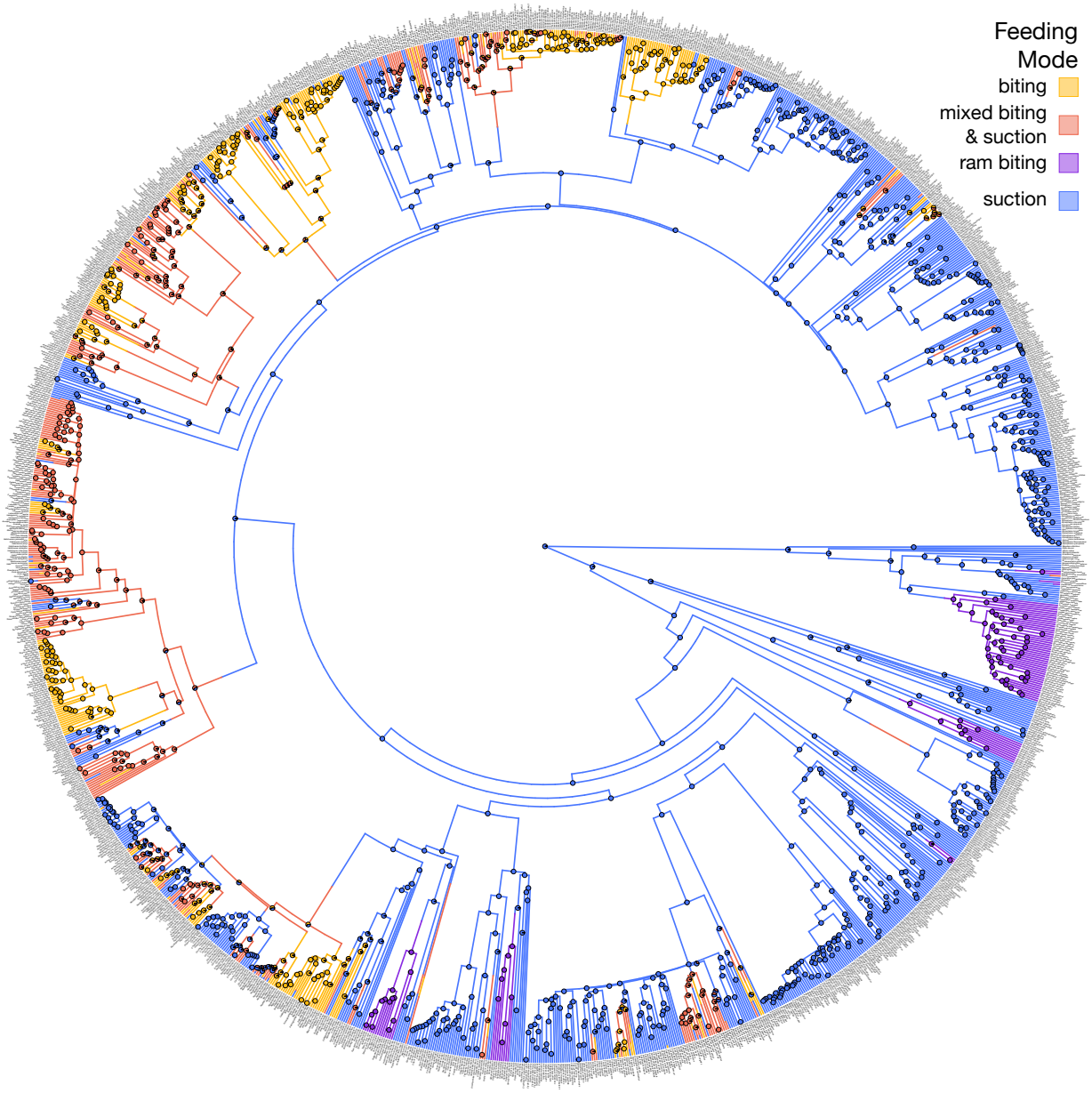

Fig. S1. A sample stochastic character map showing a simulated character history of feeding mode, with tips labeled by species. Branch mapping shown is a single map chosen at random, but pie charts at nodes summarize estimated states at each node over the full distribution of 100 stochastic character maps.

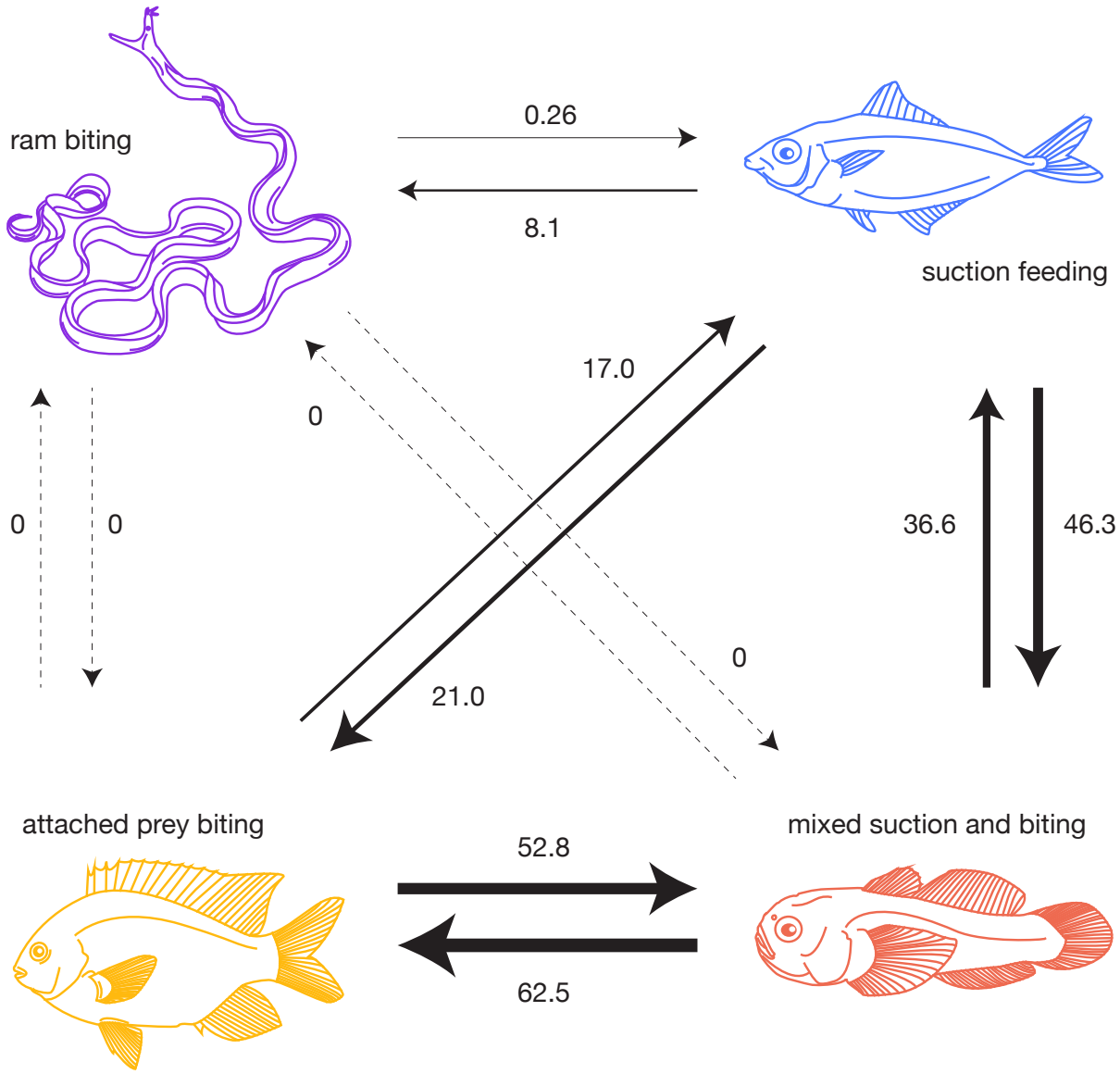

Fig. S2. Transition rate matrix between character states, from a distribution of 100 stochastic character mappings. Thickness of arrows and number beside each arrow indicates the number of transitions between the two indicated states. Notably, there are no transitions from either attached prey biting or mixed suction and biting to ram biting, and there are almost no transitions from ram biting to any other state.

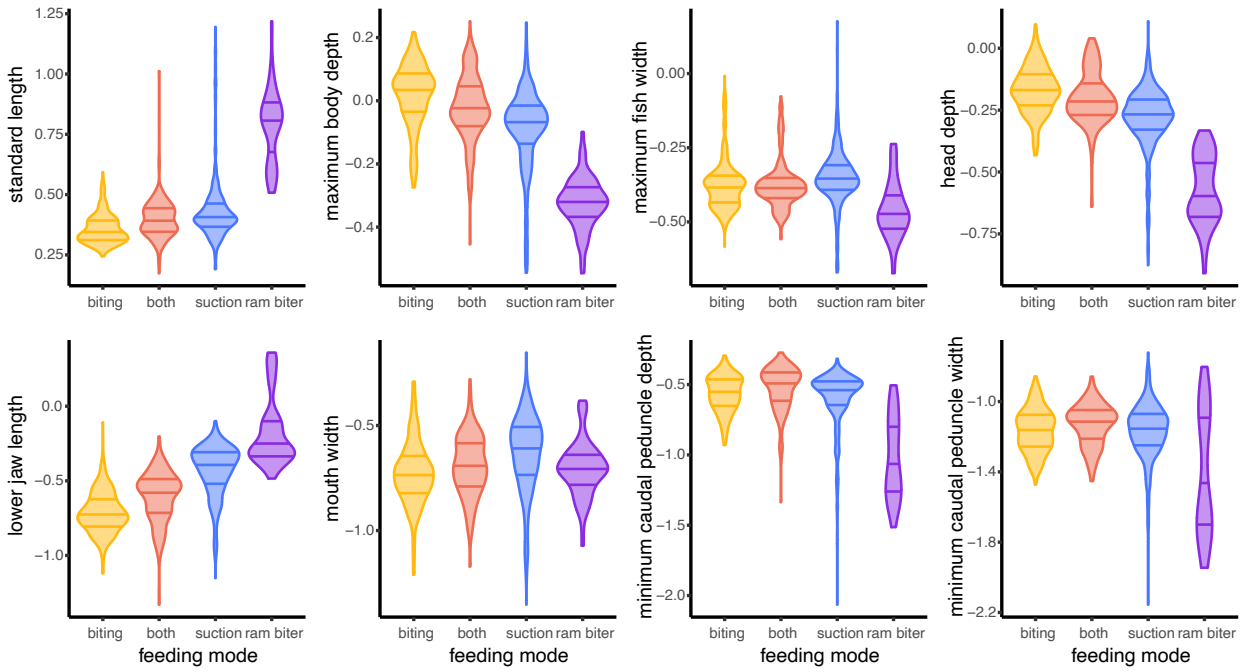

Fig. S3. Distributions of morphological traits by feeding mode. All traits were different in univariate phylogenetic ANOVAs at α = 0.05. Only fish width was not significantly different between feeding mode groups at α = 0.01.

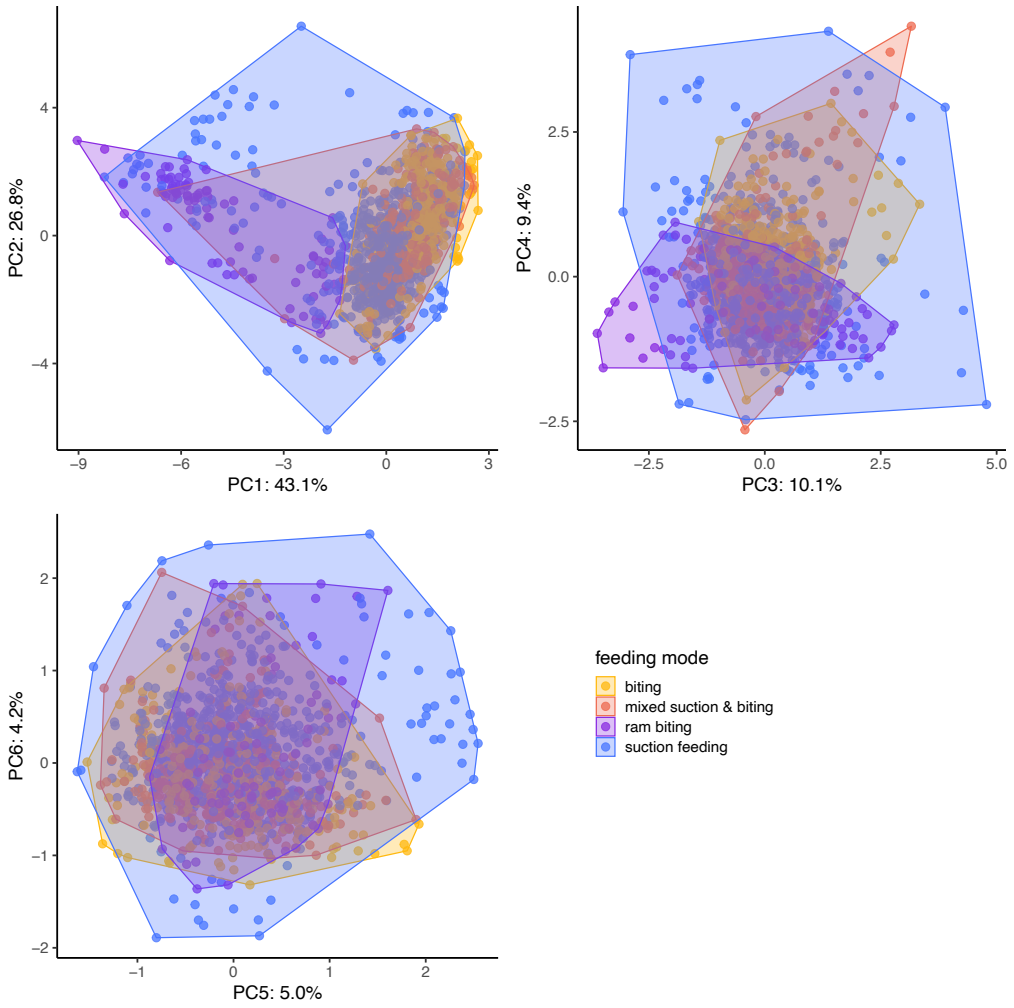

Fig. S4. Data used for generating 6-dimensional hypervolumes (principal components 1-6) plotted bivariately with convex hulls to demonstrate unique shape space occupation; together these six axes account for 98.5% of the variance in the data. Each point represents a species; points and convex hulls are colored by feeding mechanism. The primary region of unique shape space occupation by biters and mixed feeders lies along the right margin of PC1, and includes a range of species from several families using biting or mixed suction and biting, such as *Monacanthus chinensis, Acanthurus coeruleus, Canthigaster janthinoptera, Platax batavianus,* and *Pervagor janthinosoma*. These fishes are characterized by laterally compressed, shortened bodies with small mouths.

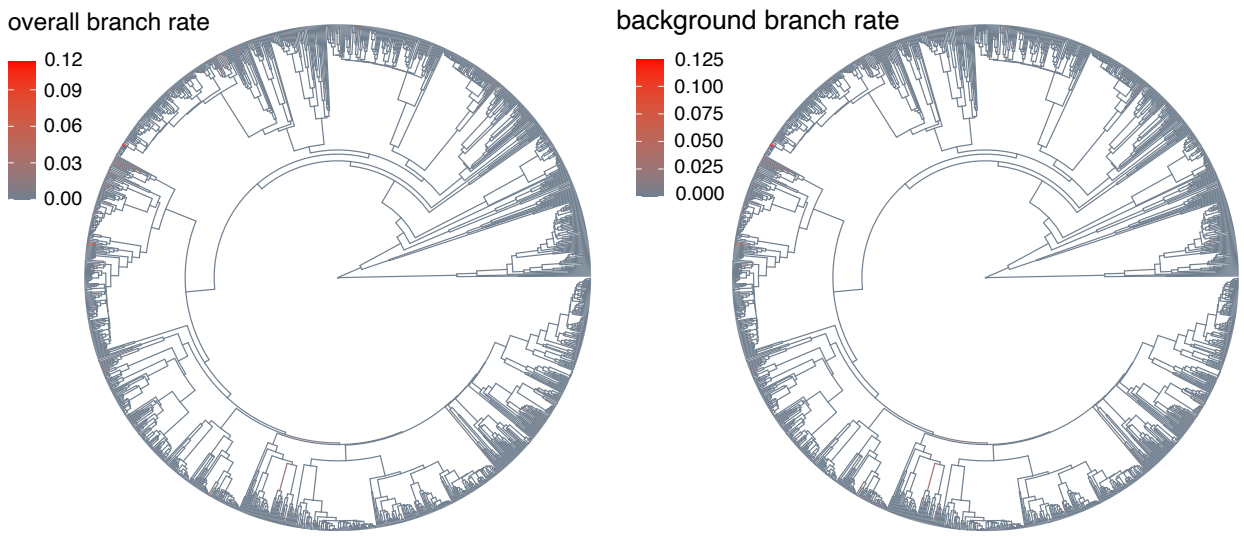

Fig. S5. Additional branch-specific rates of evolution from evolutionary model-fitting. Left, overall branch rates plotted onto the phylogeny, calculated as the product of state-dependent rates and background rates for each branch. Right, background rates, which absorb rate variation not attributed to feeding mode. Homogeneity of background rates on a broader scale suggests that a small number of short branches have elevated rates in comparison to longer branches clades, a pervasive phenomenon in evolutionary rate modeling (Harmon et al. 2021).

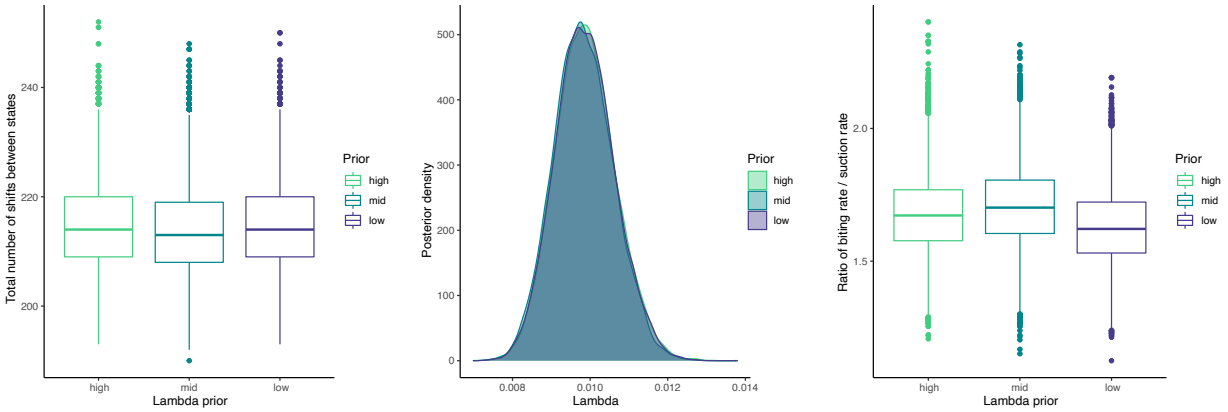

Fig. S6. Relevant statistics from alternative prior testing on the log uniform prior on the number of state changes for evolutionary rate modeling. Left, total number of transitions between discrete character states; center, estimate of lambda, the transition rate parameter; and right, sample of rates of continuous character evolution in different discrete states shown as a rate ratio of “biting” group and “suction” group. The model using the “mid” prior was used for interpretation of results in the main text.

Table S1. Loadings from a principal component analysis on the correlation matrix.

Trait	PC1	PC2	PC3	PC4	PC5	PC6	PC7	PC8
Standard length	-0.50	0.09	-0.32	0.06	-0.08	-0.27	0.32	-0.07
Maximum body depth	0.46	0.27	0.08	-0.33	0.15	0.027	-0.45	-0.06
Maximum fish width	0.12	-0.54	0.41	0.40	-0.10	0.40	0.14	-0.04
Head depth	0.49	0.11	0.03	-0.13	0.32	-0.10	0.78	5.55×10^{-17}
Lower jaw length	-0.23	-0.40	-0.26	-0.66	0.22	0.48	0.07	-2.78×10^{-17}
Mouth width	0.01	-0.59	0.21	-0.19	0.21	-0.71	-0.14	2.08×10^{-16}
Minimum caudal peduncle depth	0.39	-0.22	-0.33	-0.20	-0.79	-0.11	0.08	-5.55×10^{-17}
Minimum caudal peduncle width	0.28	-0.25	-0.70	0.45	0.36	0.03	-0.19	8.33×10^{-17}
Cumulative variance explained	0.43	0.70	0.80	0.90	0.94	0.98	1.00	1.00

Table S2. Results from phylogenetic ANOVAs.

Regression	d.f.	p-value	r^2	Z score
Standard length ~ feeding mode	3, 1526	p < 0.01	0.0084	1.88
Maximum body depth ~ feeding mode	3, 1526	p < 0.0001	0.021	2.84
Maximum fish width ~ feeding mode	3, 1526	p < 0.05	0.0074	1.77
Head depth ~ feeding mode	3, 1526	p < 0.001	0.010	2.12
Lower jaw length ~ feeding mode	3, 1526	p < 0.0001	0.062	3.82
Mouth width ~ feeding mode	3, 1526	p < 0.01	0.010	2.02
Minimum caudal peduncle depth ~ feeding mode	3, 1526	p < 0.0001	0.022	2.89
Minimum caudal peduncle width ~ feeding mode	3, 1526	p < 0.0001	0.021	2.80
All traits ~ feeding mode (MANOVA)	3, 1526	p < 0.0001	0.028	5.98

Table S3. Random forest results.

Trait	Importance (weighted mean decrease in accuracy when trait is excluded)
Lower jaw length	0.201
Head depth	0.0533
Standard length	0.0401
Minimum caudal peduncle depth	0.0307
Maximum body depth	0.00500
Minimum caudal peduncle width	0.00448
Maximum fish width	0.00275
Mouth width	0.00149

Table S4. Morphological disparity results, computed using *geomorph*.

Trait	Biters variance	Mixed suction & biting variance	Ram biting variance	Suction variance
Standard length	0.0037	0.0060	0.022	0.020
Maximum body depth	0.0098	0.011	0.0063	0.015
Maximum fish width	0.0071	0.0064	0.0086	0.0081
Head depth	0.0088	0.011	0.018	0.015
Lower jaw length	0.019	0.028	0.049	0.028
Mouth width	0.023	0.021	0.016818	0.033
Minimum caudal peduncle depth	0.016	0.024	0.080	0.044
Minimum caudal peduncle width	0.015	0.0135	0.12	0.025

Table S5. Hypervolume results, computed using *hypervolume*.

Hyper-volume 1	Hyper-volume 2	Unique fraction of hyper-volume 1 (unique frac. 1)	Proportion of permuted distribution less than unique frac. 1	Unique fraction of hyper-volume 2 (unique frac. 2)	Proportion of permuted distribution less than unique frac. 2
Biting	All not Biting	0.13	0.597	0.84	0.542
Mixed suction & biting	All not Mixed suction & biting	0.10	0.831	0.80	0.188
Suction	All not Suction	0.44	0.201	0.54	0.779
Ram biting	All not Ram biting	0.91	0.267	0.82	0.960
Biting + Mixed suction & biting	Suction + Ram biting	0.19	0.110	0.83	0.870

APPENDIX 2 REFERENCES

Blonder B., Lamanna C., Violle C., B. J. Enquist B.J. 2014. The n-dimensional hypervolume. Glob. Ecol. Biogeogr. 23:595–609.

Blonder, B., Morrow, C.B., Maitner, B., Harris, D.J., Lamanna, C., Violle, C., Enquist, B.J., Kerkhoff, A.J. 2018. New approaches for delineating n-dimensional hypervolumes. Methods Ecol. Evol. 9(2):305-319.

Bollback J.P. 2006. SIMMAP: Stochastic character mapping of discrete traits on phylogenies. BMC Bioinformatics 7.

Harmon, L.J., Pennell, M.W., Henao-Diaz, L.F., Rolland, J., Sipley, B.N., Uyeda, J.C. 2021. Causes and Consequences of Apparent Timescaling Across All Estimated Evolutionary Rates. Annu. Rev. Ecol. Evol. Syst. 52:587-609.

Hothorn T., Hornik K., Zeileis A. 2006. Unbiased recursive partitioning: A conditional inference framework. J. Comput. Graph. Stat. 15:651–674.

Hothorn T., Lausen B., Benner A., Radespiel-Tröger M. 2004. Bagging survival trees. Stat. Med. 23:77–91.

Huelsenbeck J.P., Nielsen R., Bollback J.P. 2003. Stochastic mapping of morphological characters. Syst. Biol. 52:131–158.

Revell L.J. 2012. phytools: An R package for phylogenetic comparative biology (and other things). Methods Ecol. Evol. 3:217–223.

Strobl C., Boulesteix A.L., Kneib T., Augustin T., Zeileis A. 2008. Conditional variable importance for random forests. BMC Bioinformatics 9: 1–11.

Strobl C., Boulesteix A.L., Zeileis A., Hothorn T. 2007. Bias in random forest variable importance measures: Illustrations, sources and a solution. BMC Bioinformatics 8.

APPENDIX 3

SUPPLEMENTARY MATERIALS FOR CHAPTER 3

FASTER BODY SHAPE EVOLUTION AT THE EDGES OF FISH MORPHOSPACE

SUPPLEMENTAL METHODS

Linear model fitting. In addition to fitting ordinary least squares models with log10-transformed data, we also fit linear models without log10 transformations to ensure these transformations did not have an undue effect on our results.

We performed stepwise regression on the phylogenetic least squares model (PGLS) fitting habitat traits to distance from centroid. We began with the fully saturated model containing all nine habitat traits. As the habitats in our dataset were largely mutually exclusive among species, we chose not to include the effects of interaction terms. At each step, we removed the trait with the highest p-value until we reached a model where all traits had a significant effect on distance from centroid at alpha = 0.05.

Stochastic character mapping. Stochastic character maps were generated using 'make.simmap' in the R package *phytools* (Huelsenbeck et al. 2003; Bollback 2006; Revell 2012). We used a fixed value of the Q matrix and estimated the stationary distribution using the Q matrix, which was set as a prior on the root state. We used the same parameters when building distributions of stochastic character maps for simulated datasets used to generate a "null" distribution of the transition rate between extreme shapes and non-extreme shapes.

For these simulated datasets, we generated 100 datasets sequentially using 'fastBM' in *phytools* (Revell 2012). Each of these datasets was simulated using the tree for the 5,940 species in our dataset, and we set the state at the root = 0 and the rate = 1, with no trend. We generated 8 traits, all using these parameters, for each simulated dataset.

SUPPLEMENTAL RESULTS

Linear model fitting. Linear models without log10-transformed continuous variables showed the same patterns as those with the transformations (Table S2). However, the pattern was much stronger in an ANOVA of the effect of branch directionality on log10-transformed branch rates than non-transformed branch rates.

The full phylogenetic least squares model (PGLS) containing all habitat traits found significant effects among just three habitat traits: depth zone, reef habitation, and cave habitation (Table 3).

SUPPLEMENTAL FIGURES & TABLES

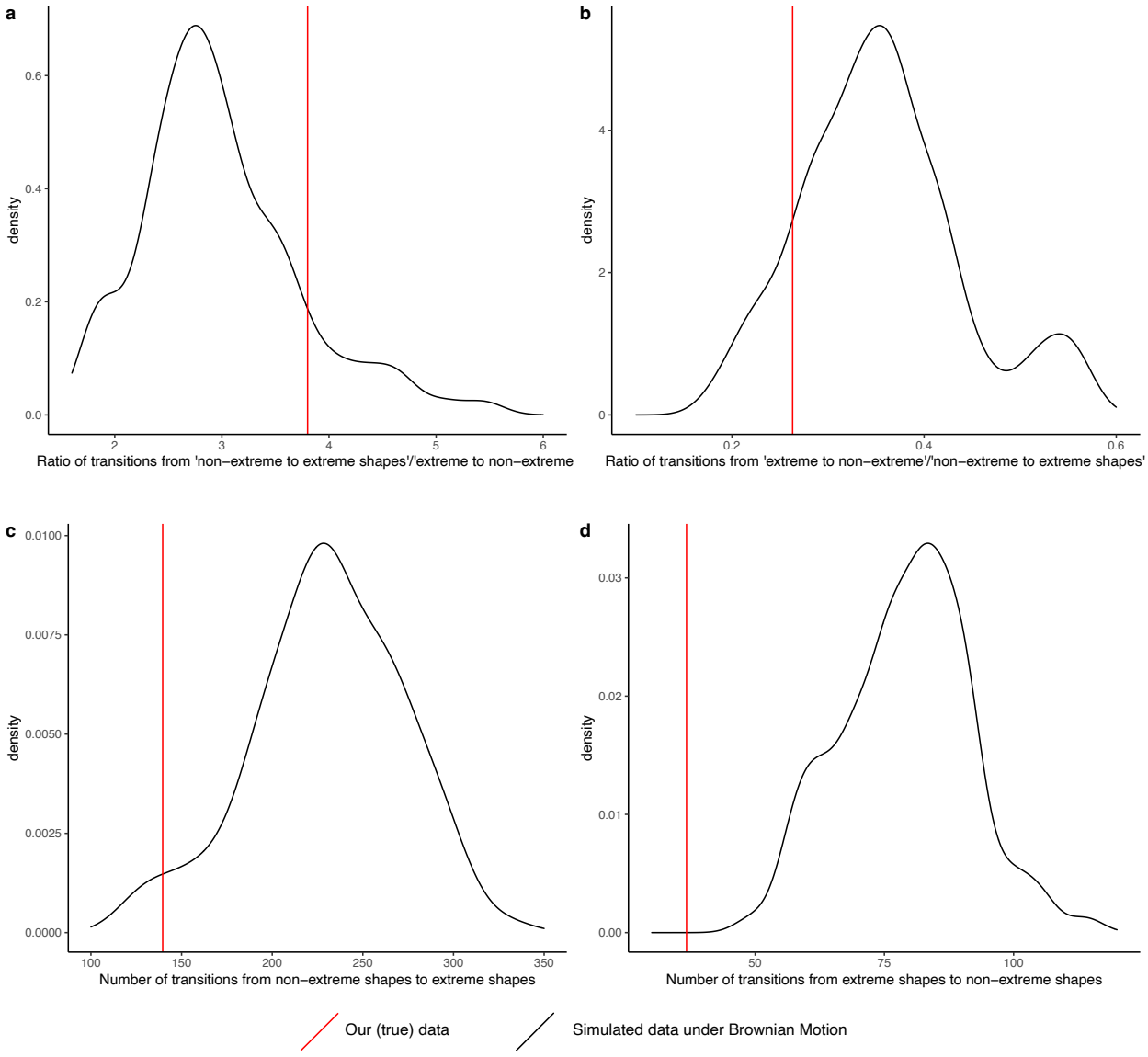

Figure S1. Results of the distribution of stochastic character maps of our true data (red) and of simulated data (black). Comparisons of the ratio of transitions between states are largely overlapping between our true data and the simulated data (a, b). However, the absolute number of transitions in our data was much lower than the number of transitions in data simulated under Brownian motion (c, d).

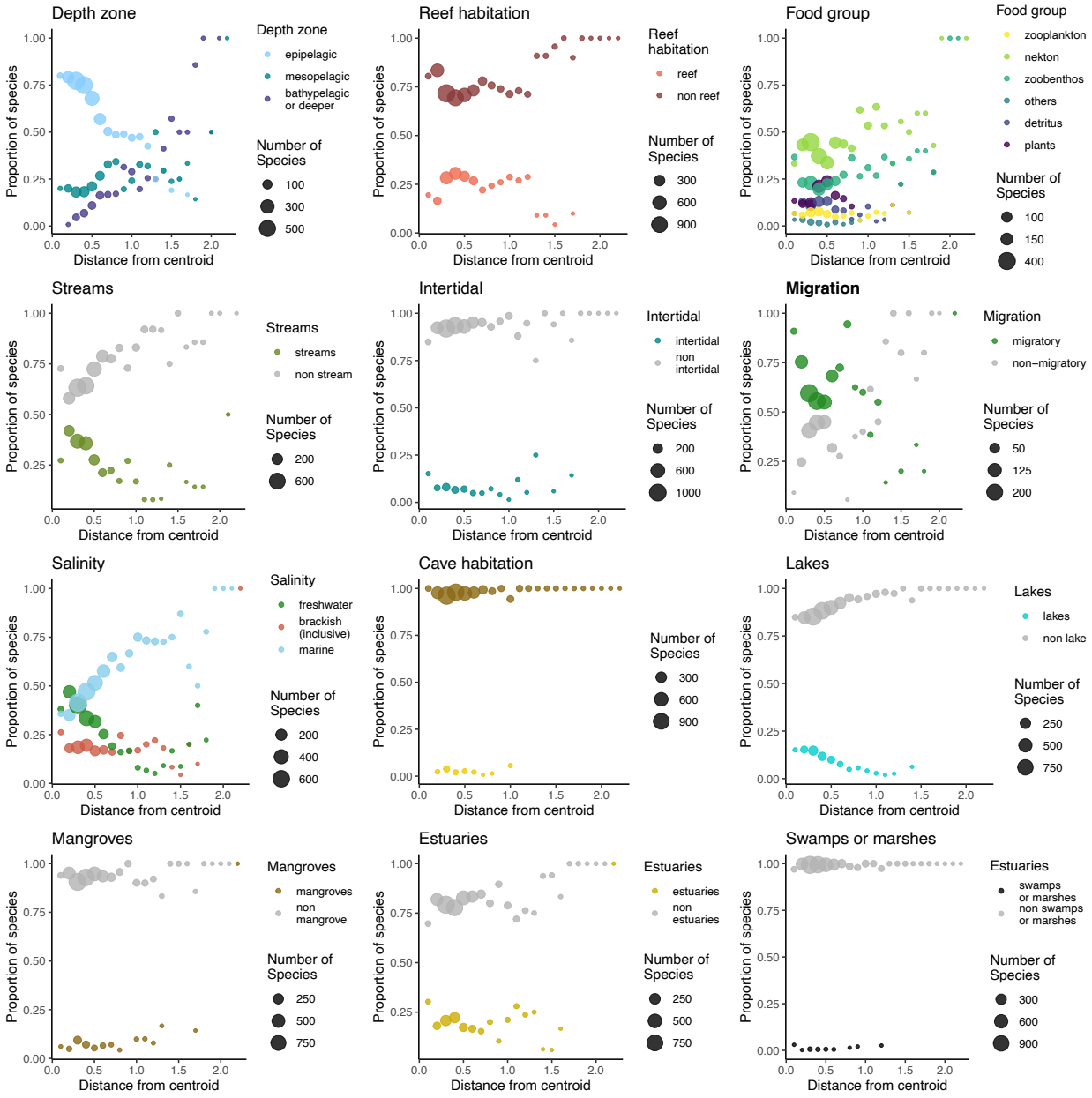

Figure S2. Representation of fishes along a gradient of extremeness in a range of ecological groups.

Table S1.

Loadings from a Principal Components Analysis on the covariance matrix of 5,940 species of extant teleost fishes.

Trait	PC1	PC2	PC3	PC4	PC5	PC6	PC7	PC8
Standard length	0.285	-0.012	0.324	-0.348	-0.086	0.523	0.281	-5.77E-01
Maximum body depth	-0.233	-0.266	-0.016	0.446	0.130	0.112	-0.559	-5.77E-01
Maximum fish width	-0.052	0.277	-0.308	-0.099	-0.044	-0.635	0.278	-5.77E-01
Head depth	-0.217	-0.122	-0.053	0.526	0.376	0.187	0.694	-5.55E-17
Lower jaw length	0.174	0.500	0.714	0.390	0.038	-0.230	-0.057	-1.11E-16
Mouth width	0.046	0.721	-0.470	0.170	-0.035	0.459	-0.128	1.80E-16
Minimum caudal peduncle width	-0.549	0.247	0.185	-0.460	0.614	0.044	-0.109	-5.55E-17
Minimum caudal peduncle depth	-0.693	0.080	0.179	0.024	-0.673	0.104	0.129	2.22E-16
Proportion of Variance	0.424	0.229	0.130	0.110	0.070	0.022	0.015	0.00E+00
Cumulative Variance Explained	0.424	0.653	0.783	0.892	0.963	0.985	1.000	1.00E+00

Table S2. Results from ordinary least squares models without log transformed data.

Regression	Intercept	Slope	d.f.	Adj. R-sq	p-value
Mean trait contrast ~ Distance from centroid (for nodes)	0.0095	0.010	1, 5937	0.041	< 2.2e-16
Rate as distance of a branch ~ Branch directionality	0.0087	-0.0012	1, 11876	0.00032	0.02785
Rate as distance of a branch ~ Distance of the start of the branch from the centroid	0.0030	0.013	1, 11876	0.013	< 2.2e-16
Length of PC space traversed by branch ~ Distance of the start of the branch from the centroid	0.019	0.063	1, 11876	0.061	< 2.2e-16

Table S3. Results the fully saturated model of a phylogenetic least squares regression of habitat traits.

Regression	d.f.	Adj. R-sq	p-value	Z-score
Distance from centroid ~	Total: 2950			
Depth zone	2	0.01276	1.00e-04	4.1927
+ Reef habitation	1	0.00257	0.0122	2.1118
+ Intertidal habitation	1	0	0.9305	-1.5424
+ Stream habitation	1	0.00046	0.2546	0.698
+ Cave habitation	1	0.00214	0.0197	1.9457
+ Mangrove habitation	1	0.00002	0.8327	-1.0259
+ Swamp/Marsh habitation	1	0.00009	0.5364	-0.0643
+ Lake habitation	1	0.0007	0.1666	0.987
+ Estuary habitation	1	0.00002	0.8154	-0.9509

APPENDIX 3 REFERENCES

Bollback J.P. 2006. SIMMAP: Stochastic character mapping of discrete traits on phylogenies. BMC Bioinformatics 7.

Huelsenbeck J.P., Nielsen R., Bollback J.P. 2003. Stochastic mapping of morphological characters. Syst. Biol. 52:131–158.

Revell L.J. 2012. phytools: An R package for phylogenetic comparative biology (and other things). Methods Ecol. Evol. 3:217–223.